

POLITECNICO DI TORINO

Corso di Laurea Magistrale
in Automotive Engineering

Master degree thesis

Fuel Cell Vehicle simulation: an approach based on Toyota Mirai



Supervisor:

Chiar.^{mo} Prof. Ing. Andrea Tonoli

Co-supervisor:

Ing. Sara Luciani

Applicant:

Marco Bonci

Academic Year 2020/2021



Acknowledgements

Un sentito ringraziamento va a tutta la mia famiglia che mi ha sostenuto a livello economico ed emotivo durante tutto il percorso di studi e ha continuato a credere nelle mie possibilità nonostante le difficoltà. Una menzione speciale va alla nonna Lily la quale purtroppo non potrà mai vedermi raggiungere questo importante traguardo.

Vorrei ringraziare i miei amici storici Francesco e Federico per il tempo passato assieme. Un grandissimo ringraziamento va anche a tutto il gruppo di CXVIII: Luca, Federico, Andrea, Andrea, Mattia e Matteo per tutte le avventure trascorse e per il solido legame creato.

Ringrazio il mio relatore, Professor Andrea Tonoli, e la mia correlatrice Sara Luciani, i quali nonostante tutti i problemi e gli impegni, specialmente in una situazione così difficile a causa della pandemia, hanno trovato il modo di dedicarmi del tempo.

Un ultimo ringraziamento va ai miei coinquilini a Torino, Andrea e Luigi, senza i quali il percorso sarebbe stato molto più pesante.



Abstract

The high expectations on hydrogen in the global energy system of the early 2000s failed to be met. In recent years, because of the more stringent emission legislation framework, the European funding for low emission innovations and the technology improvement combined with cost reduction, hydrogen and Fuel Cells are regaining momentum.

In this context, the present thesis work focuses on the modelling of performance and fuel consumption of Fuel Cell vehicles (FCVs). Starting from the models present on Advisor, a MATLAB/Simulink model capable to simulate the whole vehicle system during various driving cycles has been created.

The main components are modelled as follows. The vehicle is represented through its load parameters and longitudinal dynamics. The motor is described through a torque-speed map with efficiency curves. The battery is modelled through its main parameters such as the state of charge, the capacity, the voltage and the internal resistance. The whole system is considered for the Fuel Cell. The stack is modelled with its polarization curve while the auxiliaries are modelled with operational maps if present like for example in the air compressor or with their efficiencies in the case of the pumps.

Firstly, the data of an average small car are considered. The simulation is run over five different driving cycles, namely FTP, NEDC, UDDS, US06 and WLTP, and different control strategies are evaluated. Thus, a comparative analysis on the collected results is performed. The control strategy which highlighted the best performance in terms of fuel consumption and driving range is selected for the second part of this work. Afterwards, the main parameters of the model, such as the battery, fuel cell stack, electric motor, aerodynamic drag and vehicle parameters, have been set accordingly to those of 2017 Toyota Mirai Fuel Cell Vehicle.

The analysis has been carried out considering both the tests made on Toyota Mirai vehicle by Argonne National Lab (ANL) in 2017, and looking at available data relative to similar vehicles. Finally, a model which closely represents the Toyota Mirai vehicle has been built. For validation purposes, the simulation has been run on the NEDC and US06 cycles and the results have been compared to those found by the Argonne National Lab. The thesis work ends with critical comments about the obtained results and the possible future works perspectives.



Table of Contents

Acknowledgements	2
Abstract	3
1. Introduction	8
2. Fuel Cells	10
2.1. Fuel Cell technologies	13
2.1.1. Alkaline Fuel Cells (AFC).....	14
2.1.2. Phosphoric Acid Fuel Cells (PAFC).....	15
2.1.3. Molten Carbonate Fuel Cells (MCFC).....	15
2.1.4. Solid Oxide Fuel Cells (SOFC).....	16
2.1.5. Direct Methanol Fuel Cells (DMFC).....	16
2.1.6. Proton Exchange Membrane Fuel Cells (PEMFC).....	17
2.2. PEM Fuel Cell operating conditions	18
2.2.1. Operating pressure.....	18
2.2.2. Operating temperature.....	19
2.2.3. Reactant flow rates.....	19
2.2.4. Reactant humidity.....	20
2.3. Fuel Cell auxiliary systems	21
2.3.1. Oxidant supply system.....	22
2.3.2. Hydrogen supply systems.....	22
2.3.3. Water management systems.....	23
2.3.4. Heat management systems.....	23
2.4. Hydrogen storage	25
2.4.1. Compressed Hydrogen.....	25
2.4.2. Liquid Hydrogen.....	26
2.4.3. Solid State.....	26
2.5. Hydrogen production methods	26
2.5.1. Steam reforming.....	27
2.5.2. Electrolysis.....	28
3. Vehicles powered by Fuel Cells	29
3.1. Pure Fuel Cell traction system	30
3.2. Series hybrid traction system propulsion	30
3.2.1. Range extender solution.....	31



3.2.2.	Load follower and Full performance solution	32
3.3.	Fuel Cell durability and performance during vehicle usage	33
3.4.	Technology comparison	33
3.4.1.	FCEVs vs ICE hybrids vs BEVs	33
3.4.2.	Trends and perspectives for future development.....	35
4.	Advisor	37
4.1.	Advisor structure.....	37
4.2.	Advisor approach	39
4.2.1.	Backward approach	39
4.2.2.	Forward approach.....	39
4.2.3.	Advisor approach	39
4.3.	Fuel Cell hybrid electric vehicle modelling in Advisor	40
4.3.1.	Vehicle (longitudinal dynamics) block	41
4.3.2.	Fuel Cell control strategy block	42
4.3.3.	Fuel Cell KTH model	42
5.	Hybrid Fuel Cell vehicles control strategies	45
5.1.	Control strategies testing parameters.....	48
5.1.1.	Simulation set-up.....	48
5.1.2.	Vehicle used for testing	51
5.2.	Thermostat control strategy	52
5.2.1.	Results using the FTP driving cycle	53
5.2.2.	Results using the NEDC driving cycle	54
5.2.3.	Results using the UDDS driving cycle	55
5.2.4.	Results using the US06 driving cycle.....	56
5.2.5.	Results using the WLTP driving cycle	57
5.3.	Range extender control strategy	58
5.3.1.	Results using the FTP driving cycle	59
5.3.2.	Results using the NEDC driving cycle	60
5.3.3.	Results using the UDDS driving cycle	61
5.3.4.	Results using the US06 driving cycle.....	62
5.3.5.	Results using the WLTP driving cycle	63
5.4.	Mode based control strategy	64
5.4.1.	Results using the FTP driving cycle	65
5.4.2.	Results using the NEDC driving cycle	66



5.4.3.	Results using the UDDS driving cycle.....	67
5.4.4.	Results using the US06 driving cycle.....	68
5.4.5.	Results using the WLTP driving cycle.....	69
5.5.	Constant Fuel Cell output control strategy.....	70
5.5.1.	Results using the FTP driving cycle.....	71
5.5.2.	Results using the NEDC driving cycle.....	72
5.5.3.	Results using the UDDS driving cycle.....	73
5.5.4.	Results using the US06 driving cycle.....	74
5.5.5.	Results using the WLTP driving cycle.....	75
5.6.	Strong load following control strategy.....	76
5.6.1.	Results using the FTP driving cycle.....	77
5.6.2.	Results using the NEDC driving cycle.....	78
5.6.3.	Results using the UDDS driving cycle.....	79
5.6.4.	Results using the US06 driving cycle.....	80
5.6.5.	Results using the WLTP driving cycle.....	81
5.7.	Adaptive control strategy.....	82
5.7.1.	Results using the FTP driving cycle.....	83
5.7.2.	Results using the NEDC driving cycle.....	84
5.7.3.	Results using the UDDS driving cycle.....	85
5.8.	Control strategies considerations and comparison.....	86
6.	Simulating Toyota Mirai.....	90
6.1.	Chassis and load parameters modelling.....	90
6.2.	Battery modelling.....	91
6.3.	Electric motor modelling.....	92
6.4.	Fuel Cell system modelling.....	92
6.5.	Parameters not taken into account: humidifier-less stack.....	95
6.6.	Simulation results.....	96
6.6.1.	Results using the FTP driving cycle.....	97
6.6.2.	Results using the NEDC driving cycle.....	98
6.6.3.	Results using the UDDS driving cycle.....	99
6.6.4.	Results using the US06 driving cycle.....	100
6.6.5.	Results using the WLTP driving cycle.....	101
6.7.	Cycle results comparison.....	102
7.	Comparison with Argonne National Lab results.....	103



7.1. NEDC.....	103
7.2. US06.....	104
8. Conclusions	105
References	106

1. Introduction

Fuel Cells are devices able to directly convert chemical energy into electricity, without combustion and without moving parts. This is obtained through the electrochemical combination between hydrogen and oxygen, which produces electricity, water and heat.

Fuel cell vehicles (FCVs) use fuel cells to generate electricity, which is used to drive the vehicle through an electric motor or is stored in an energy storage device (battery pack or supercapacitors).

In the last decades, oil consumption derived from the transportation sector has hugely increased, mainly due to the high usage of personal-use vehicles powered by internal combustion engines (ICEs).

Since important problems such as environmental pollution and green house effect are directly related to vehicle emissions, government organizations have developed more stringent standards on their emissions and consumptions.

After the Paris agreement, signed on 12th December of 2015, Europe has become united with the goal of fighting the climate change through the usage of clean technologies and sustainable energy sources. This is a common challenge, which leads to decarbonization in different sectors. One of the most affected is mobility, which includes many vehicles such as cars, buses, trucks, trains, ships and planes.

In the automotive field, the rise of this environmental view combined with the dieselgate scandal in which air pollution tests were found to be manipulated, lead to the replacement of the NEDC test procedure with the WLTP procedure. The transition from these two procedures started in September 2017 and ended in September 2019.

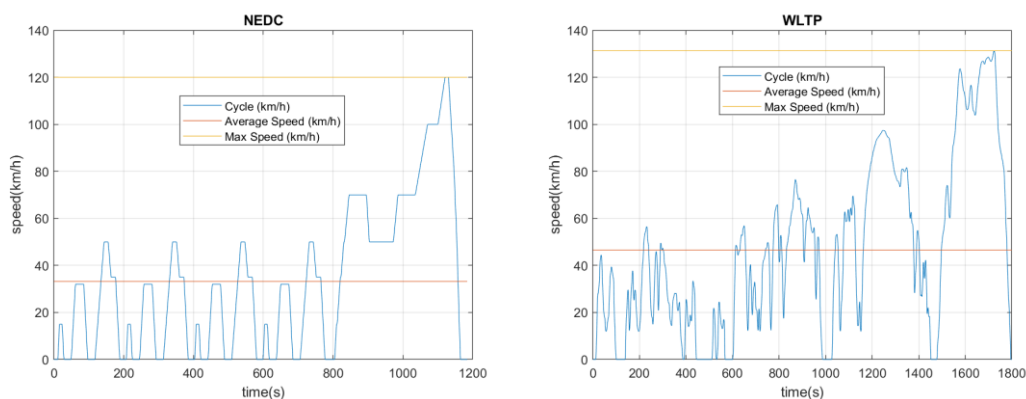


Figure 1.1 – NEDC profile vs WLTP profile

The WLTP profile represents better the real world driving conditions and the energy demand. The new procedure also takes into account Real Driving Emissions (RDE) tests, which must not be highly different from the ideal regulation limit. This difference is measured by conformity factors (CF), defined as the ratio of measured emissions to the regulated emission limit, which must be as close as possible to 1.



In addition to these changes, European Commission (EC) has set new CO₂ emission targets. The 2015 limit of 130 g/km set for an average car of the company in terms of mass has been lowered to 95 g/km in 2020, which is a quite demanding target. In the case of a vehicle equipped only by an ICE, it is a very difficult limit to reach especially in the case of gasoline engines.

A solution for both the environmental problems and the emission regulation problems could be represented by Fuel Cell Vehicles (FCVs).

Since Fuel Cells work without combustion, they enable a carbon free propulsion which both impacts on carbon based noxious emissions (CO, HC, etc.) and on carbon dioxide ones. In addition to that, Fuel Cells have the potential to be highly efficient especially at low load. Other important features of Fuel Cells are their higher specific energy and energy density compared with Li-ion batteries which are the most performing ones on the market.

Hydrogen is not a primary energy source (such as oil) but an energy carrier (like electricity), which can be obtained from a wide variety of energy sources such as hydrocarbons, renewables and nuclear. For this reason, it is important to remark that that the Fuel Cell propulsion is carbon free from a Tank-to-Wheel point of view, but its global carbon emissions are a function of the way hydrogen is produced and distributed to the vehicles (Well-to-Tank analysis). Hydrogen can be produced from fossil fuels or from water. This second way is much cleaner but unfortunately is more expensive (up to ten times more than fossil fuels).

A more complete view of real emissions is given combining both the upstream and downstream stages (Well-to-Wheel analysis).

Due to the lack of hydrogen distribution and due to the fact that hydrogen refueling infrastructures have still to be constructed, Fuel Cell vehicles could be a long term solution.

Within this context, a consumption and performance modelling of Fuel Cell vehicles can be extremely useful for car manufacturers and car component producers in order to understand the grade of maturity of the technology and to understand if it is convenient to enter the market and in which position. Good modelling results that indicate the convenience of this technology could accelerate its spread into the market, opening a new age of zero emission driving. Consequently, the work carried out in the development of the thesis focuses on the simulation of the performances and fuel consumption of hybrid Fuel Cell vehicles. In particular, various control strategies, which determine how the output power is split between the Fuel Cell stack and the battery, have been tested. In the second part of the thesis, for validation purposes, the simulation model parameters have been set accordingly to those of 2017 Toyota Mirai and the results have been compared with those obtained in reverse engineering tests by the Argonne National Lab (ANL).

2. Fuel Cells

Fuel cells are devices that directly convert the chemical energy of hydrogen and oxygen into electricity, heat and water. It is important to notice that the fuel cells work with the hydrogen and the oxygen coming from outside and for this reason they continue to run as far as the reactants are present. A single cell has two electrodes (the negative one is called anode while the positive one is called cathode) where the reactions take place and an electrolyte which allows ions (often protons which are the positively charged) to move from the anode to the cathode while blocks the passage to the electrons. At the same time, electrons are moving from one electrode to the other through an external circuit and so they produce direct current electricity. If free electrons or other substances could travel through the electrolyte, they would destroy the chemical reaction.

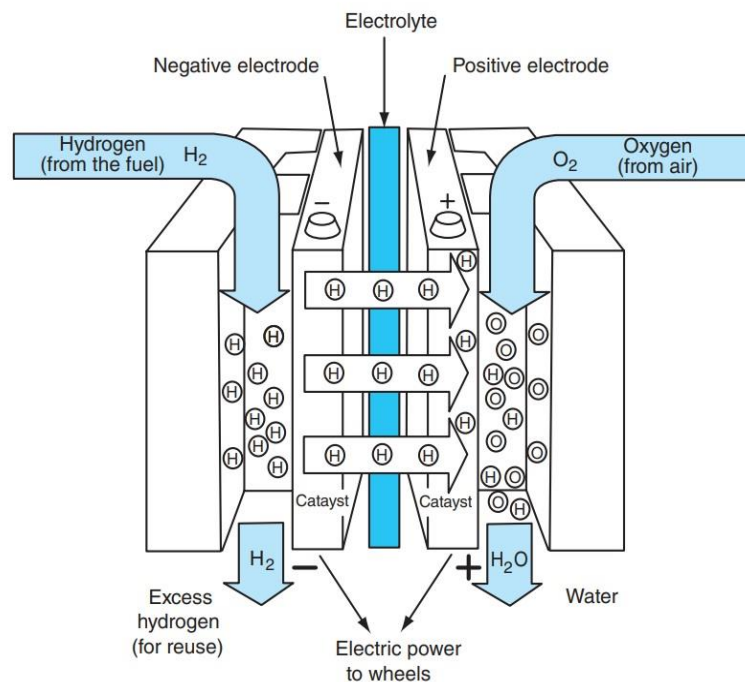


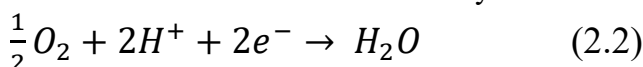
Figure 2.1 – All Fuel cells contain two electrodes and an electrolyte in the middle [1]

The operation of the fuel cell is so based on the following overall reactions, which happen simultaneously at the anode and at the cathode.

At the interface between the ionically conductive electrolyte and the anode:



At the interface between the ionically conductive electrolyte and the cathode:



The electrodes are porous in order to allow the gases to arrive and let the water leave the reaction sites.

It is important to note that these are global reactions and in both cases there are lots of intermediary sequential and parallel steps to reach the final form.

Fuel cells have some interesting and important features:

- Their electrical efficiency is very high (it can arrive to ≈ 0.6) and a lot higher than the efficiency achievable by an internal combustion engine (ICE). Some recent co-generation power plants can reach this value.
- The high efficiency area is wide and the efficiency depends poorly on the plant size (also small scale cells can give good efficiency).
- A wide variety of reactants can be used (hydrogen, methane, methanol, etc...).
- They have high modularity and their environmental impact is limited
- They are able to be used for co-generation (combined generation of heat and power)

If a fuel cell is supplied by its reactant gases but the electrical circuit is kept open, there will be no current and so the potential will be the open circuit voltage (OCV). This value is lower than the theoretical cell potential for given conditions (reactants concentration, temperature, pressure) because there are some losses even if no external current is generated.

Closing the electrical circuit with a load, the potential drops even more as a function of the current generated due to the losses. The polarization curve of a cell represents the relation between the DC voltage at the cell terminals and the current density (current measured per unit membrane area) drawn by the external load.

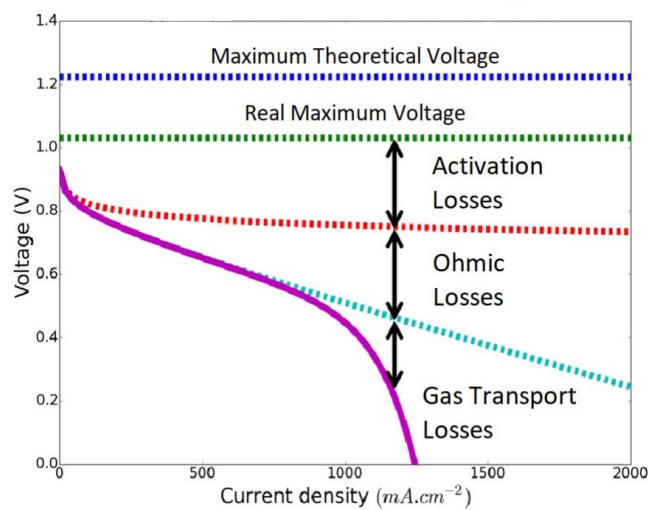


Figure 2.2 – Example of a polarization curve for a PEM cell [2]

The energy conversion efficiency of a cell can be measured as follows:

$$\eta_{conversion} = \frac{V_{at\ a\ given\ current\ density}}{Open\ circuit\ voltage-OCV} \quad (2.3)$$

There can be different types of voltage losses:

- **Activation losses:** they are given by the slowness of the reactions taking place on the surface of the electrodes. To reduce them there are some possible actions: increase the cell temperature, improve the effectiveness of the catalyst, increase the concentration of the reactant or use electrodes with higher roughness.

- **Ohmic losses:** which are given by the resistance of the electrodes material to the flow of the electrons. These losses generally change linearly with the current density.
- **Concentration (gas transport) losses:** are given by the concentration change of the reactant at the surface of the electrodes during the fuel usage. They can be reduced increasing the conductivity of the electrodes, using better materials for the bipolar plates or reducing the thickness of the electrodes.
- **Fuel crossover losses:** they are present because a part of the fuel flow passing through the electrolyte is wasted and due to the fact that a small amount of electrons could pass through the electrolyte. Generally, these losses are a small amount but which can be relevant in cells that operate at low temperatures.

The proportions between the types of losses in a fuel cell are shown in the next figure. Activation losses are the largest for every current density value.

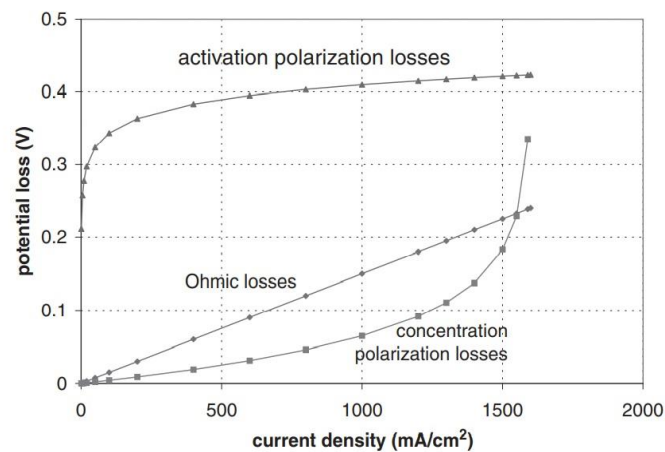


Figure 2.3 – Example of voltage losses in a fuel cell [3]

Since a single fuel cell produces a voltage which is very low ($< 1V$), to provide the power needed by the vehicle many fuel cells are connected in series. This connection forms the fuel cell stack.

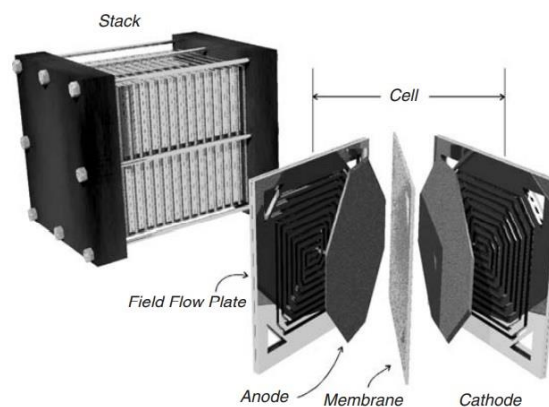


Figure 2.4 – Stack made up of many single cells put in series [4]

For proper working, the fuel cell stack needs some auxiliaries. In fact, the fuel cell system includes all the components needed to operate the stack i.e. fuel supply, air compressor, humidifiers, water pumps, heat management, valves and control systems.

The stack efficiency is represented as follows:

$$\eta_{stack} = \frac{P_{stack}}{m_{H_2} LHV} \quad (2.4)$$

Where:

η_{stack} = efficiency of the stack

P_{stack} = output power of the stack

m_{H_2} = hydrogen feed

LHV = hydrogen lower heating value (used instead of the higher heating value – HHV which includes the heat of vaporization to remain coherent with the automotive industry conventions)

The system efficiency is represented as follows:

$$\eta_{stack} = \frac{P_{stack} - P_{aux}}{m_{H_2} LHV} \quad (2.5)$$

Where:

P_{aux} = power requested by the auxiliaries (parasitic)

In the following figure, some considerations on the efficiencies are done.

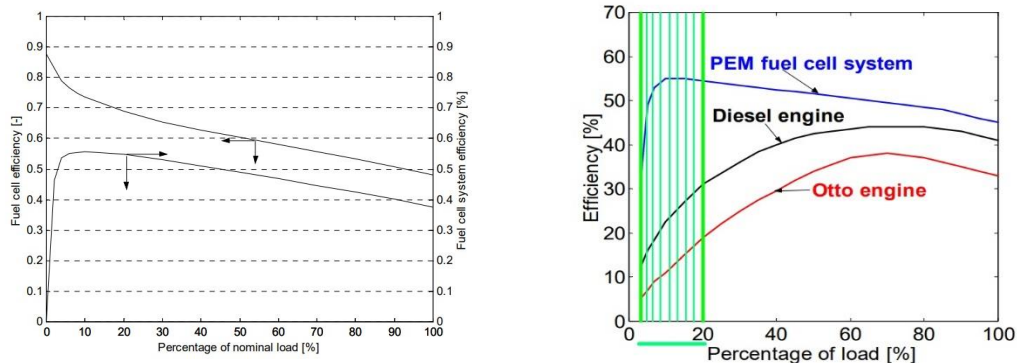


Figure 2.5 – Stack and system efficiency comparison (at the left)/ Fuel cell efficiency compared with that of a diesel engine and a gasoline engine (at the right) [5]

The system efficiency is always lower than the stack one, especially at very low loads. In any case, a fuel cell system has an evident partial load advantage in efficiency respect to diesel and gasoline engines (even direct injection ones).

2.1. Fuel Cell technologies

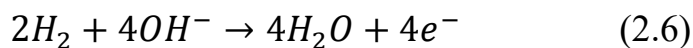
According to the basis of the electrolyte type and operating temperature, there are six major types of fuel cells.

Cell system	Operating temperature (°C)	Electrolyte
PEMFCs	60-100	Solid
AFCs	100	Liquid
PAFCs	60-200	Liquid
MCFCs	500-800	Liquid
SOFCs	1000-1200	Solid
DMFCs	100	Solid

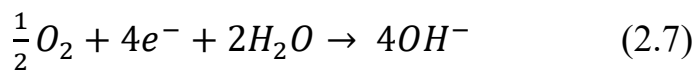
Table 2.1 – Types of fuel cells [6]

2.1.1. Alkaline Fuel Cells (AFC)

These cells use an electrolyte consisting of an alkaline aqueous solution of potassium hydroxide (KOH). For this reason, the ion conduction method is different from the classical PEMFC. The electrolyte carries a hydroxide ion (OH^-). The reactions at the electrodes are:
At the anode:



At the cathode:



It is interesting to observe that at the anode there is water formation while at the cathode there is water request for oxygen reduction. Water management becomes difficult and so sometimes waterproof electrodes are used keeping so the water in the electrolyte. The temperature operating range of these cells is between 80 °C to 230 °C. The efficiencies achievable are very high (≈ 0.7) because of the fast kinetics due to low activation losses especially of the reaction at the cathode. For this reasons they are sometimes used for space missions. Their biggest problem is the susceptibility of the electrolyte to carbon dioxide contamination. Carbonate ions, which do not participate to the reaction and have the risk of obstructing the electrodes reducing the cell performance, are created. For this reason, pure hydrogen and pure oxygen are needed to feed this cell.

Advantages:

- High operating efficiency and low operating temperature
- Catalyst and electrolyte are cheap

Disadvantages:

- At the anode (fuel electrode) water is produced
- Corrosive electrolyte can reduce durability
- Carbon dioxide can poison the electrolyte

2.1.2. Phosphoric Acid Fuel Cells (PAFC)

These cells use an acidic electrolyte for hydrogen ions conduction. Since the freezing point of the phosphoric acid is 42 °C, its temperature must be kept higher than this limit. Continuous freezing and thawing of the acid would stress the stack too much, but on the other side keeping the stack over this temperature requires higher fuel consumption, higher cost, system complexity, bigger volume involved. If the usage is intermittent every time the cell is started some energy is required to heat the cell and this heat is loss every time the cell is switched off. Generally, these cells are used for co-generation and have the advantage of having a big choice of fuels usable.

Advantages:

- Inexpensive electrolyte
- Reasonably small start-up time
- Low operating temperature

Disadvantages:

- Low efficiency
- High cost catalyst (platinum)
- Possible carbon (CO) poisoning

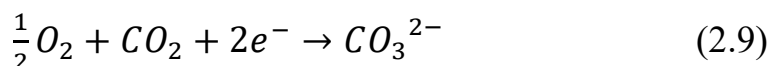
2.1.3. Molten Carbonate Fuel Cells (MCFC)

These cells use molten carbonate salt for ions conduction and work in the range of temperatures between 500 and 800 °C. The electrode reactions change respect to the other types:

At the anode:



At the cathode:



Carbon dioxide must be provided at the cathode, but it can be found recycling it from the anode. These cells can be used with hydrocarbons instead of pure hydrogen, which are a more available fuel. The high temperature allows the decomposition of the hydrocarbons into hydrogen on the electrodes and speeds up the reaction kinetics so much that a cheap catalyst can be used. The reactions are fast and this cell is flexible. The drawbacks are the high temperature needed for usage which could be unsafe and requires fuel for heating and the problem of corrosion on the electrodes. For this reasons usually MCFCs are used in steady applications like ships.

Advantages:

- Can be fueled with hydrocarbons
- Cheap catalyst
- Low sensitivity to poisoning

- High efficiency (fast reactions)

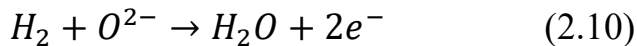
Disadvantages:

- Gradual start-up which requires time
- Corrosive electrolyte
- Small material choice (due to the high temperature working range)
- Slow power response
- Complicated cell system design because of the CO_2 cycling

2.1.4. Solid Oxide Fuel Cells (SOFC)

This name has been given to these cells because their conduction method is similar to the one of semiconductors (solid-state devices). Ions are conducted at very high temperature (1000-1200 °C) in a ceramic membrane.

At the anode:



At the cathode:



The anode (fuel electrode) produces water. Since the operating temperature is high, as in MCFC it is possible to use hydrocarbon fuels. Again because of the temperature range, the activation losses are strongly reduced and the dominant component becomes the ohmic one. Another advantage is that there is no moving part in the electrolyte (auxiliaries excluded). On the contrary, the disadvantages are not only the ones related with the cell temperature (fuel economy and safety) but also due to the fact that that ceramic materials are brittle (which is a strong negative point if vibrations occur frequently). In any case they are normally not used because the system around and the electronics close to the cell require high cost for packaging.

2.1.5. Direct Methanol Fuel Cells (DMFC)

The fuel used for the working of the cell is directly methanol in this case.

There can be different motivations for the usage of this technology:

- Methanol used for vehicle propulsion is easy to store, distribute and sell
- Methanol is simple and cheap to produce on large scale from fossil fuels (coal and natural gas) and can be produced from agricultural products

Platinum is the catalyst for both the anode and the cathode. The anode catalyst can draw hydrogen from the liquid methanol. The main disadvantages of this technology are:

- It is an immature technology
- Respect to direct hydrogen fuel cells they have lower power density, efficiency and their power response is too slow

2.1.6. Proton Exchange Membrane Fuel Cells (PEMFC)

The electrolyte in these cells is a solid polymer membrane made of perfluorosulfonic acid also named as NAFION. Hydrogen positive ions are transported (H^+). The fuels used are pure hydrogen and an oxidant, which can be directly air or oxygen.

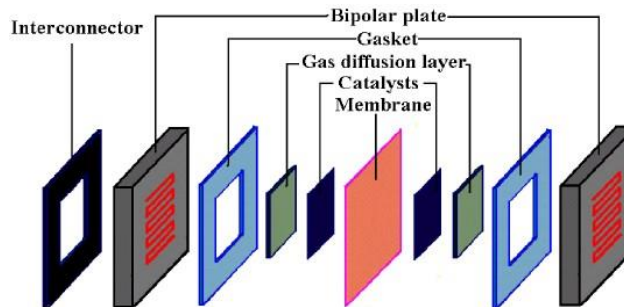


Figure 2.6 – An exploded view of PEMFC components

The bipolar plates distribute uniformly the reactants in the surface (they are forced to travel all the surface) and also distribute cooling fluid through the stack without having cooling fluid and reactant gases mixed. In fact, Plates are larger than the membrane and gaskets (generally Teflon made) are present to avoid gas escape from the perimeter.

A carbon-supported catalyst covers the membrane. To maximize the interface of the catalyst, it is in contact with both the membrane and the diffusion layer. The catalyst made of noble metals is very important and increasing the technology, its loading has been reduced year after year. The catalysts are the electrodes. The cathode is more critical because the reaction of oxygen reduction is more difficult than the reaction of hydrogen oxidation. Water management is important in these cells because for proper operation the membrane must be kept at the correct humidity level (if it is too dry there are not enough acid ions for protons carrying, in the opposite case the pores of the diffusion layer are blocked by water and so the reactants cannot reach the catalyst) [6]. Generally, stacks run an excess of air that would normally dry the cell and solve the problem using external humidifiers to supply water by the anode.

Also poisoning is an important issue in this type of cell. The platinum catalyst has strong performance but as a drawback has a stronger affinity to CO and sulfur products respect to oxygen. This could poison the catalyst and so the reactants cannot reach it. Carbon residuals could reach the fuel cell air from the reformer which feeds hydrogen or from the air stream if it is taken from a polluted atmosphere. As a rule of thumb, less than 10 ppmv of CO must be contained. Poisoning is reversible but has high cost since it requires the individual treatment of each cell.

Other important characteristics are the high power density (which helps in having small size systems while satisfying the power request), the low temperature usage that allows a fast start-up and the low risk of corrosion (the only liquid is water).

Summarizing, the peculiarities of PEM fuel cells are:

- Cheap technology respect to the other cells
- Low operating temperature (70-100 °C)

- Fast response (almost only function of the velocity of introduction of the inputs)
- Functional life more or less of 3000-5000 h
- Resistance to vibrations
- Good safety
- Uses generally air as an oxidant

This solution is the one that is generally used in the automotive field.

2.2. PEM Fuel Cell operating conditions

Since the PEM fuel cells are the most used in the automotive field from now on, the discussion will be focused on this type of cell. Its typical operating conditions are listed in the following table, but they are obviously not rigid boundaries.

Parameter	H_2 /air: Ambient to 400 kPa
Pressure	H_2/O_2 : up to 1200 kPa
Temperature	50 °C to 80 °C
Flow rates	H_2 : 1 to 1.2 O_2 : 1.2 to 1.5 Air: 2 to 2.5
Humidity of reactants	H_2 : 0 to 125% O_2 /air: 0 to 100%

Table 2.2 – Typical operating conditions of PEM fuel cells [3]

2.2.1. Operating pressure

There are two types of reactant gas supply: from a high pressure tank with a downstream valve which regulates the back-pressure or by an upstream mechanical device (compressor or blower). In the first case, the outlet pressure is monitored (even if the inlet pressure is higher because of the pressure drop in the channels of the fuel cell). In the second case, it is the inlet pressure to be important. The compressor must deliver the required flow rate at the required pressure. Backpressure regulator can still be present to avoid the gas leaving at atmospheric pressure (which is variable).

Increasing the operating pressure of the cell, also the voltage increases (proportionally to the logarithm of the pressure ratio) and so the output power. However, as a drawback also the power needed to push the air inside increases and so the problem must be addressed by a whole system point of view. It is to avoid the condition in which the power required by the compressor is higher than the output advantage.

Summarizing, increasing the operating pressure there are the following effects:

- Better stack performance due to the reduced activation and concentration polarization losses
- Lower water requirements for membrane humidification

- Higher power consumption related to the air compressor
- Higher problems in transient management

2.2.2. Operating temperature

Usually a higher temperature gives a higher potential, which gives more power but every cell has its optimal temperature (by design). A fuel cell could work even at temperatures under 0 °C but cannot reach its maximum power. The upper limit is given by the hydration of the membrane. At high temperatures close to 100 °C, it is difficult to keep the membrane hydrated. The temperature (as the pressure) must be chosen through a system perspective considering also the characteristics needed by the heat management subsystem.

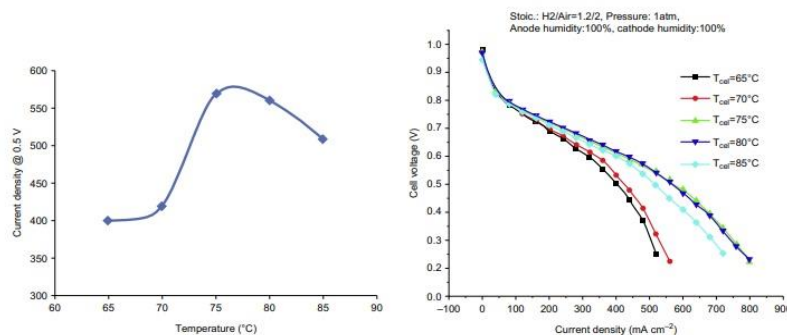


Figure 2.7 – Effect of temperature on the cell performance [3]

Since the temperature inside the cell is not uniform, the temperature that is measured and is approximated to it can be the surface temperature, the temperature of the air leaving the cell or the temperature of the coolant leaving the cell. The precision of the approximations made is a function of the flow rates of air and coolant and of the thermal conductivity of the materials inside the cell.

2.2.3. Reactant flow rates

The mass flow rates of reactants consumed in the cell (g/s) are:

$$m_{H_2} = \frac{i}{2F} M_{H_2} \quad (2.12)$$

Where:

m_{H_2} = hydrogen flow rate

i = current

F = Faraday's constant

M_{H_2} = hydrogen molar mass

$$m_{O_2} = \frac{i}{4F} M_{O_2} \quad (2.13)$$

Where:

m_{O_2} = oxygen flow rate

M_{O_2} = oxygen molar mass

The mass flow rates of water generation in the cell (g/s) is:

$$m_{H_2O} = \frac{i}{2F} M_{H_2O} \quad (2.14)$$

Where:

m_{H_2O} = water flow rate

M_{H_2O} = water molar mass

Gas flow rates can also be expressed in Normal liters per minute (NLpm), which is the gas quantity that would occupy 1 liter of volume at standard normal conditions (101.3 kPa and 0°C). Using the ideal gas law in normal conditions, the molar volume of any gas is 22.414 l/mol. In case of dry air, they correspond to 28.964 g/mol, which are a little less in case of humid air.

The orders of magnitude of the reactants consumption and water generation are shown in the following table:

Measure unit	Hydrogen consumption	Oxygen consumption	Water generation
mol/s	5.18×10^{-6}	2.59×10^{-6}	5.18×10^{-6}
g/s	10.4×10^{-6}	82.9×10^{-6}	93.3×10^{-6}
NLpm	6.970×10^{-6}	3.485×10^{-6}	N/A

Table 2.3 – Orders of magnitude of the consumptions and generation (per Amp and per Cell)

At the inlet, the reactant rate must be equal or higher than their consumption rate inside the cell. The produced water flow is disposed by the excess flow at the cathode. Also at the anode side there can be excess flow. Dead-end mode means to deliver the hydrogen exactly at the rate at which it is consumed, instead if there is excess of hydrogen the mode is called Flow-through. An excess of hydrogen respect to the ideal amount needed to produce that current is needed to compensate the crossover permeation and internal current losses. Excess of hydrogen can also be supplied to avoid having the periodical purging of the cells because of the inert gas or water accumulation. In case of pure hydrogen and/or oxygen the excess of flow needed can be found by recirculation from the exhaust to the inlet through a pump/compressor or a Venturi. The stoichiometric ratio in this case can be higher because the excess flow is re-used. In anycase periodic purging could be needed because of the inert gases accumulated in the electrodes. At low flow rates there will not be enough power while at too high flow rates the hydrogen wasted would be too much and so the efficiency would be too low.

2.2.4. Reactant humidity

As it has been seen in the PEM description part, to maintain the proton conductivity, both the air and the hydrogen must be humidified before entering the cell. Sometimes an excess of humidity is needed only for the hydrogen at the anode and not saturated conditions are

sufficient for the air at the cathode. At the cathode side, the heat needed for humidification is remarkable if air at ambient pressure is to be saturated at high temperatures. Usually the cell generates enough heat and water to humidify the cathode side, but humidification is still used to prevent the membrane part near the air inlet from drying.

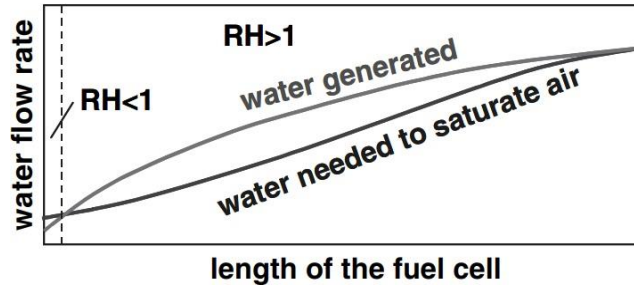


Figure 2.8 – Water profile in the fuel cell

At 20-30 °C small amounts of water are sufficient to reach saturation. At higher temperatures and lower pressures, the water needed would increase. With a well-planned design it is possible to match the water generated and the water needed for saturation. It is important to remark that even if the reactants are saturated at cell temperature, there could be dehydration due to the water drag. Since the cathode allows higher drag module before saturation than the anode does, the humidity excess is generally more important at the anode.

2.3. Fuel Cell auxiliary systems

The conditions required for the stack to work are provided by some auxiliaries, which in turns require power. The main component of this parasitic power is generally the one required by the air compressor.

The fuel cell system is the whole plant made by the stack and its auxiliary circuits needed for proper operation (air, hydrogen, water, cooling etc..).

The main components of the fuel cell system are described by the following picture.

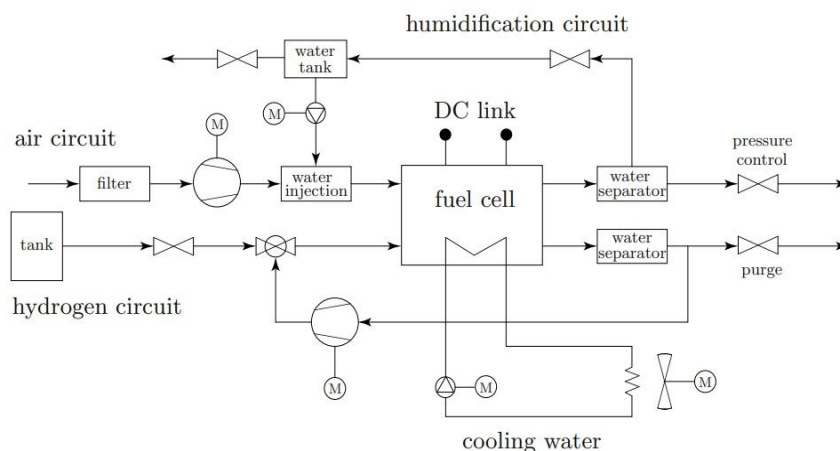


Figure 2.9 – Fuel Cell system [7]



The main components of the system in addition to the stack are:

- Oxidant supply (with air compressor or blower)
- Hydrogen supply (generally there is a hydrogen recirculating pump)
- Water management (for humidification purposes)
- Heat management generally made by a cooling circuit with heat exchangers and a radiator (with coolant circulating pump and ventilation fan)

Depending on the fuel and oxidant used there are different types of systems:

- Hydrogen/Oxygen systems: used when air is not available for example in submarines or space applications
- Reformate/Air systems: they are not treated in this thesis
- Hydrogen/Air systems: they are the most used in the automotive industry and so they are the systems that will be referred to in the following discussion

2.3.1. Oxidant supply system

Oxygen is present in air for 20.95% and its dilution gives a voltage penalty. In addition to that, since it is necessary a device to pump the air inside the cell, this device will reduce the power and the efficiency of the system.

There are two types of air supply:

- For low pressure systems a blower is used
- For high pressure systems (up to 3 bars) an air compressor is used generally in combination with a backpressure valve for regulation (they allow smaller and compact fuel cell stacks even if there is the compressor that requires power)
- For very small systems requiring a small power output natural convection is sufficient

Two types of compressors can be used: positive displacement ones (such as piston, screw or scroll) or centrifugal ones (axial or radial).

In positive displacement ones the air flowrate can be changed only by changing the speed of the motor (without changing backpressure).

Centrifugal compressors must be operated at the right of the surge line and so especially at low flow rates pressure regulation is needed.

Turbo-compressors have higher efficiency than twin-screw compressors especially at low flow rates. Despite of this, screw compressors are more used for fuel cells because it is easier to keep a neutral water balance using this solution.

2.3.2. Hydrogen supply systems

There are two common types of hydrogen supply schemes:

- Dead-end: only with a pressure regulator. To operate this system extremely pure gases are needed
- Closed-loop system: excess of hydrogen is run through a recirculating pump and a humidifier and a hydrogen purge are added. Hydrogen purging may be programmed

as a function of the voltage or as a function of time. This type is the more used in the automotive industry.

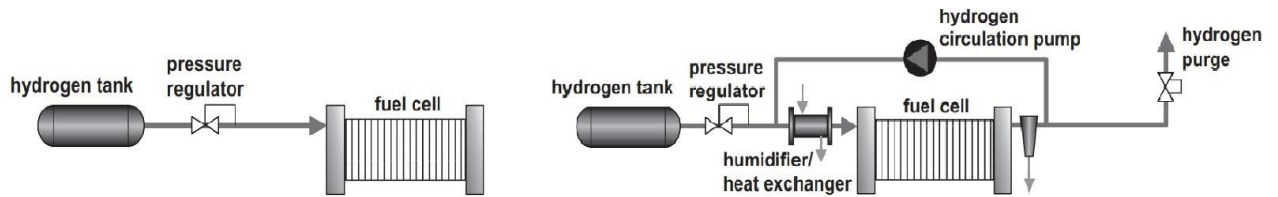


Figure 2.10 – Dead-end at the left and Closed-loop at the right [3]

2.3.3. Water management systems

Hydrogen is humidified to prevent the anode side of the membrane from drying out. Air is humidified to make sure that the excess of air at the entrance region (most critical part) of the cathode does not remove water faster than the rate at which it is created by the reaction. The gases must be maintained close to their saturation level and the drying up of the membrane must be avoided. On the contrary, too much humidity would condensate water and block the flow (it would be impossible for the reactant gases to reach the catalyst if the pores of the diffusion layer are blocked). The correct amount of humidity must be kept.

There are different types of air humidification methods:

- Bubbling air in water: this method gives a large contact area but is difficult to control and so it is used only in LABs
- Direct injection of water/steam: it is a compact and easy solution. A fine mist of water is injected to increase the contact area. Additional heat is needed since water enthalpy alone is generally not enough to humidify the air. This heat can be found in the stack or in the air compressor. Water injection during compression can reduce the temperature and so increase the process efficiency but not all compressors can afford it. In case of steam injection there would not be the problem of additional heat required but the system cannot be used because the stack needs to work at temperatures higher or equal to 100°C
- Use the exhaust water and heat of the cathode side of the fuel cell and exchange them with the inlet air

For automotive systems it is important to have the condensed water equal to the one required for humidification. This makes the fuel cell system autonomous from a water point of view. In fact, components to condense the exhaust gases, and to store and use again the water are present.

2.3.4. Heat management systems

To keep physical stability and constant temperature of the fuel cell stack, a cooling circuit dissipates the heat wasted by the system. This heat can be used for example for the air conditioning system.

Another important point to look is the integration between the water and heat management.

The water that is used to remove the heat from the stack can be then used for humidification purposes. The heat remaining is dissipated to the external ambient through a radiator. Since the PEM stack does not have high operating temperatures, thermal exchange with the ambient is not so effective (small temperature difference) and so heat exchanger dimensions need to be big. It would be more effective a higher temperature difference to reduce the cooling system sizing. This has to be done without penalizing the system in terms of: current density, internal resistances and lifetime. In the operating temperature decision, also operating pressure and water balance must be considered, since the system must work without any external water supply. The water generated by the fuel cell must be the same needed for humidification. At the exit of the stack, there are some liquid/gas separators to gather the exit water and recirculate it to the humidifier. When the amount of water of the separators is not sufficient, the exhaust could be cooled to condense and separate more water.

The water balance of the system is:

$$m_{in} + m_{gen} = m_{out} \quad (2.15)$$

Where:

m_{in} = water entering the system

m_{gen} = water generated by the fuel cell

m_{out} = water leaving the system and entering the separators

This balance depends on the ambient conditions, the operating pressure and temperature and the inlet flowrates of the reactants. All these parameters must be chosen together to have the proper balance.

If the same water is used for cooling and humidification, water and heat management are integrated in a single subsystem and deionized water must be used. Instead, if the system works at freezing temperatures, in order to use anti-freeze coolants the coolant loop and the water system are divided.

In case of a very small stack (of an order of magnitude of less than 2-3 kW) an air cooling can be used trying to increase as much as possible the surface area.

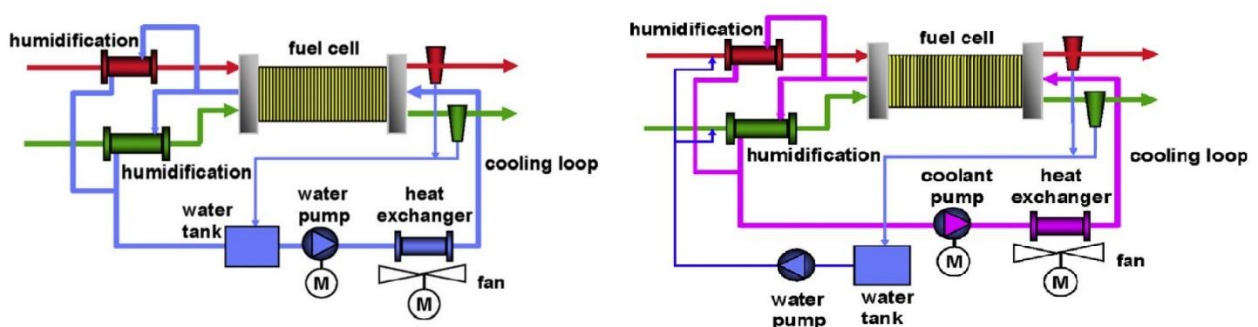


Figure 2.11 – Integrated system at the left and Separated system at the right [3]

In the last years, new thinner membranes have been developed which operate at higher temperatures (90-120 °C) allowing to reduce the cooling radiator dimensions and which don't need reactants humidification due to a well-designed 3D flow field channel geometry.

This is all done without penalizations in terms of maximum current density, internal resistance (which directly affects efficiency) and lifetime.

In this case, the humidification circuit and its components can be skipped and the cooling heat exchangers and radiators mass/volumes are drastically reduced giving more compactness to the system.

2.4. Hydrogen storage

To store on-board hydrogen there are three methods: compressed (gaseous) hydrogen at ambient temperature, liquid hydrogen reducing its temperature (cryogenic) or solid state (metal hydride). Sometimes there could also be some mixed solutions (instead of 700 bar at ambient temperature or $-270\text{ }^{\circ}\text{C}$ at ambient pressure, there could be intermediate values like 80 bars at -80°C). It is important to remark that hydrogen has better gravimetric energy density (MJ/kg) but worse volumetric energy density (MJ/l) than normal fuels such as gasoline, diesel and natural gas.

2.4.1. Compressed Hydrogen

This method consists in pressurizing pure hydrogen in a tank. In the following picture, it is shown the energy per liter of hydrogen and its equivalent liters of gasoline, both represented as a function of pressure and at fixed ambient temperature of $25\text{ }^{\circ}\text{C}$. For every pressure value, the energy of one liter of hydrogen is equivalent to one order of magnitude less of gasoline liters. In addition to that, also the energy for hydrogen compression is to take into account, which is about 25% of the hydrogen energy taking into account the losses of the compressor and electric motor. To store this gaseous hydrogen, polymer liners with a reinforced resistant external shell and a regulator valve are used. Since also the lightness of the tank is important, composite materials such as carbon fiber are used and for this reason it is difficult to predict ageing and the costs of this solution are high. There is also the leakage risk in the tank to take into account and the fact that the explosive range of hydrogen in air is very large (4%–77%) increasing the risks should there be a crash. For a rapid comparison, in liquid gasoline the explosive range is (1%–6%). It must also be taken into account that the autoignition temperature of hydrogen is 571°C while for gasoline it is $220\text{ }^{\circ}\text{C}$. In the case of gasoline before having autoignition there must be vaporization.

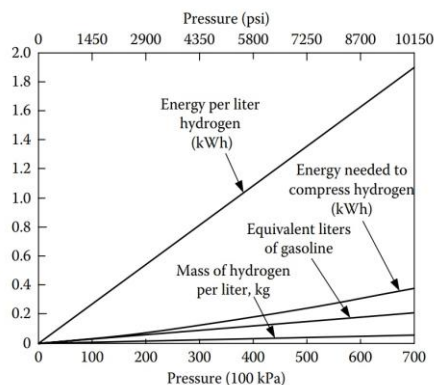


Figure 2.12 – Energy per liter of hydrogen and equivalent liters of gasoline as a function of pressure [6]

2.4.2. Liquid Hydrogen

Another method is to liquefy the hydrogen at low cryogenic temperatures (≈ -270 °C). Liquid hydrogen has low density and this helps to reduce the weight. The tank must be strongly insulated in order to reduce the heat transfer from the ambient to the hydrogen and so prevent the hydrogen from boiling. If boiling occurs, the larger volume of gas will increase the tank pressure and so the tank must be dimensioned in order to have a strength sufficient to withstand some of the excess pressure. A security valve can release the excess pressure to the atmosphere. In this case, some fuel is lost but the pressure is controlled. If there is some boil-off in a closed area, the risk to have some gaseous hydrogen in the explosive range, which would cause an explosion in presence of a spark, is high. In an open atmosphere at ambient temperature, the cryogenic liquid evaporation speed is fast enough to limit or eliminate the risk of explosion.

The advantages of this technology are:

- Low pressure
- High storage density

The disadvantages of this technology are:

- High energy needed for liquefaction
- Evaporative losses

2.4.3. Solid State

Another method is to use the property of some metals or metal alloys to combine with hydrogen forming some stable compounds, which are then decomposed when the pressure and temperature levels allow it. This type of technology has a very strong drawback. Hydrogen must be extracted from a metallic matrix, which for safety issues needs to have high weight. This condition is very bad for cars but is acceptable for a hydrogen station.

2.5. Hydrogen production methods

Hydrogen can be extracted from different substances with a process that breaks its bonds with other elements. It is possible to pull out hydrogen from water, coal, fossil fuels and biomasses. Even if fuel cell vehicles are commonly thought to be zero-emission vehicles, this is not strictly true because also the hydrogen production process must be considered. It is possible so to say that they are zero-emission vehicles from a Tank-to-Wheel point of view but not from a Well-to-Wheel point of view.

Hydrogen production is generally very expensive (much more expensive than it is to produce other fuels used for automotive traction such as gasoline).

The possible hydrogen production pathways are represented in the following picture.

The two main hydrogen production ways are steam reforming and electrolysis.

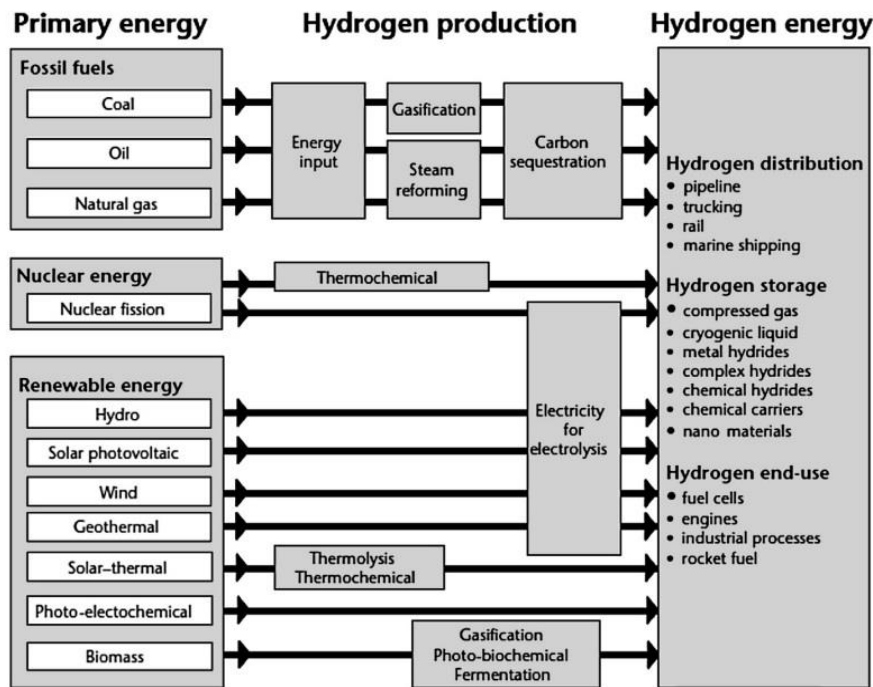


Figure 2.13 – Hydrogen production pathways [8]

2.5.1. Steam reforming

It is the method by which more than 95% of the hydrogen available is produced. Reforming is a chemical process which aim is to pull out hydrogen from hydrocarbons. In order to extract hydrogen from hydrocarbon fuels such as gasoline, methane or methanol, high temperature steam is used. Methane is the hydrocarbon with more simple chemical structure and the most easily available. It can be extracted by oil or natural gas fields and coal beds. Even if this method uses fossil fuels to create hydrogen and generates emissions, it is the most used production way because it is the most convenient in terms of costs.

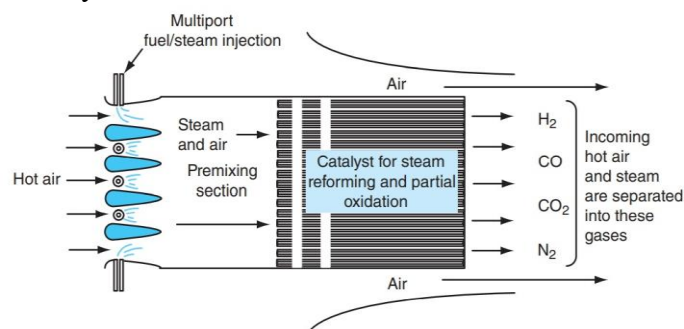


Figure 2.14 – Steam reformer example

Reforming could also be done using solar energy to provide the heat required for the steam reforming and in this case it is called Solar-Thermal reforming.

If instead of transforming gaseous carbonaceous raw materials into hydrogen, solid carbonaceous raw materials are transformed, the process is called gasification instead of reforming. Examples of gasification can be Coal gasification or Biomass (plants or agricultural wastes) gasification.



2.5.2. Electrolysis

It is the cleaner method to produce hydrogen but unfortunately it is the most expensive. Hydrogen production from electrolysis can cost up to 10 times more than the production from steam reforming [1]. Using electricity derived from renewable sources is estimated to cost from 3 to 5 times more than that derived from fossil fuels. For this reason only few percent of total hydrogen world production is obtained this way.

In this process, direct electric current (DC) is given to two electrodes placed in the water. The current is used to decompose water in hydrogen, which is collected at the cathode and oxygen, which is collected at the anode.

Water molecule is very stable, decomposition can start only at very high temperatures, and this requires a lot of energy. To produce hydrogen at lower temperatures, some catalysts for decomposition reaction combined with membranes for effective gas separation have been tested, but these variants are only at early testing stages. If solar light captured through photovoltaic cells is used as electricity to start electrolysis, the method is called Photo Electrolysis. Instead if the properties of hydrogen production of some algae or bacteria during their exposure to light are used it is a Photo Biological process.

3. Vehicles powered by Fuel Cells

Fuel Cell vehicles operating with hydrogen and PEM stack are seen by many people as the solution for the environmental problems in road transportation. In these vehicles, combustion engines are substituted by fuel cells as continuous energy source. To allow regenerative braking, also a battery is needed. This is implemented in a series hybrid layout. Since internal combustion engines have more than a century of development and know how, while PEM fuel cells are a more recent technology, the cost of the latter is higher. Technical challenges to reduce costs of materials and manufacturing must be addressed to reach economic competitiveness. In addition, hydrogen fueling infrastructure diffusion problems must be addressed. Hydrocarbon fuel could be stored in a tank and then be processed in an on-board reformer to be transformed in hydrogen. This method is called the reforming method. Some tests of this technology have been done by General Motors with the Zafira Projects [9].

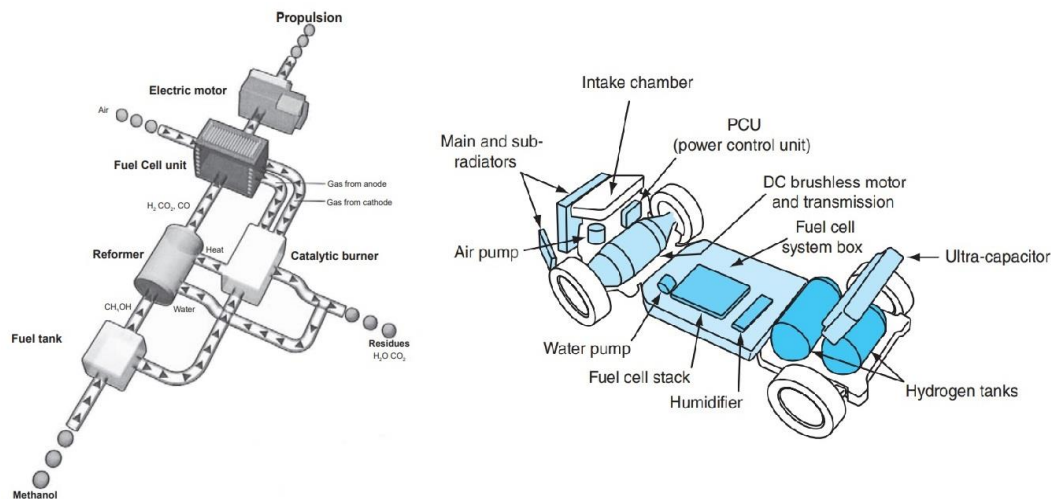


Figure 3.1 – At the left the flow diagram of a reforming prototype of Opel Zafira and at the right the layout of a non-reforming fuel cell powertrain of Honda FCX

Supplying directly the hydrogen needed from an outside source to a pressurized tank inside the vehicle has been found to be an easier solution and that reduces the net output power losses. This method is called the non-reforming method.

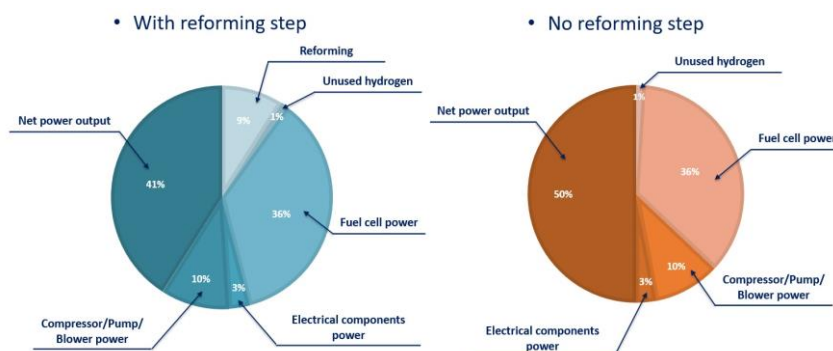


Figure 3.2 – System power distribution with and without reforming step

Since it has been found to be a lot more efficient, the configuration without the reformer is the one which is almost always adopted.

Depending on the layout, different categories of fuel cell systems can be obtained. If when doing a hybridization with an internal combustion engine it is necessary to take into account that the engine has more efficiency at high load, in fuel cells this is not true. The fuel cell has its higher efficiency at low loads.

Fuel cell systems can be divided in pure fuel cell traction systems and simple series hybrids. The series hybrids can be further subdivided as a function of the fuel cell sizing in full power sized, load follower sized and range extender sized.

3.1. Pure Fuel Cell traction system

In this solution, there is only the fuel cell without any other power source (except a little 12 V battery for the car auxiliaries). With this layout, obviously the Fuel Cell system must be sized for the maximum transient power. It is not possible to have regenerative braking since a fuel cell cannot store energy and a battery is not present. The Fuel Cell system must manage the instantaneous dynamics of the system and face the problems of the system warm-up and the vehicle must start up without external sources.

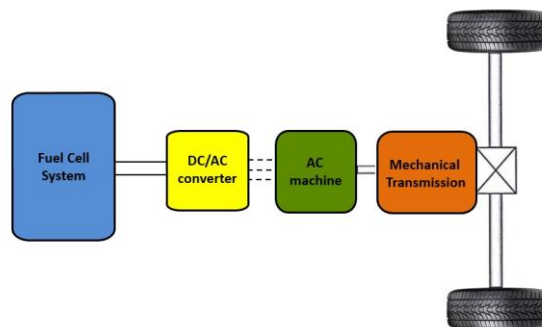


Figure 3.3 – Pure FC traction system

3.2. Series hybrid traction system propulsion

The Fuel Cell system is series coupled (the connection is at the on-board energy source level even if it is done electrically in parallel) with a second energy and/or power electric source which can be:

- A second energy and power source: a traction battery pack
- A second power source (buffer): it can be a power sized battery or a super capacitor pack (which has higher specific power for dynamic assisting but very poor specific energy and so can be used for very small amount time respect to a classical battery used as traction assist). Choosing supercaps instead of batteries make so less effective all the functions asking not only power but also a certain duration.

In the following figure it is shown a scheme which compares the pure FC system with a series hybrid FC system with order 2 and index 1. It is important to remember that the order is the

number of different elementary traction systems present while the index is the number of linking components of the traction system.

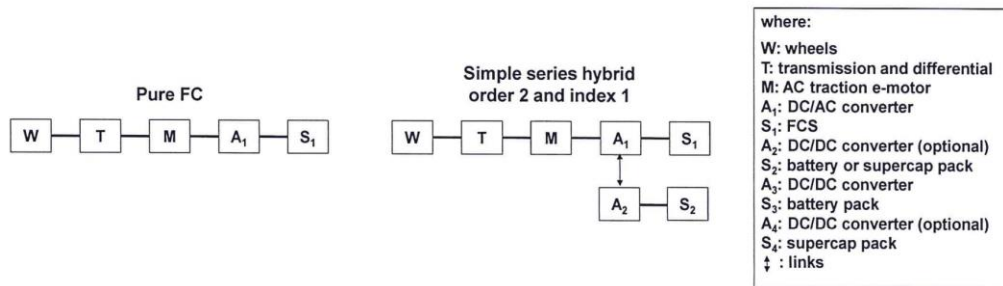


Figure 3.4 – Schematic system comparison [10]

A battery or supercap based hybridization of a pure fuel cell electric traction system has the following advantages:

- Limit the Fuel Cell stack stress in dynamic acceleration conditions
- Enable the ‘classic’ electric regenerative braking
- Simplify the vehicle start-up, transiently supplying the fuel cell system air compressor (at the beginning the FCS voltage and available power are zero)
- Enable energy management strategies to increase the efficiency
- Speed-up the FCS warm-up, supplying in the meantime the traction system

3.2.1. Range extender solution

The goal of hybridization in this case is to increase the original battery electric vehicle range (on the sizing cycle) reducing the volume and weight of the battery pack. Hybridization is realized adding to a battery electric traction system a limited Fuel Cell system (sized for the average power on a defined cycle). The result is a range extender architecture functionally similar to the one realized with an engine and electric generator hybridization unit. In this case since the Fuel Cell system power is lower than the battery pack one, it is better to put the DC/DC converter (monodirectional) on the fuel converter side.

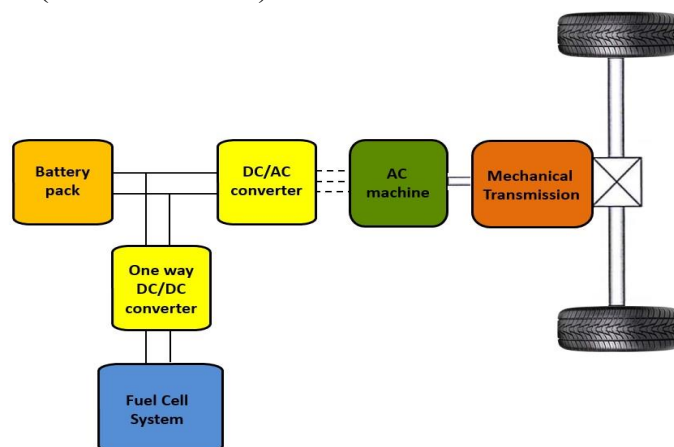


Figure 3.5 – Range extender system

3.2.2. Load follower and Full performance solution

In the load follower case, the Fuel Cell system has to give the maximum continuous power while in the Full performance solution the Fuel Cell system has to give the maximum transient power (which is higher). The second case (in which the installed on-board power is more than the maximum requested one) can be justified by the fact that differently from an internal combustion engine (ICE), the fuel cell system doesn't have the maximum efficiency at the maximum power but at lower loads.

In both cases, the fuel cell system gives a remarkable amount of power and so it is convenient to put the bidirectional DC/DC converter on the buffer side.

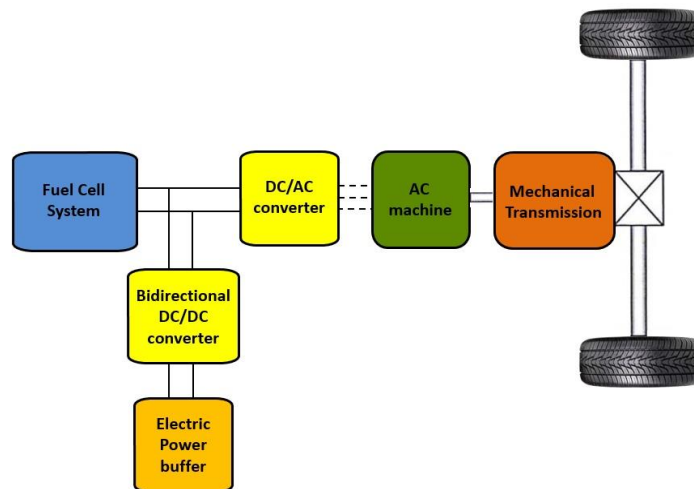


Figure 3.6 – Load follower and Full Performance system

It is important to observe that the coupling between the fuel cell system and the electric power buffer could be realized also through a direct electric parallel connection without the DC/DC converter but with an energy split between the two systems obtained acting on the fuel cell system reactants angulation. This solution at the fuel cell system level is not efficient and the fuel cell system efficiency reduction would be bigger than the benefit coming from the removal of the DC/DC converter.

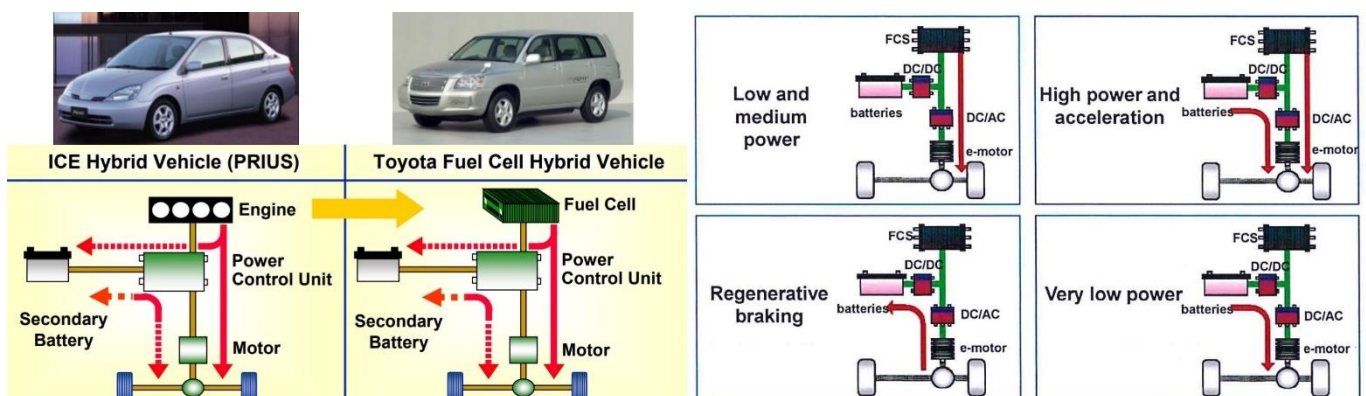


Figure 3.7 – Power path flow comparison between Toyota Prius and Toyota FCHV at the left and Toyota FCHV working strategies at the right

An example of the operating modes in this type of solution is given by the Toyota FCHV working strategies. The power path flows are the same of the old Toyota Prius (2002) which is a hybrid electric vehicle powered by an internal combustion engine and a NiMe battery. Even if the power path flows are the same, the working modes are different because of the different efficiencies of the fuel cell system compared to the internal combustion engine. At very low power only the battery is used. At low and medium power the fuel cell system is used alone. When high power is requested during strong accelerations, the fuel cell system and the battery are used together. The presence of the battery also allows the possibility to have regenerative braking.

3.3. Fuel Cell durability and performance during vehicle usage

The standards in terms of fuel cell stack durability and fuel cell performance have been assessed by the National Renewable Energy Laboratory (NREL) through testing of vehicles provided by the main project partners (General Motors, Honda, Hyundai, Mercedes-Benz, Nissan, and Toyota) [11].

The durability target has been set at 5000h (≈ 150000 miles in conventional driving) with less than 10% loss of performance. The 10 % performance loss is referred to a 10% voltage degradation and it is not an end-life performance. At this degradation level there is more or less 9.73% power loss. At the current state of art, the maximum fleet durability can respect this range while the average fleet durability cannot respect it jet.

For what concerns performance, the target of 65% peak efficiency at 25% rated power for direct hydrogen fuel cell power systems for vehicles has been set. The fleet fuel cell system efficiency at that rated power is 57% and so even if the value is close; to reach the target a lot of improvements must be done.

3.4. Technology comparison

3.4.1. FCEVs vs ICE hybrids vs BEVs

Fuel cell hybrids offer three main advantages respect to hybrid electric vehicles with an internal combustion engine (ICE):

- The fuel cell system alone does not produce carbon emissions such as CO_2 , CO and not even particulate matter or nitrogen oxides.
- The fuel cell system has 30% higher energy efficiency than an internal combustion engine. In fact, even if the specific energy density of hydrogen (142 MJ/kg) is more or less 3 times the specific energy density of gasoline (46 MJ/kg), the km per kg of hydrogen achieved by a fuel cell vehicle are more or less 5 or 6 times higher than those achieved by a standard internal combustion engine. It is also important to take into account the volume limitation. In fact, cylinders in pressure occupy a lot more volume than a gasoline tank and the volume available determines the quantity of hydrogen that can be carried which in turns determines the range obtainable.

- Hydrogen used for propulsion can be produced in various ways some of which exploit renewable energies such as the electrolysis of water, which does not produce carbon emissions.

The hybrid fuel cell vehicle has three main advantages in compared with battery electric vehicles:

- A hydrogen vehicle with full tank full has a longer driving range than a battery electric vehicle considering the actual battery technology.
- Refueling for fuel cell vehicles is very fast (5-10 min) while battery recharging is quite long (1h -1 day as a function of the vehicle needed range and of the charging technology).
- Fuel cell can be warmed up faster than a battery in cold weather conditions and so can reach full power faster.

The main disadvantages of fuel cell vehicles are their high cost due to the small production units, the lack of refueling infrastructures (present only in California), the poor volumetric energy density of the hydrogen storage system and the inadequate life of the stack.

An interesting work of comparison between hydrogen systems and batteries has been done by C.E. (Sandy) Thomas [11]. The useful specific energy and useful energy density of different types of battery have been compared with those of a PEM fuel cell system, which includes the hydrogen storage tanks and the buffer batteries used to capture regenerative braking and boost power on the Fuel cell electric vehicle.

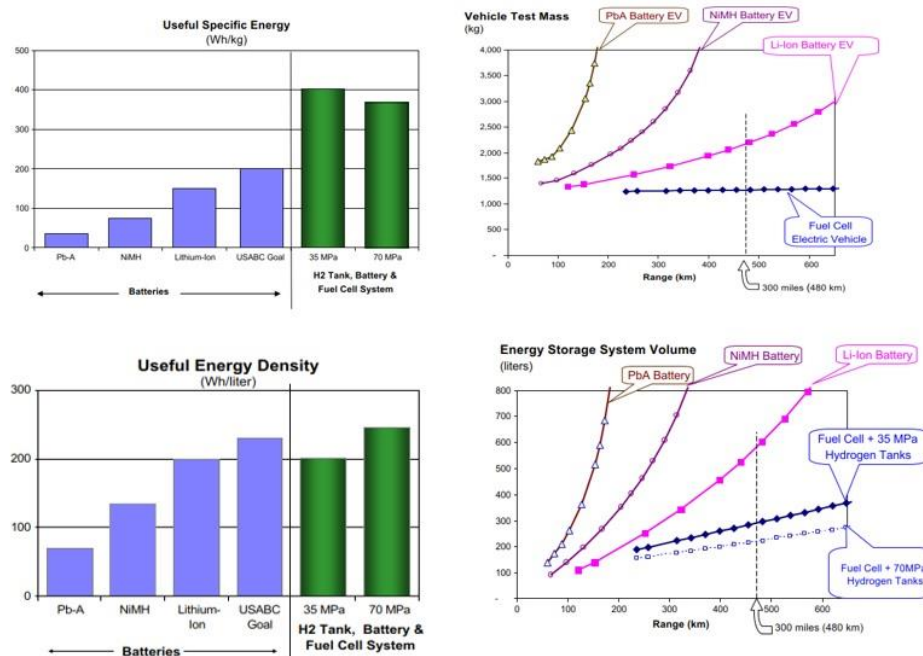


Figure 3.8 – Batteries vs Fuel Cells: specific energy and energy density comparison

The energy plotted is the useful one delivered to the vehicle motor controller. For the fuel cell vehicle, it is the electrical energy at the output of the fuel cell system while for the battery electric vehicle it is the energy delivered to the motor (not the whole energy stored



in the battery). The results found out suggest that Fuel cell hybrids could be also used efficiently in buses, naval applications and industrial vehicles.

In fact, in the case of buses, hybrid electric ones are becoming an interesting idea respect to the ones powered only by a battery because of some important reasons:

- Large batteries needed by pure-battery buses are very expensive
- Having only a battery as a source of power gives a strong range limitation
- During all the recharging time, the pure-battery bus can't be used

Since hybrid electric buses powered also by an internal combustion engine are not zero-emission vehicles, they cannot fulfill the need of having a totally clean vehicle without the range limitations of the pure-battery design. These specifications can be met by fuel cell buses. The high cost of fuel cell vehicles is reduced by subsidies and by the fact that they are bought by state public bodies and not by privates. The wide space and roof area allow a comfortable disposition of the fuel cell stack and of the storage cylinders.

Since the routes driven are the same and known in advance, the refueling network in this case can be more standardized and less widespread than the network needed for private use fuel cell cars. Urban transport can be an important opportunity for the diffusion of fuel cells. A first step if the cost of fuel cells is still high and the hydrogen infrastructure remains weak may be to use battery dominant buses with fuel cells acting as a range extender [8].

3.4.2. Trends and perspectives for future development

The main points to be highlighted for the diffusion of fuel cell vehicles are:

- The cost, efficiency and lifetime of the stack. It is important to remember that the catalyst and the membrane represent more than 80% of the stack cost.
- For what concerns the fuel cell system and the fuel cell auxiliaries it is important to improve the efficiency, the cost competitiveness, the integration level and the possibility to park the vehicle even at very low temperatures (-20 °C).
- The capacity and safety of the hydrogen on-board storage. Also the weight in case of solid storage (metal hydrides), the volume in case of gaseous storage and the cost in case of liquid storage.
- The planning of the hydrogen distribution infrastructure. The choice of which type of infrastructure (if centralized or distributed), and its availability, diffusion times and costs. The techno-economical barriers from this point of view are the high capital cost of pipelines, the high cost of compression and liquefaction, the presence of leakages in the pipelines and of hydrogen embrittlement.
- Standardization for what concerns both the connectors for refueling and the test procedures (vehicle and components point of view).

With current technology, the production of some well working hydrogen driven prototypes is very easy but the passage to mass producible cars at an acceptable price is still in progress. The main issue from this point of view could be the difficulties in updating the grids and infrastructures.



The diffusion of these type of vehicles could be seen as a typical chicken and egg problem: 'I would make a product if there were a market' contraposed to 'a market could exist if there were a product'. In the case of hybrid electric vehicles, Toyota broke the loop reducing the prices to the equivalent of the diesel engine version of the same car. In order to brake the loop there are two possible approaches:

- The top-down approach: consists in adding a high complexity from the beginning of the diffusion in order to satisfy from the beginning all the end-user needs at the same time.
- The bottom-up approach: consists in adding the minimum possible complexity level at the beginning to satisfy, at least partially, the needs and to have the less possible impact on the production extra cost.

For any approach chosen, after a certain period of time, the car maker must make profits.

4. Advisor

Advisor (also called Advanced Vehicle Simulator) is an analysis model written in the MATLAB/Simulink environment and developed by the U.S. Department of Energy (DOE) in collaboration with the National Renewable Energy Laboratory (NREL) in November 1994, which allows the simulation of various types of vehicles.



Figure 4.1 – Advisor home screen

Its main advantage is the high flexibility in component and vehicle configuration modelling which is commonly used for the evaluation of performance (fuel economy and emissions) of vehicles that use new and alternative technologies. In hybrid systems, the most common applications of this program are the evaluation of the effect of single part improvements in the total system, the derivation of the performance requirements for the vehicle subsystems and the optimization of the vehicle system. The main features and user interfaces of this simulation model are well described by T. Markel [12] and P.K. Prathiba [13]. The analysis of fuel cell vehicles using this software is instead described by A. Turkmen [14].

Advisor's first public release was in September 1998 and since then the public users grew exponentially. The users are generally industry members, academia members or government entities. The big user community provided many feedbacks for the modelling improvement and for the component data knowledge. Large community combined with the high possibility of customization of the simulations gives high potential to this tool.

In 2005, the license of the program was transferred to AVL powertrain limited, which then developed its own software called AVL Cruise.

4.1. Advisor structure

Three graphical user interface (GUI) steps for the user during the simulation are present: vehicle input window, simulation setup window and results window.

The user interface has the goal of choosing the vehicle parameters and drive cycles and to evaluate their impact on the global vehicle performance. The connection of the components of the vehicle is described through Simulink block diagrams, which read the input data from the

MATLAB workspace and then gives the output results again to the workspace. The input data and the outputs are viewed by the GUI, which interacts with the workspace.

In the first window, the user can ‘build’ the vehicle to simulate considering various configurations and components through the menus. It is possible to change the size of the components, their performance maps are showed and any scalar parameter can be changed.

In the simulation setup window the various drive cycle parameters over which it is possible to test the vehicle are chosen. Single and repeated cycle possibility is present and it is also possible to implement acceleration and grade tests. Speed trace of the cycle and a statistical analysis of it is present.

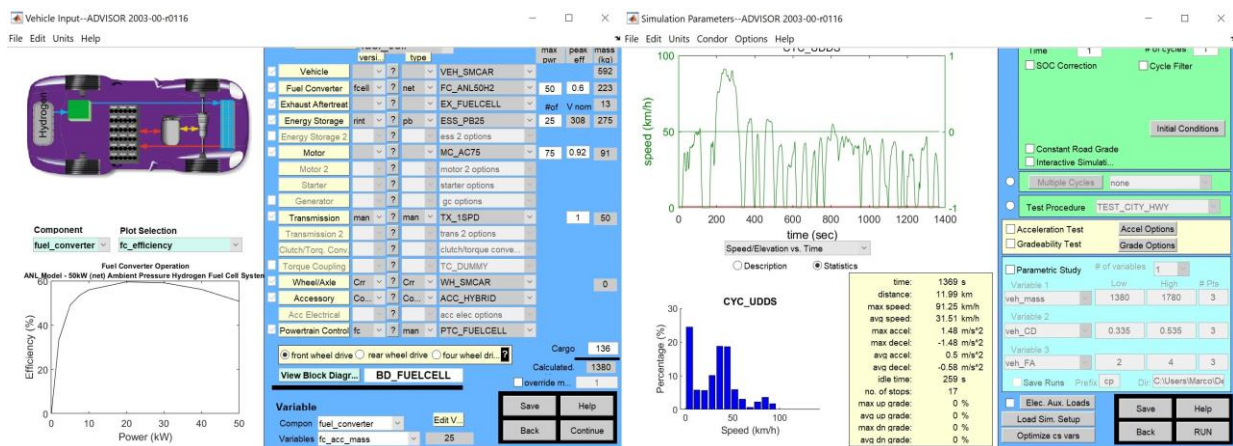


Figure 4.2 – Vehicle input window at the left and Simulation setup window at the right

In the results window, performance, fuel consumption, emissions and state of charge history are shown. The outputs viewed are also editable and so can be changed as a function of the investigated parameters and tests to make. Both overall values and instantaneous values of the parameters can be chosen.

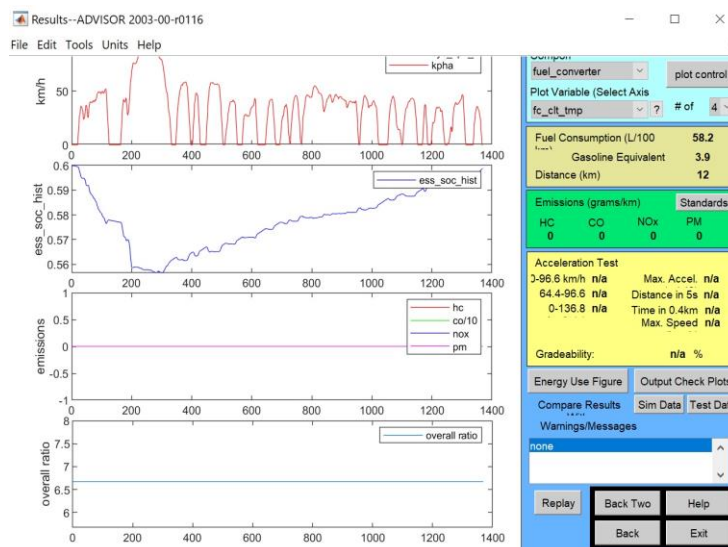


Figure 4.3 – Results window



4.2. Advisor approach

Vehicle simulators can have different simulation approaches.

4.2.1. Backward approach

The backward-facing approach determines the power demand due to the imposed cycle and transmits it to the various vehicle components, with the advantage of taking into account the actual power needs and not requiring any driver model. The calculation of the maximum vehicle performance is therefore carried out without iterations that take into account the actual power availability. The convenience of this approach is that if the testing is done in a laboratory, efficiency versus torque and speed maps can generally be made and this allows doing more straightforward calculations starting from the maps and simple integration methods (as the Euler method) can be used. Since this approach implies assuming that the speed profile is respected, it is not optimal for simulating best-effort performances (the requests could be higher than the powertrain capabilities). Efficiency maps are generally built up through steady state testing and so generally the dynamic effects are not included in the maps.

4.2.2. Forward approach

The forward-facing approach calculates the achievable performance of the vehicle based on its actual power availability, thus being intrinsically more faithful to its real potential. This approach requires a series of iterations to take into account the actual usability for traction of the power delivered by the propulsion system, and a model, even if simplified, of driver, who gives the system its commands. This approach is good for hardware development and vehicle controller testing since it deals with quantities that are measurable in a real drivetrain. Also dynamic models are easily added to this approach and maximum effort events are easily simulated as wide open throttle conditions. High order integrations with small time steps are needed for these types of calculations which require high computational efforts which are too much especially for preliminary design studies.

4.2.3. Advisor approach

The Advisor approach combines the backward and forward approach in almost all the blocks. The demand for power deriving from the cycle of guide imposed is transmitted through the chain of propulsion, but the power that every block demands to the previous element is never greater than the one it is able to manage. In the case a component of the system has caught up its own limit of performance, the intervention of the component "in ahead" of the simulation limits to such value its distribution of power. This can be seen easily in the block diagram where every top input of a component block represents a request from the previous component and the bottom input represents what the upstream component can achieve. Generally, the requested value and the achievable value are the same unless a performance limit of a component has been faced. Advisor can be considered so a backward simulation with the possibility to calculate in parallel the wide-open throttle conditions

without iterations needed. A big limitation of this model is that the component modelling is quasi-static (a succession of equilibrium states) and so can't be used for the prediction of phenomena with small time scales such as vibrations, fast dynamics and electric field oscillations. For these analysis other tools must be integrated (for example Saber for electrical systems and ADAMS/Car for vehicle dynamics).

4.3. Fuel Cell hybrid electric vehicle modelling in Advisor

In hybrid fuel cell electric vehicles, a fuel storage system, a fuel cell stack, an energy storage device (battery or supercapacitor) to allow regenerative braking, a power-processing unit and an electric motor to transmit the power to the wheels are present. Generally, in hybrid systems, the fuel cell supplies the base power needed for driving while the battery supplies the power assist needed for accelerations and high load operation. Every component is modelled through a simplified description which considers its most important parameters. The vehicle is represented through its load parameters and longitudinal dynamics. The motor is described through a torque-speed map with efficiency curves. The battery is modelled through its main parameters such as the state of charge, the capacity, the voltage and the internal resistance. The whole system is considered for the Fuel Cell. The entire fuel cell system is picked as a single element function of the net power output of the system and so the complexity of the system is not taken into account. Just a system map that takes into account of every aspect without entering in the details about the system auxiliaries is given. In the following picture, the fuel cell vehicle block diagram is shown.

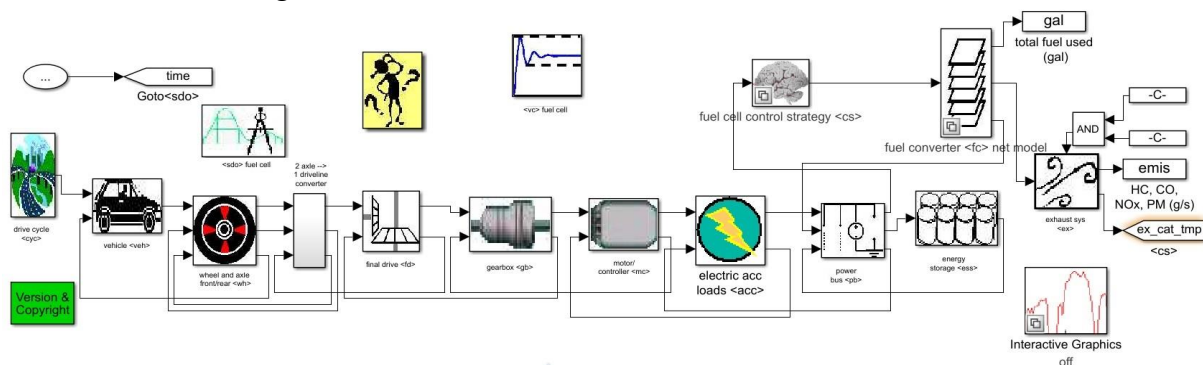


Figure 4.4 – Advisor Fuel cell hybrid electric vehicle block diagram

It is interesting to notice that the ‘Advisor approach’ is respected and so every top input of a component block represents a request from the previous component and the bottom input represents what the upstream component can achieve. An overall system explanation of all the blocks is given in the following picture.

For what concerns single blocks deep explanation, the vehicle block (which has the longitudinal dynamic implemented) and the fuel cell control strategy blocks will be explained.

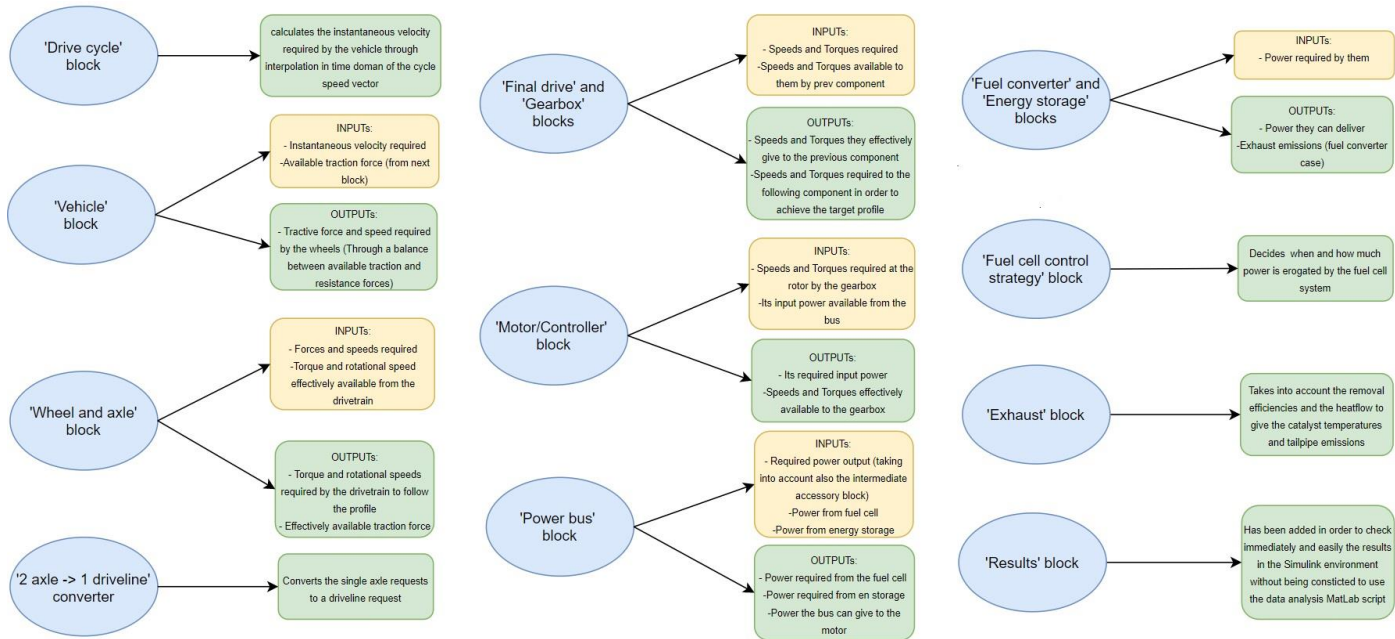


Figure 4.5 – Block Diagram explanation (overall view)

4.3.1. Vehicle (longitudinal dynamics) block

The 'Vehicle' block receives as upper input from the 'Drive Cycle' block the information about the instantaneous speed required by the drive cycle at the end of the single time step. As lower input, the 'Vehicle' block receives from the following 'Wheel and Axle' block the information about the available traction force and the speed actually reachable. The block expresses the balance of the traction force and the resistant forces (rolling resistance, aerodynamic resistance, resistance due to inertia, resistance due to the possible slope), each calculated for the average speed value between the one required at the end of the time step and the one reached at the end of the previous step.

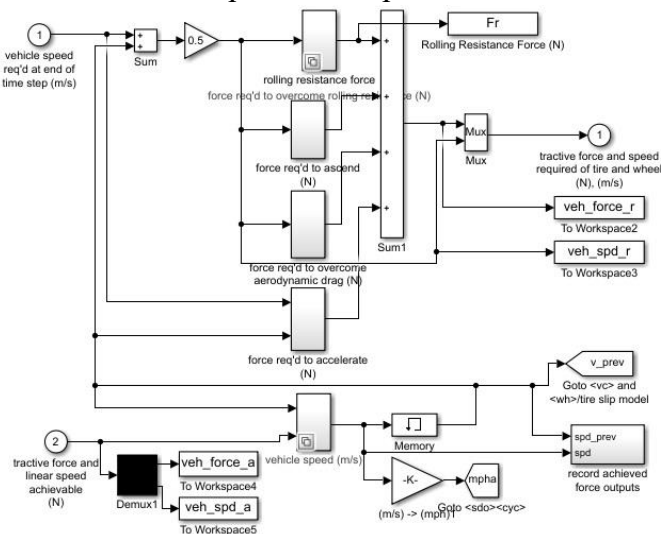


Figure 4.6 – Vehicle block diagram

The equation that represents the force balance is represented as follows:

$$\begin{aligned}
 F_{traction} &= F_{rolling} + F_{aero} + F_{inertia} + F_{slope} \\
 &= mg\cos\alpha(f_0 + f_1v) + 0.5c_x\rho Av^2 + ma + mg\sin(\alpha) \quad (4.1)
 \end{aligned}$$

The forces are reduced to the single material point with which the vehicle is schematized. The tractive force and speed that must be required of the propulsion system to meet the imposed drive cycle is thus calculated, and the same equation is used to calculate the attainable speed for a given available tractive force. If these demands are not met by some element in the propulsion chain, the calculation of the attainable speed is done based on the available power and speed.

4.3.2. Fuel Cell control strategy block

The fuel cell control strategy block is mainly based on the ‘FC on’ sub block. This sub block gets in input the bus-required power, the FC power command, the SoC and the difference between the maximum battery power and the requested one. On the basis of the SoC limits, of the type of the battery discharge (charge depleting or sustaining) and of the Fuel Converter power limits, determines when the Fuel Converter is activated and when not.

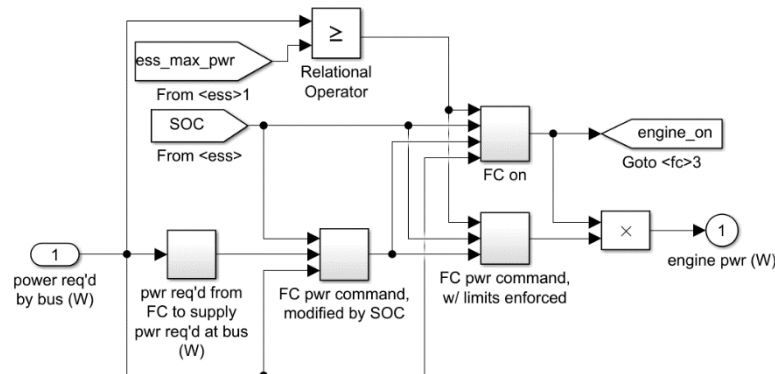


Figure 4.7 – Fuel Cell control strategy block

4.3.3. Fuel Cell KTH model

In order to consider in a detailed way all the fuel cell system and in particular to consider the thermal balance and the auxiliaries power loss, Kristina Haraldsson [5] of the KTH institute has developed a more advanced fuel cell block which can be added to the Advisor folders.

The model has the following procedure:

1. The stack power output is set to the chosen value. The current density to achieve the fuel cell power is calculated iteratively as a function of the initial value of the cell voltage
2. Number of cells needed is calculated from the current density at fixed cell area
3. Then are calculated:
 - The anode and cathode flows

- The heat developed in the stack and in the condensers and cooling circuit components
- Water management system specifications
- Auxiliary system power requirements
- Fuel cell system electric efficiency

Inputs of the model

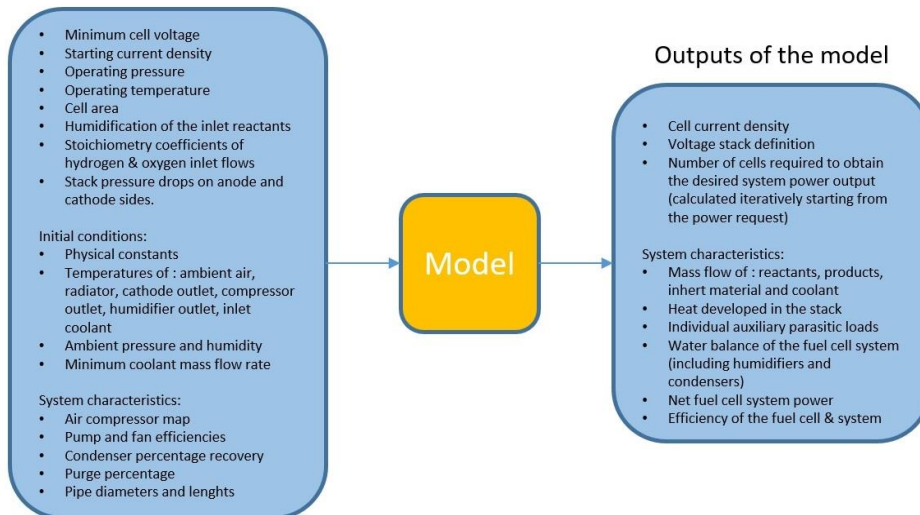


Figure 4.8 – Global overview of the fuel cell KTH model

The whole fuel cell system is considered. As it has been discussed in the previous chapters, some auxiliary systems are needed for the working of the stack. Some water is required to maintain proton conductivity and avoid the drying due to electroosmotic drag (especially of the membrane part near the inlet). For this reason, humidifiers on both the anode and cathode side are added. Hydrogen excess respect to that necessary for the ideal reactions is given in input through a recirculation system. The water generated by the cell and collected inside the condensers (modelled as evapcoolers) must be equal to the one needed for humidification and is so recirculated by a pump. A cooling system is present in order to keep the cell at the most efficient working temperature and release the thermal loads.

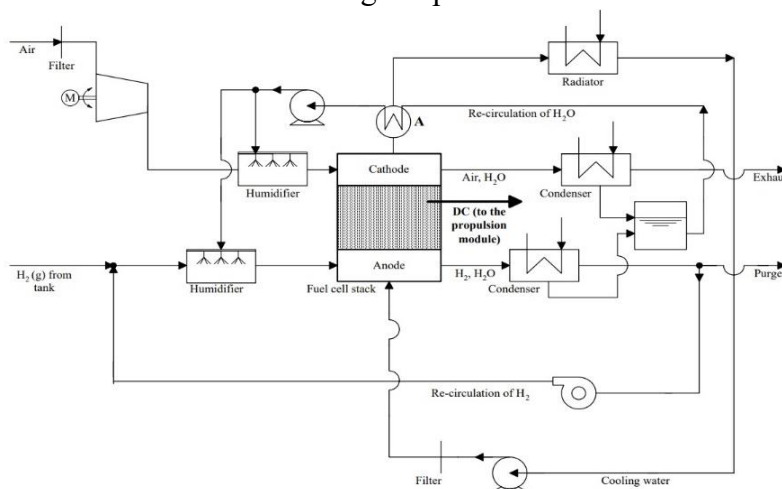


Figure 4.9 – Fuel cell KTH system scheme

The final goal is to evaluate the global efficiency of the fuel cell system which equation has been already described (2.5). The unknown to evaluate is the parasitic power of the auxiliaries P_{aux} .

$$\begin{aligned}
 P_{aux} &= P_{air\ compressor} + P_{cooling} + P_{for\ humidifiers} + P_{H2\ recirc} \\
 &= P_{air\ compressor} + P_{radiator\ fan} + P_{cooling\ pump} + \\
 &\quad + P_{pump\ of\ water\ recirc\ (for\ both\ anode\ and\ cathode)} + P_{H2\ recirc\ pump} \quad (4.2)
 \end{aligned}$$

The power loss due to the air compressor is calculated with the component map having as input the air flowrate and as output the power. In the next figure, the map of the Opcon autorotor 1050 compressor that is the one used by the KTH model is shown.

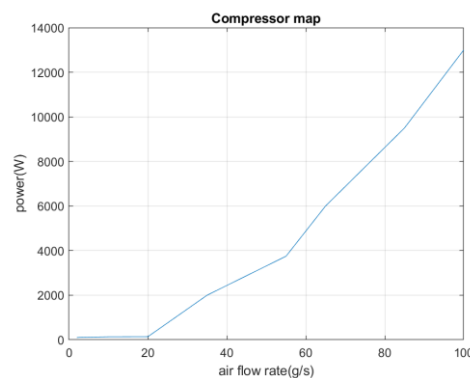


Figure 4.10 – Opcon autorotor 1050 compressor map

All the other components powers are calculated with the Bernoulli formula imposing the diameters of the ducts, the pressure differences and piezometric differences and finding the velocity with the inverse function from the inlet flowrate (which is given). The Reynolds number is calculated to know which formula to use for the friction coefficient f (different in case of turbulent or laminar flow).

$$P_{component} = \frac{\dot{m} \left[\frac{\Delta p}{\rho} + g\Delta z + \Sigma f v^2 \right]}{\eta_{component}} \quad (4.3)$$

5. Hybrid Fuel Cell vehicles control strategies

Hybrid vehicles offer great potential as an alternative to conventional vehicles because of the advantages they offer. Being equipped with an electric energy source and a thermal energy source capable of ensuring the propulsion of the vehicle, their operation can be optimized by exploiting them appropriately in various driving conditions. In parallel with the technical development of hybrid vehicles, arises the need to determine a procedure that allows to properly coordinate the powertrain components, since their inappropriate management would lead to clear penalties in terms of fuel consumption and efficiency. These procedures are called control strategies for hybrid vehicles. Lots of studies and publications have been done in the recent years relative to this topic. For what concerns general electric hybrid vehicles an important work has been done by Michele Zoppello [15], while for works more focused on fuel cell hybrids it can be noticed what has been done by Michael Karpinski-Leydier [16] and by R. Cipollone [17]. Therefore, a control strategy is defined as an ordered sequence of operations (both control and implementation) designed to regulate the operation of the various components of the drive train. In fuel cell hybrid vehicles the control strategy must control the power flow between the fuel cell system, the electric power buffer and the drivetrain.

The following conditions should be met:

- The power demand of the vehicle is always met by the electric motor
- The energy level in the electric power buffer must be kept in its optimal region
- The fuel cell system is operated in its best efficiency zone

These concepts can be expressed in an analytical way as follows. The vehicle propulsive power is equal to the road power P_{road} , which is calculated in the following equation:

$$P_{road} = (F_{inertia} + F_{rolling} + F_{aero})V \quad (5.1)$$

The energy given by the fuel cell to the traction motor $E_{FC,trac}$ is:

$$E_{FC,trac} = \int_0^{end\ cycle} \frac{P}{\bar{\eta}_{motor}} dt \quad \text{with} \begin{cases} P = P_{FC} & \text{if } P_{road} > P_{FC} \\ P = P_{road} & \text{elsewhere} \end{cases} \quad (5.2)$$

This expresses the fact that the optimal fuel cell power should fulfill the request of the traction motor. When this is not possible, the energy difference should be given by the battery $E_{B,trac}$:

$$E_{B,trac} = \int_0^{end\ cycle} \frac{P_{road} - P_{FC}}{\bar{\eta}_{motor}\bar{\eta}_{B,discharge}} dt \quad (5.3)$$

The extra energy (respect to the one needed for traction) given by the fuel cell can be accumulated inside the battery $E_{FC,B}$:

$$E_{FC,B} = \left(\int_0^{end\ cycle} P_{FC} dt - E_{FC,trac} \right) \bar{\eta}_{B,charge} \quad (5.4)$$

To run the cycle using the fuel cell energy, $E_{FC,B}$ must be equal or higher than $E_{B,trac}$ and for this reason $E_{FC,B}$ is also the minimum battery capacity to run the cycle.

For real capacity dimensioning it is important to consider the lower battery state of charge limit and the fact that a higher distance in full electric must be considered and so some oversizing coefficients respect to the minimum capacity value are used.

An element of distinction between the control strategies is represented by the knowledge of the future driving situation of the vehicle. From this perspective, in fact, it is possible to distinguish between:

- Rule-based control strategies
- Strategies that allow to determine an optimal solution to the problem of consumption minimization

Rule-based strategies determine the power distribution among the powertrain components by using heuristic relations and therefore do not require prior knowledge of the driving profile. Their advantage is that they are quite intuitive and simple to implement, while their disadvantage is the difficulty in controlling the threshold values of some parameters.

The strategies for optimal control determine the distribution of power between the components of the powertrain of the vehicle that moves along a predetermined path through a process of mathematical optimization aimed at minimizing energy consumption of the vehicle. These strategies require a priori knowledge of the driving profile and therefore can be effectively implemented for example in public transport where the routes are pre-determined.

In this thesis, five rule-based control strategies and one energy minimization control strategy are investigated. The rule-based ones are the thermostat control strategy, the range-extender control strategy, the mode based control strategy, the constant fuel cell output control strategy and the strong load following control strategy. The energy minimization one is called adaptive control strategy.

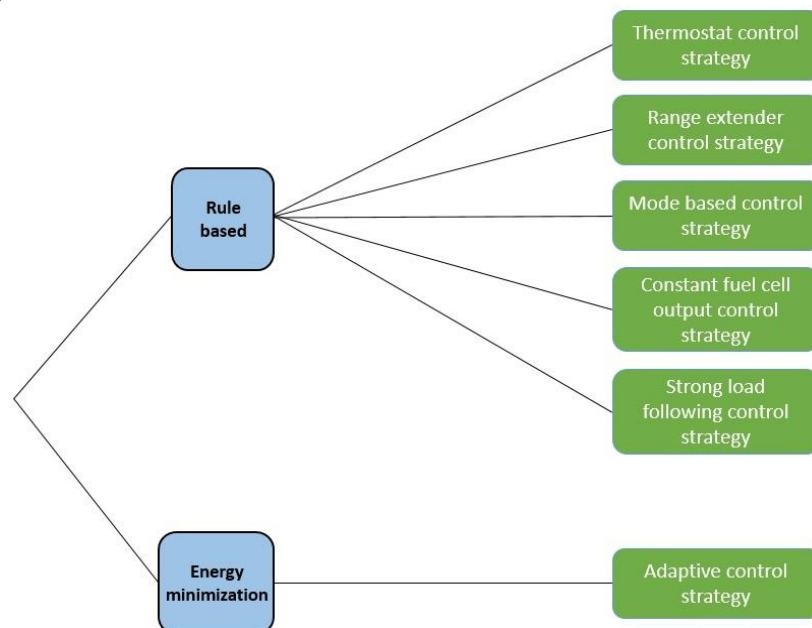


Figure 5.1 – Control strategies investigated

These control strategies have been tested in five driving cycles: three low load cycles (the Federal Test Procedure – FTP, the New European Driving Cycle – NEDC, the Urban Dynamometer Driving Schedule – UDDS) and two high load cycles (the Supplemental Federal Test Procedure – US06 and the Worldwide harmonized Light-Duty vehicles Test Procedure – WLTP). The characteristics of these cycles are shown as follows.

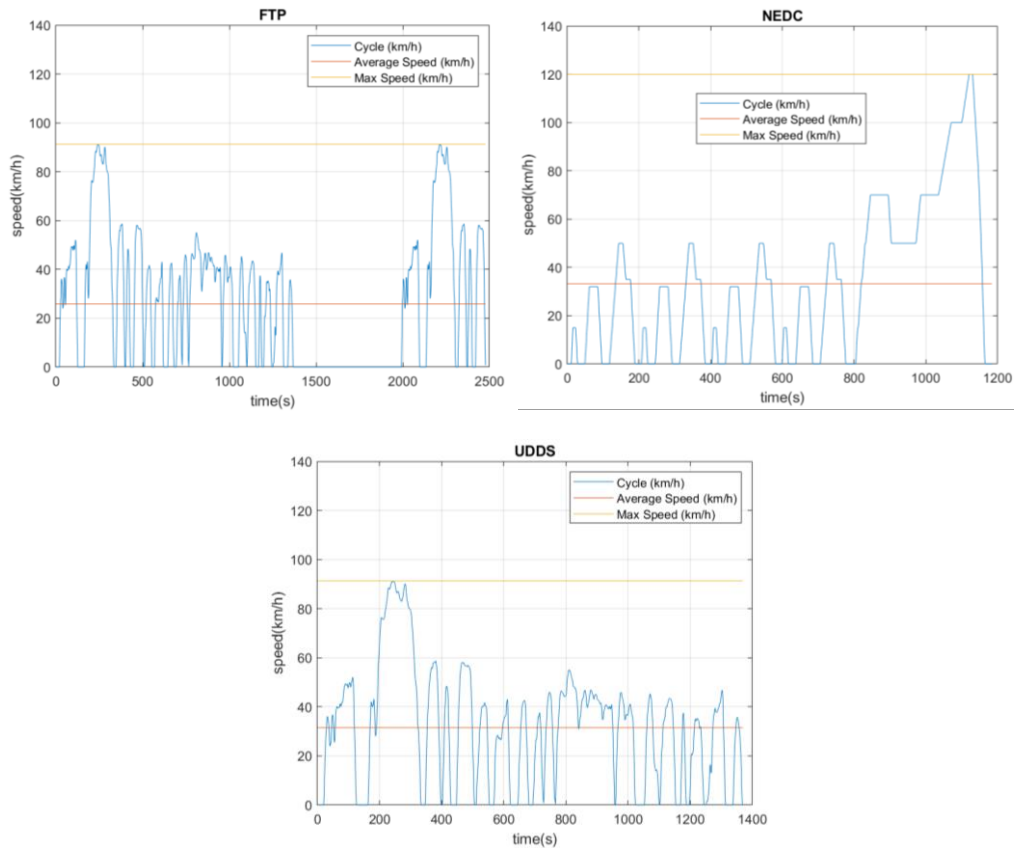


Figure 5.2 – Low load cycles

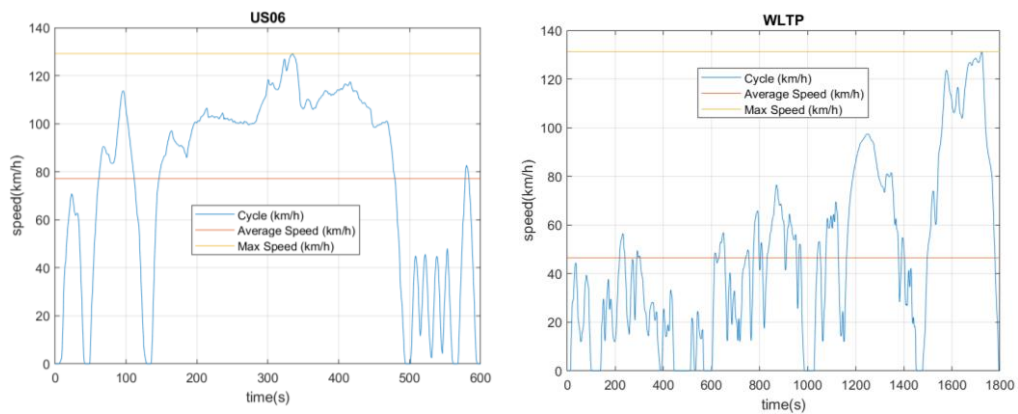


Figure 5.3 – High load cycles

5.1. Control strategies testing parameters

5.1.1. Simulation set-up

A Simulink block diagram equivalent to the Advisor one has been created. In order to initialize the vehicle and cycle data needed for the simulations a MATLAB script has been created. In this way, it was possible to stay only in the MATLAB/Simulink environment without using the Advisor interface saving time and increasing the ease in editing the simulation parameters. The Simulink method gives the same results of Advisor (running the same simulation parameters). It is also quicker because it skips the steps of the User interface.

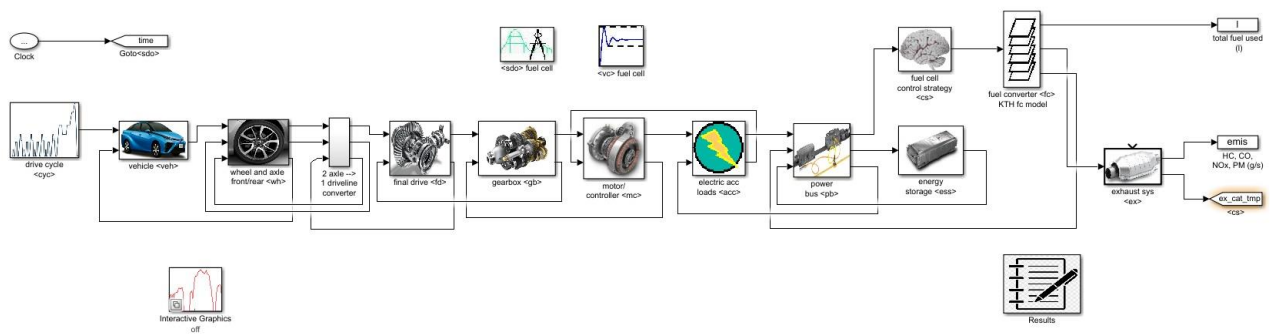


Figure 5.4 – Block Diagram used (equivalent to the Advisor one with the KTH model added)

In addition, a script for the post-processing data analysis called RESULT_ANALYSIS has been created. This script gives as output global vehicle data, fuel cell system data and power management data.

The global vehicle data displayed are: the distance travelled over the time of the cycle, the speed required profile, and the speed achieved profile, the cumulative fuel consumption measured in liters and the instantaneous specific fuel consumption measured in $\frac{l}{100km}$.

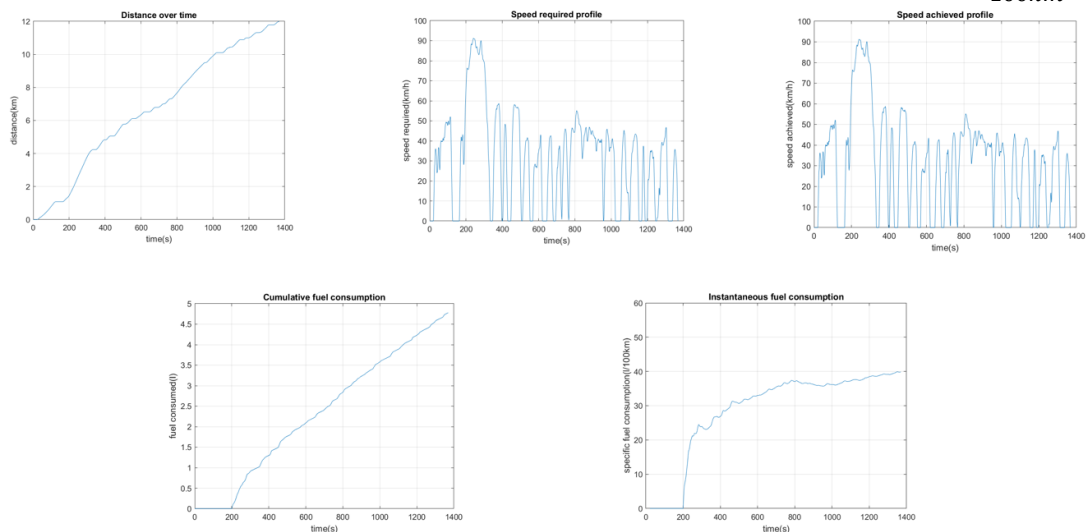


Figure 5.4 – Global Vehicle data example

The fuel cell system data displayed are: the fuel cell system output power, the fuel cell system instantaneous efficiency, the stack current density, the hydrogen inlet flowrate expressed in g/s, the compressor air flowrate expressed in g/s, the total power absorbed by the fuel cell stack auxiliaries.

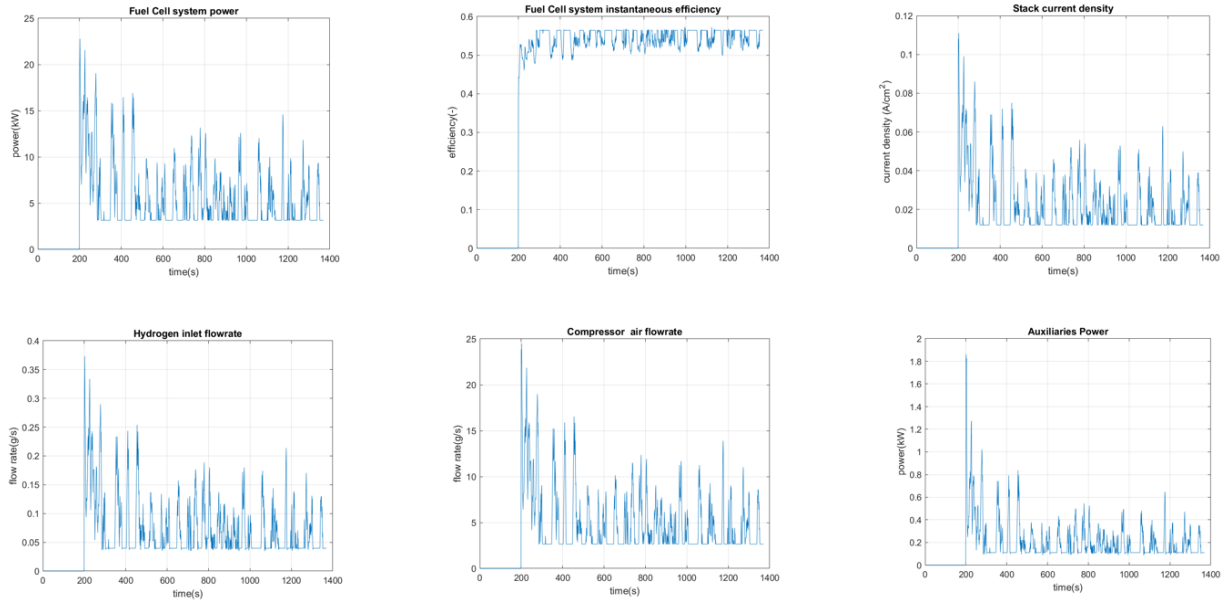


Figure 5.5 – Fuel Cell System data example

The power management data displayed are: the fuel cell system power, the power absorbed by the air compressor, the motor power, the battery power, the battery state of charge and the global hybrid system operation. In particular, the hybrid system operation is a very effective tool to understand how the power is split between the fuel cell and the battery during the cycle testing, monitoring at the same time the power absorbed by the compressor (major auxiliary contributor) and the battery state of charge.

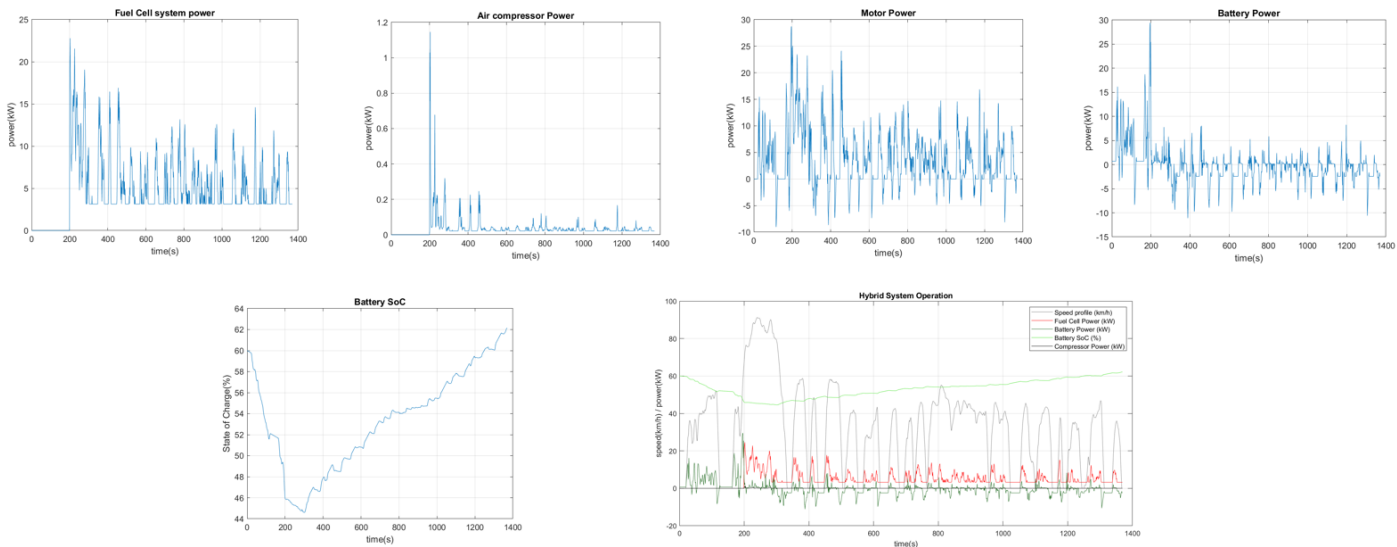


Figure 5.6 – Fuel Cell System data example

In these tests, it is important to consider the state of charge of the battery. If the state of charge is higher than the starting value, some hydrogen of the fuel cell has been used to charge the battery and not for traction purposes. If the state of charge is instead lower than the starting value, the cycle is not repeatable any more. The ISO 23274-1 regulation [18] about exhaust emissions and fuel consumption measurements in hybrid-electric road vehicles gives the following rules.

No correction in the measured fuel consumption and exhaust emissions is needed if the energy change in the battery due to the different state of charge from the starting point to the end point of the cycle $|\Delta E_{SoC}|$ is less or equal than 1% of the energy of the consumed fuel during the cycle E_{fc} .

$$|\Delta E_{SoC}| \leq 0.01 E_{fc} \quad (5.5)$$

If the energy difference is higher than the limit, it is necessary to apply a correction factor to reduce the state of charge difference effect to a negligible value. The values of ΔE_{SoC} and E_{fc} are calculated according to what seen in [19].

$$\Delta E_{SoC} = \Delta SoC \times C_{max(Ah)} \times V_{ocmean} \times n \times 3600 \quad (5.6)$$

Where:

ΔSoC = state of charge difference from the initial and final state of the cycle

$C_{max(Ah)}$ = maximum battery capacity measured in Ah

V_{ocmean} = mean open circuit voltage of the module

n = number of modules in the battery

$$E_{fc} = Q_{(l)} \times \rho_{(g/l)} \times LHV_{(J/g)} \quad (5.7)$$

Where:

$Q_{(l)}$ = cumulative fuel (hydrogen) consumption at the end of the cycle measured in l

$\rho_{(g/l)}$ = fuel density in g/l

$LHV_{(J/g)}$ = fuel lower heating value measured in J/g

The fuel consumption to add (if $SoC_{end\ cycle} < SoC_{initial}$) or to subtract (if $SoC_{end\ cycle} > SoC_{initial}$) in order to keep the cycle balanced Q_{Δ} is defined as follows:

$$Q_{\Delta} = \frac{\Delta E_{SoC}}{E_{fc}} Q_{(l)} \quad (5.8)$$

In each of these simulations, the parameters of the controller have been tuned in order to have a simulation as much balanced as possible. If the energy difference has been higher than the limit, the fuel consumption has been corrected.

5.1.2. Vehicle used for testing

Control strategies have been tested using as a reference the ‘Average small car’ data present in the Advisor folders which is roughly based on a 1994 Saturn SL1 vehicle.

However, the Fuelcell model has been improved using the KTH model and the battery pack has been changed into a more recent Li-Ion one for better performance.

Vehicle system power components:

- Westinghouse 75-kW (continuous) AC induction motor/inverter, tested by VA Tech
- KTH Fuel Cell Model - 50kW (net) Pure Hydrogen Fuel Cell System
- 6 Ah Saft Lithium Ion battery
- 700-W constant electric load (accessories)

Load parameters:

- Vehicle mass: 1191 kg
- Vehicle glider mass*: 592 kg
- Drag coefficient: 0.335
- Frontal area: 2 m^2
- Weight fraction in front when standing still: 0.6
- Centre of gravity (CoG) height: 0.5 m
- Wheelbase: 2.6 m
- Cargo Mass: 136 kg
- Wheel dimensions: 185/70R14

* vehicle mass without the propulsion system (fuel converter, exhaust aftertreatment, drivetrain, motor, energy storage system, generator)



Figure 5.7 – 1994 Saturn SL1 vehicle

5.2. Thermostat control strategy

The vehicle is started relying on the battery and is maintained in this operating condition until its charge state reaches the minimum threshold; when this threshold is reached, the fuel cell that provides power for both propulsion and battery charging starts operating. Battery increases its state of charge during the cycle from when the Fuel Cell is on.

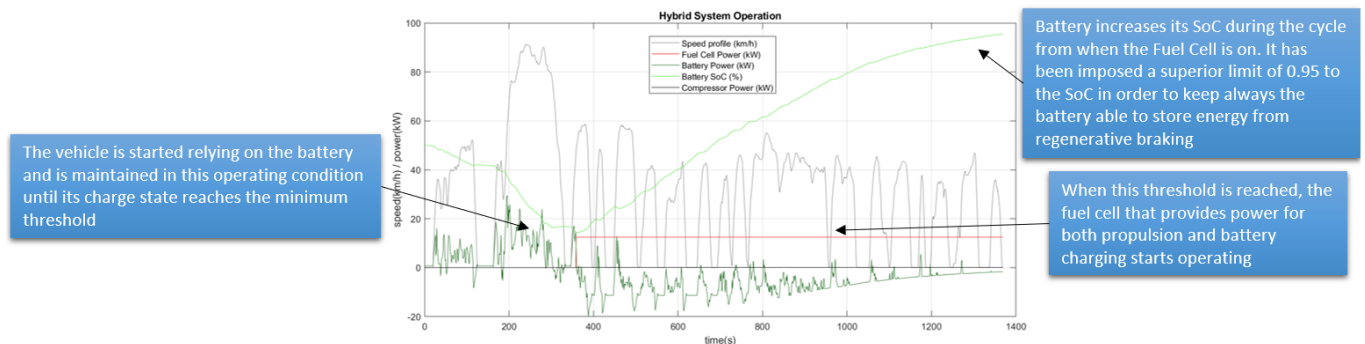


Figure 5.8 – Thermostat control strategy example

Mean controller parameters used (tuned for every cycle to balance the state of charge):

- Initial battery SoC=0.5
- Highest desired battery SoC=0.95
- Lowest desired battery SoC=0.2
- Initial FC state=off
- Minimum operating power (W)=35% of maximum fuel converter power
- Maximum operating power (W) [exceeded only if SoC<Lowest desired battery SoC]= 35% of maximum fuel converter power
- Corrective factor to keep the battery SoC inside the limits [extra FC power output (W)]=0
- Minimum time Fc remains off (s) [enforced unless SOC<=Lowest desired battery SoC]= infinite
- Maximum rate of increase of power (W/s)=0
- Maximum rate of decrease of power (W/s)=0
- Charge sustaining strategy=on
- Fuel cell not always on

5.2.1. Results using the FTP driving cycle

The main outputs of the vehicle system are represented as follows:

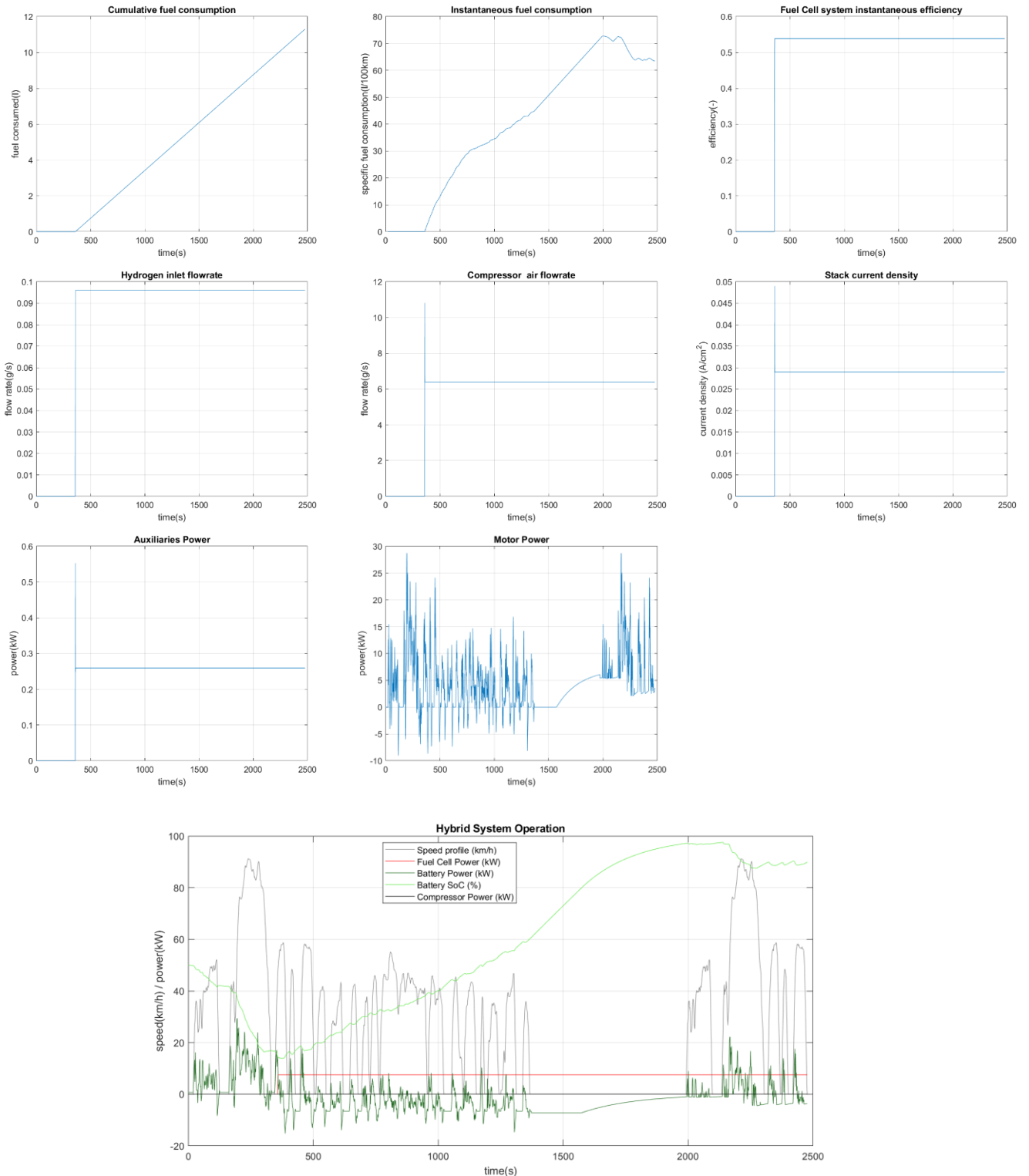


Figure 5.9 – Results on FTP driving cycle: a) Cumulative consumption b) Instantaneous specific consumption c) Fuel cell system efficiency d) Hydrogen flowrate e) Air flowrate f) Current density g) Auxiliary system power h) Motor power i) Hybrid system operation

5.2.2. Results using the NEDC driving cycle

The main outputs of the vehicle system are represented as follows:

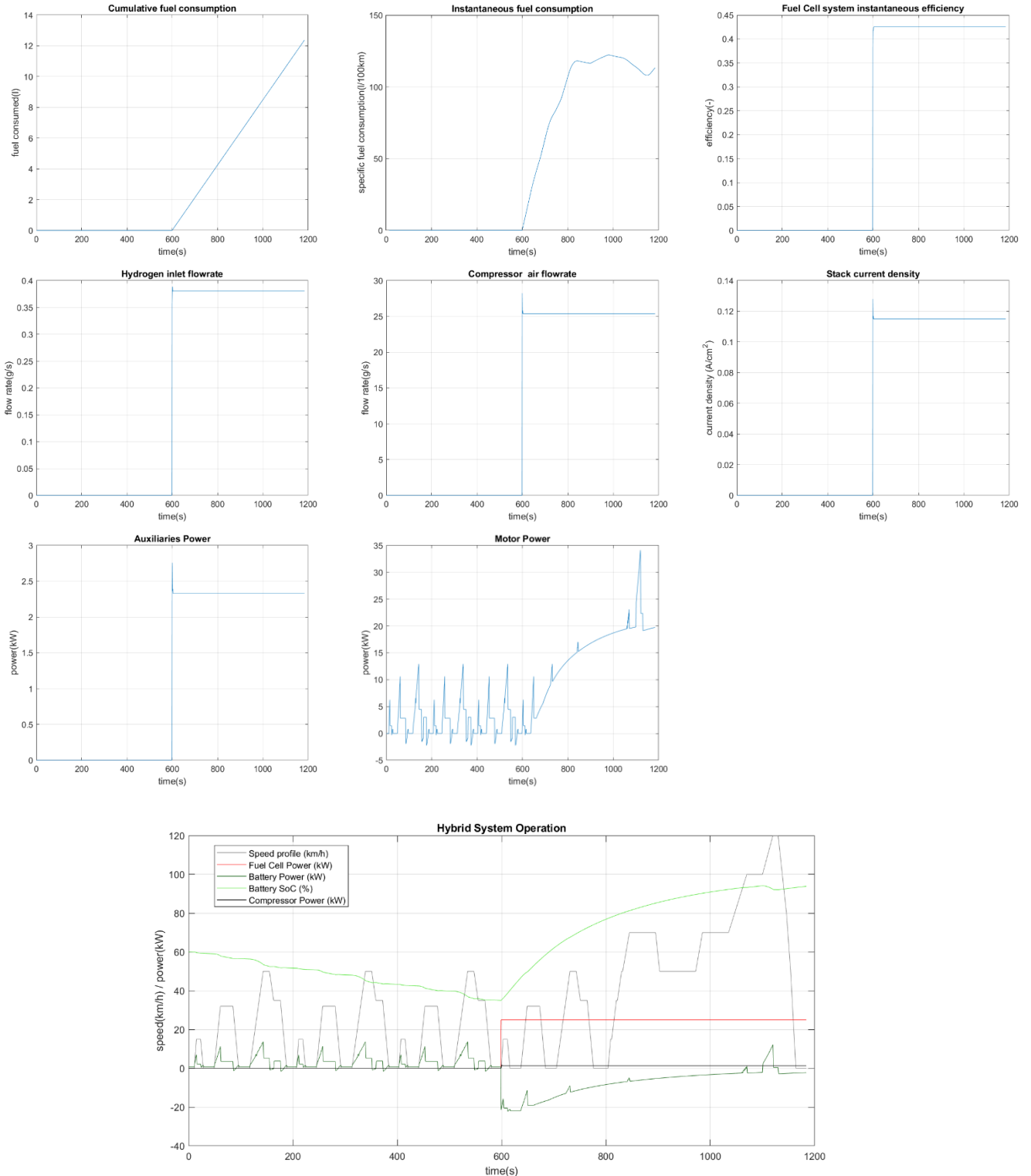


Figure 5.10 – Results on NEDC driving cycle: a) Cumulative consumption b) Instantaneous specific consumption c) Fuel cell system efficiency d) Hydrogen flowrate e) Air flowrate f) Current density g) Auxiliary system power h) Motor power i) Hybrid system operation

5.2.3. Results using the UDDS driving cycle

The main outputs of the vehicle system are represented as follows:

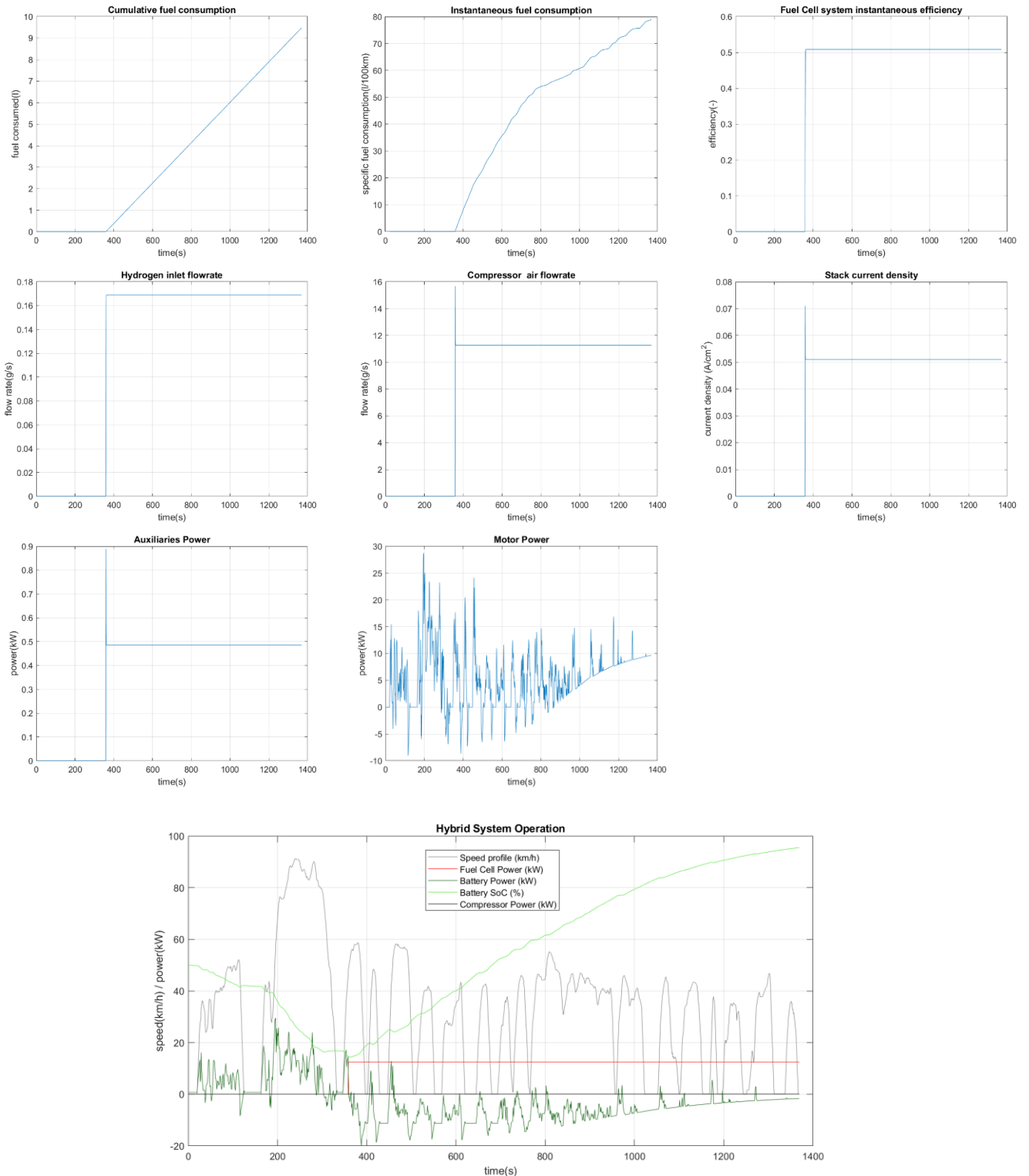


Figure 5.11 – Results on UDDS driving cycle: a) Cumulative consumption b) Instantaneous specific consumption c) Fuel cell system efficiency d) Hydrogen flowrate e) Air flowrate f) Current density g) Auxiliary system power h) Motor power i) Hybrid system operation

5.2.4. Results using the US06 driving cycle

The main outputs of the vehicle system are represented as follows:

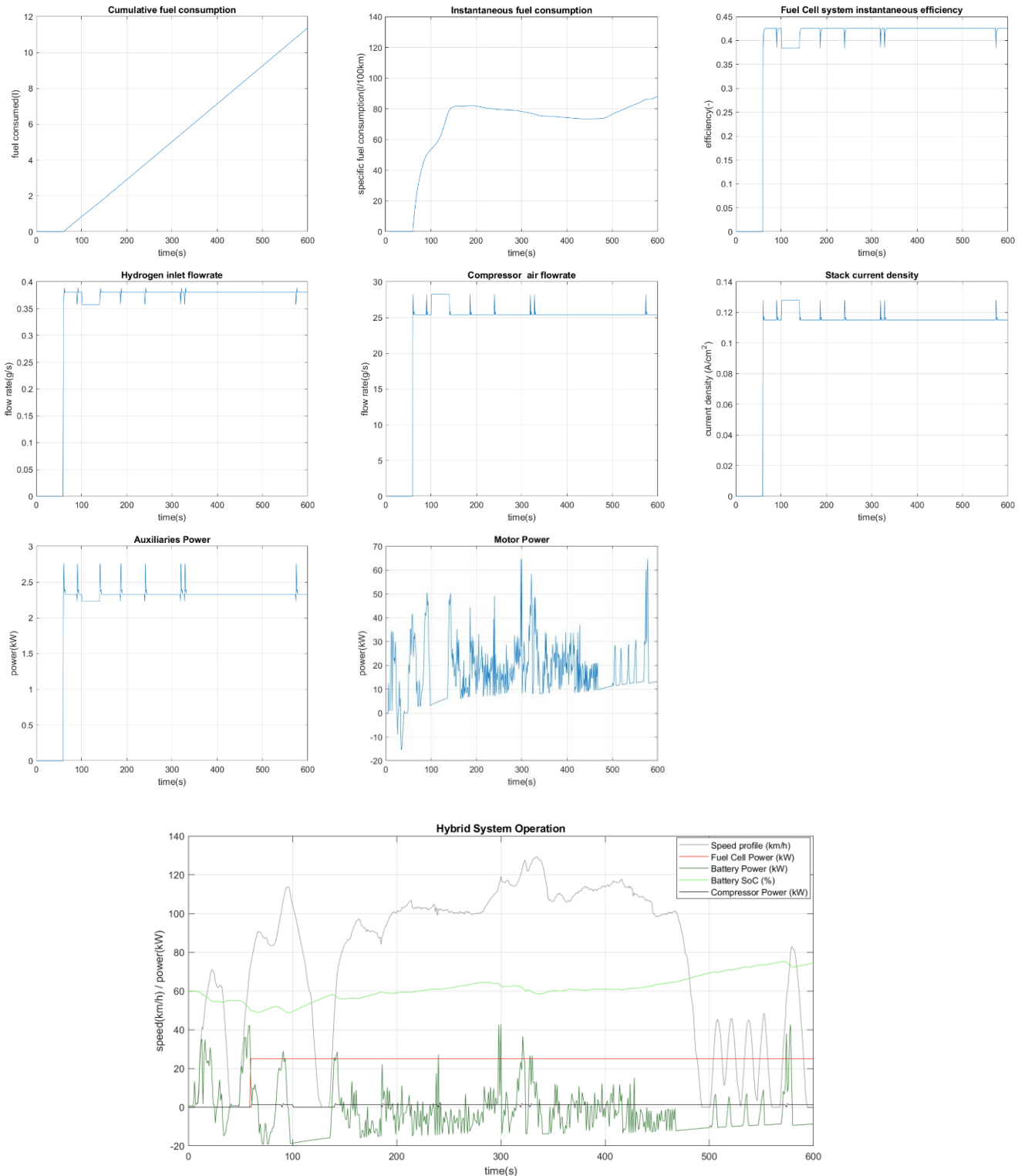


Figure 5.12 – Results on US06 driving cycle: a) Cumulative consumption b) Instantaneous specific consumption c) Fuel cell system efficiency d) Hydrogen flowrate e) Air flowrate f) Current density g) Auxiliary system power h) Motor power i) Hybrid system operation

5.2.5. Results using the WLTP driving cycle

The main outputs of the vehicle system are represented as follows:

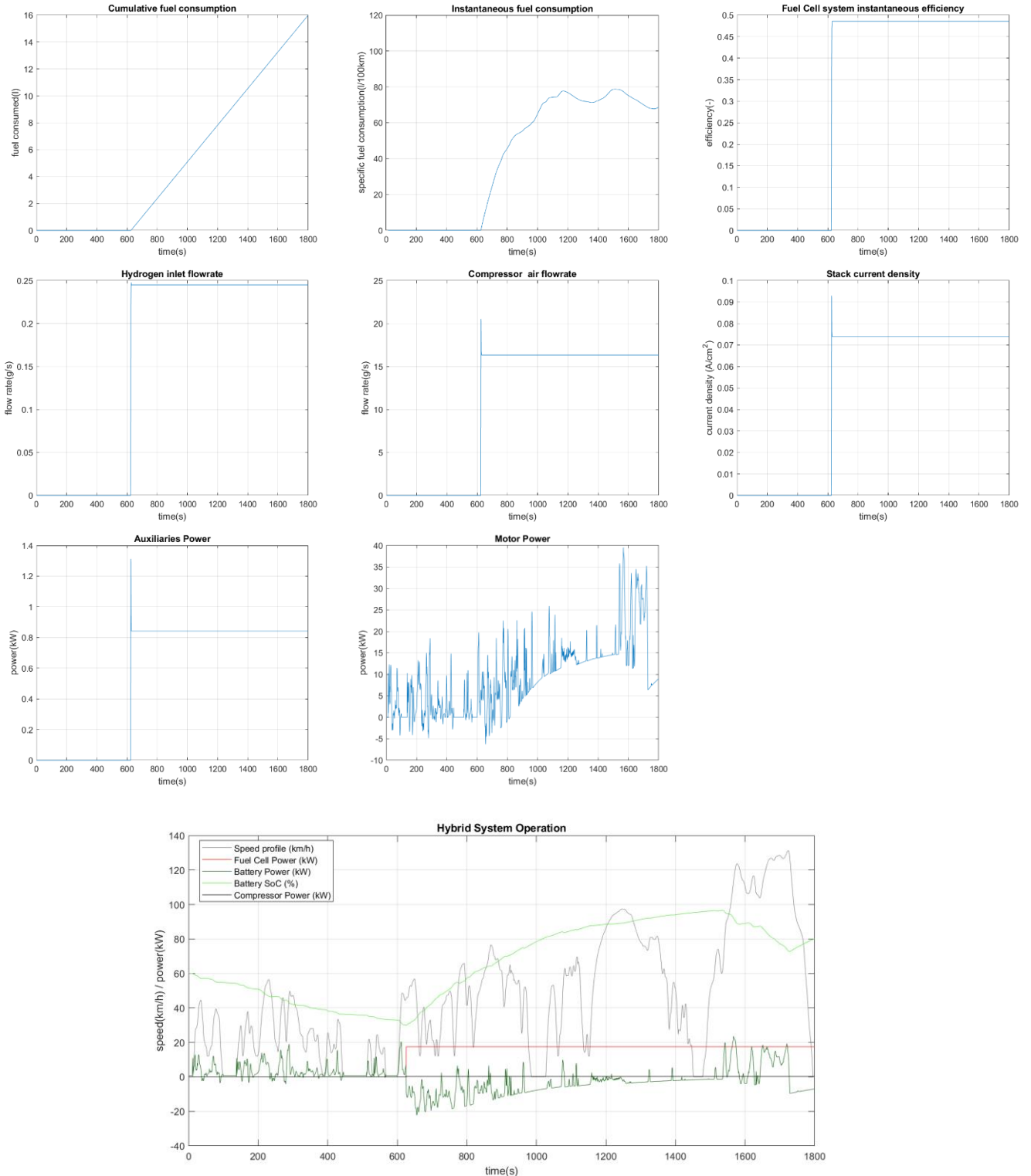


Figure 5.13 – Results on WLTP driving cycle: a) Cumulative consumption b) Instantaneous specific consumption c) Fuel cell system efficiency d) Hydrogen flowrate e) Air flowrate f) Current density g) Auxiliary system power h) Motor power i) Hybrid system operation

5.3. Range extender control strategy

The propulsion of the vehicle is mainly entrusted to the battery while the fuel cell can produce additional power to maintain the state of charge of the battery and increase its mileage. In the simulations, the power delivered by the fuel cell has been kept constant and equal to 5 kW for low load cycles and is equal to 20 kW for high load cycles. The Battery operates in charge sustaining (CS) mode.

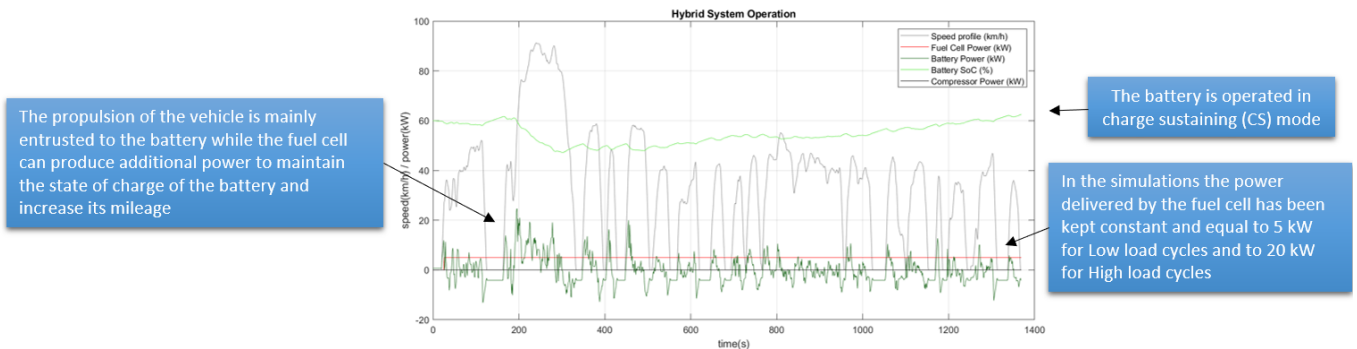


Figure 5.14 – Range extender control strategy example

Mean controller parameters used (tuned for every cycle to balance the state of charge):

- Initial battery SoC=0.60
- Highest desired battery SoC=0.8
- Lowest desired battery SoC=0.4
- Initial FC state=off
- Minimum operating power(W)=15% of maximum fuel converter power
- Maximum operating power(W) [exceeded only if SoC<Lowest desired battery SoC]= 15% of maximum fuel converter power
- Corrective factor to keep the battery SoC inside the limits [extra FC power output (W)]=0
- Minimum time Fc remains off (s) [enforced unless SOC<=Lowest desired battery SoC]=0
- Maximum rate of increase of power(W/s)=0
- Maximum rate of decrease of power(W/s)=0
- Charge sustaining strategy=on
- Fuel cell not always on

5.3.1. Results using the FTP driving cycle

The main outputs of the vehicle system are represented as follows:

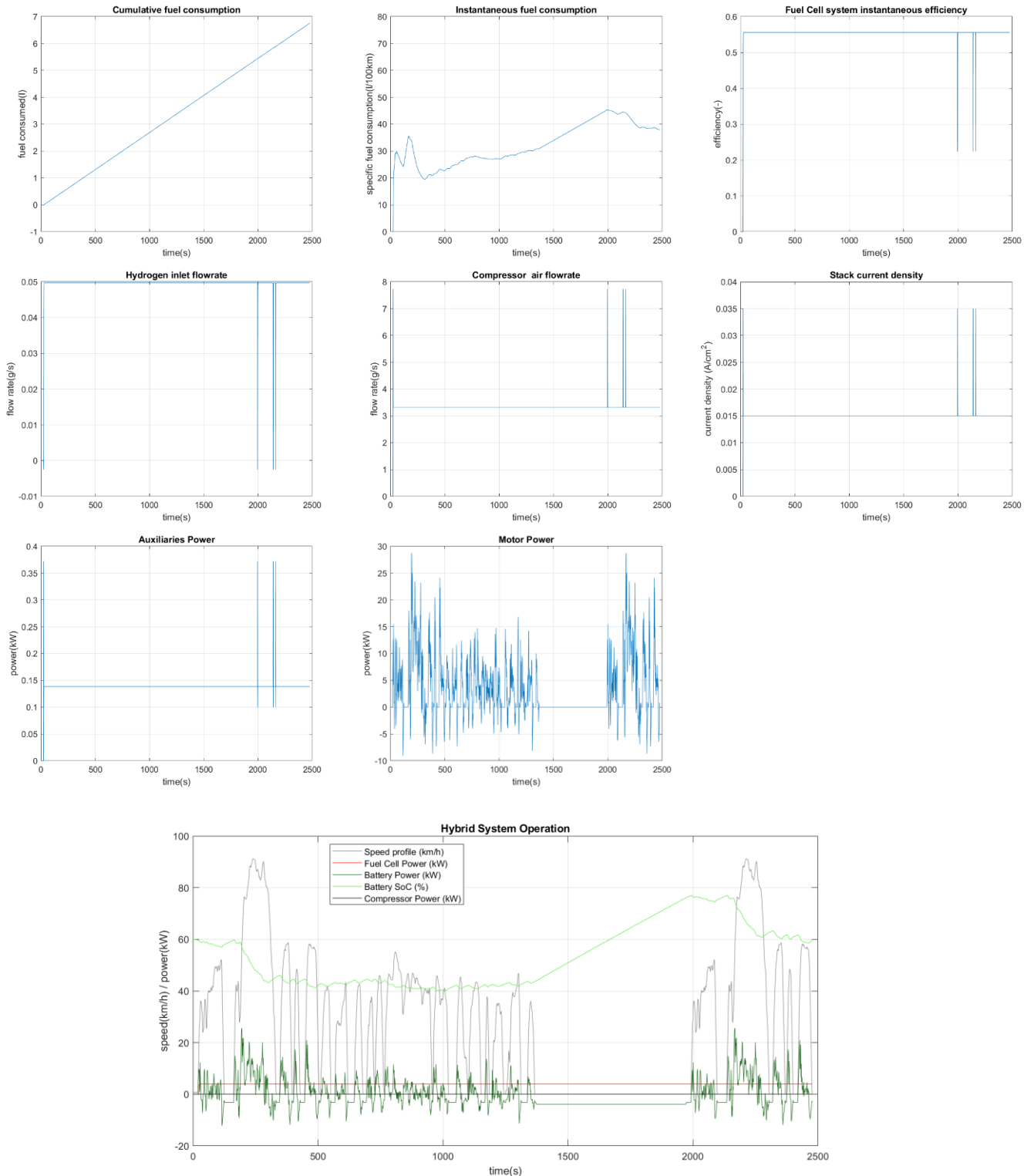


Figure 5.15 – Results on FTP driving cycle: a) Cumulative consumption b) Instantaneous specific consumption c) Fuel cell system efficiency d) Hydrogen flowrate e) Air flowrate f) Current density g) Auxiliary system power h) Motor power i) Hybrid system operation

5.3.2. Results using the NEDC driving cycle

The main outputs of the vehicle system are represented as follows:

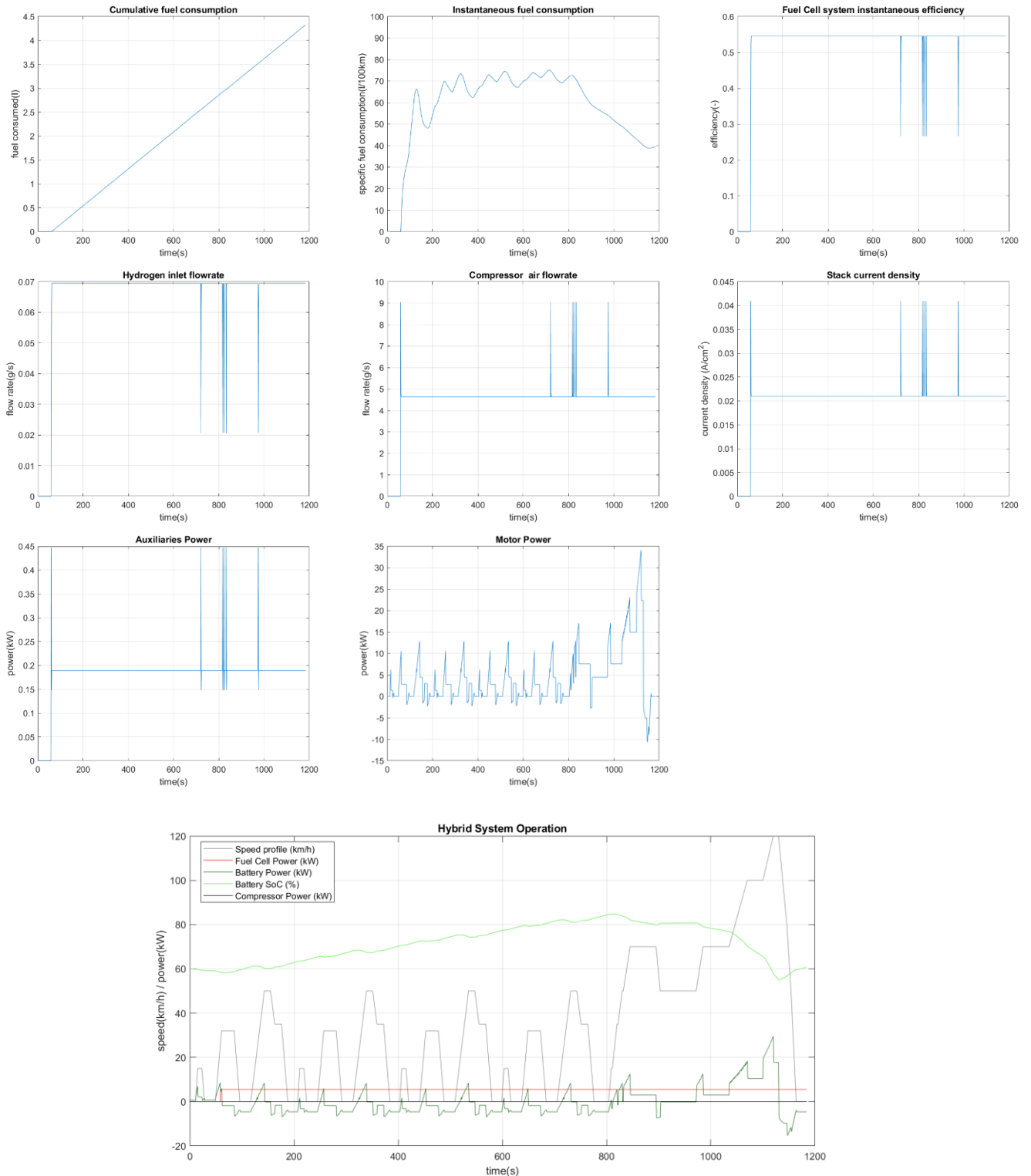


Figure 5.16 – Results on NEDC driving cycle: a) Cumulative consumption b) Instantaneous specific consumption c) Fuel cell system efficiency d) Hydrogen flowrate e) Air flowrate f) Current density g) Auxiliary system power h) Motor power i) Hybrid system operation

5.3.3. Results using the UDDS driving cycle

The main outputs of the vehicle system are represented as follows:

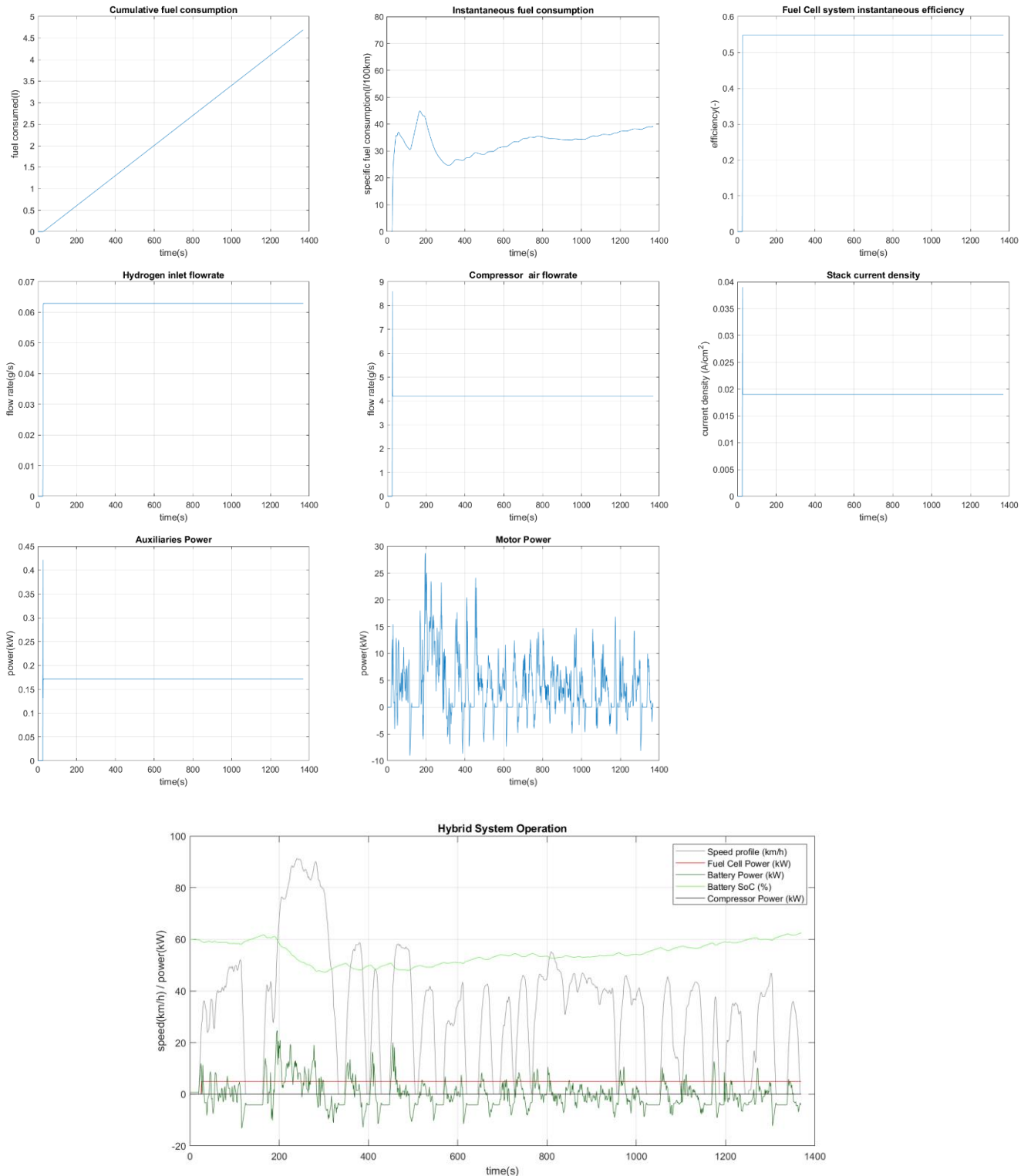


Figure 5.17 – Results on UDDS driving cycle: a) Cumulative consumption b) Instantaneous specific consumption c) Fuel cell system efficiency d) Hydrogen flowrate e) Air flowrate f) Current density g) Auxiliary system power h) Motor power i) Hybrid system operation

5.3.4. Results using the US06 driving cycle

The main outputs of the vehicle system are represented as follows:

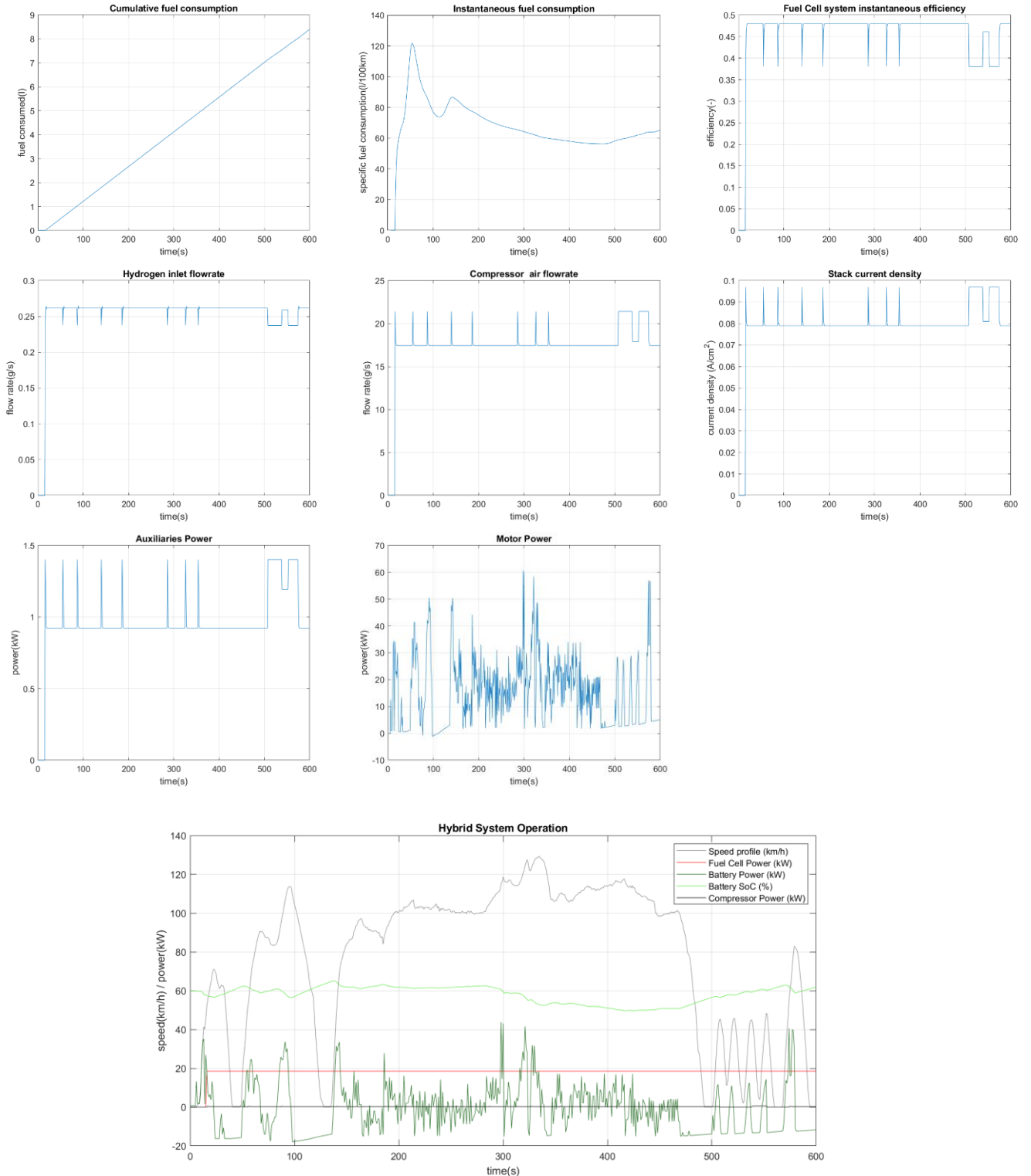


Figure 5.18 – Results on US06 driving cycle: a) Cumulative consumption b) Instantaneous specific consumption c) Fuel cell system efficiency d) Hydrogen flowrate e) Air flowrate f) Current density g) Auxiliary system power h) Motor power i) Hybrid system operation

5.3.5. Results using the WLTP driving cycle

The main outputs of the vehicle system are represented as follows:

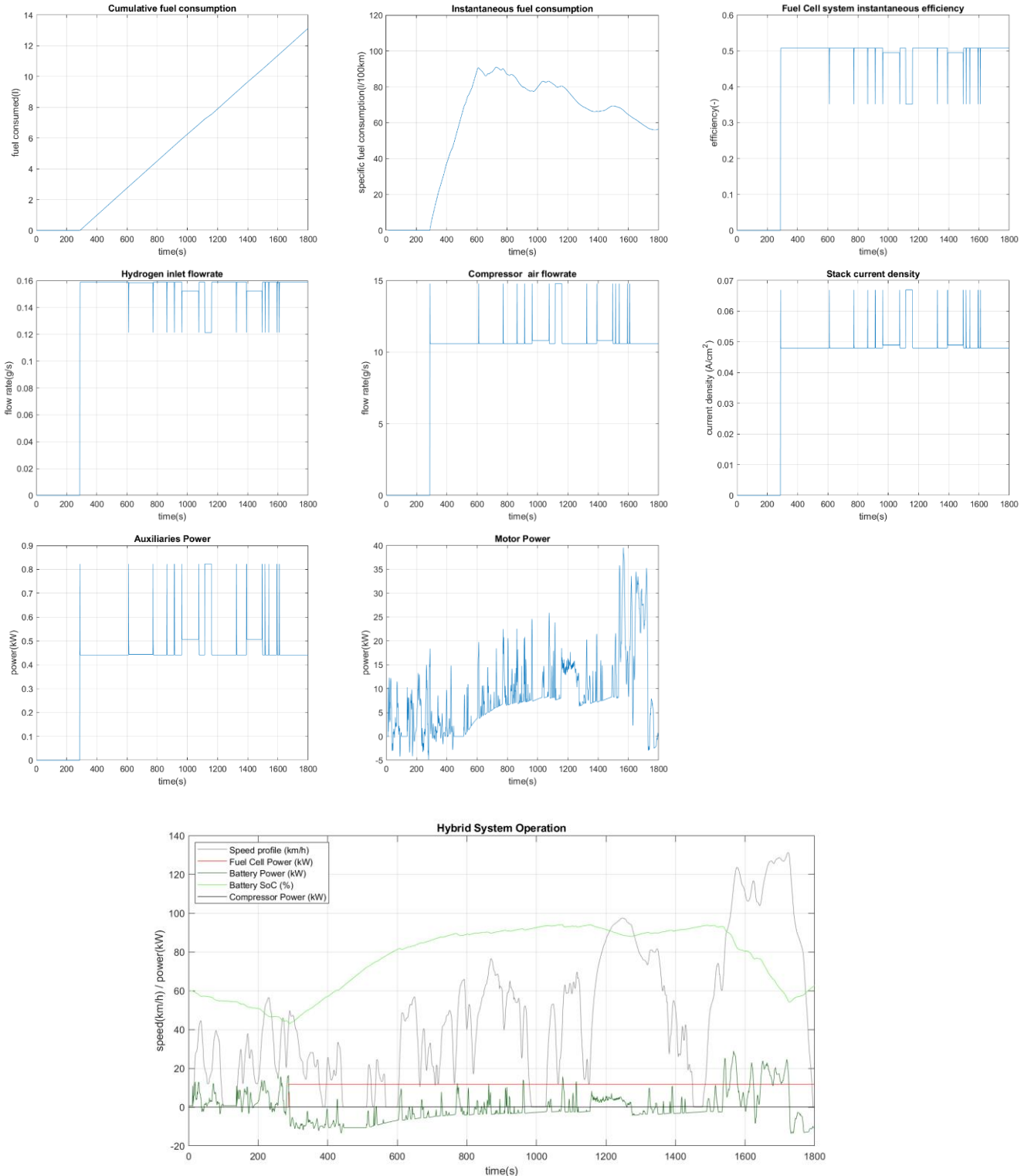


Figure 5.19 – Results on WLTP driving cycle: a) Cumulative consumption b) Instantaneous specific consumption c) Fuel cell system efficiency d) Hydrogen flowrate e) Air flowrate f) Current density g) Auxiliary system power h) Motor power i) Hybrid system operation

5.4. Mode based control strategy

The idea of this strategy is to run the vehicle in several different operating modes based on battery SOC and Fuel converter power demands. It operates the fuel cell between different modes with an On/Off operation and uses the fuel cell to follow changes in the power demand with the battery operating at a constant set-point proportional to its current SOC. Referring to the following figure, the fuel cell is always on in green area and always off in the red area. The yellow area is a transition area where the fuel cell maintains its on/off state from the previous state that it was in. The Battery operates in charge sustaining (CS) mode.

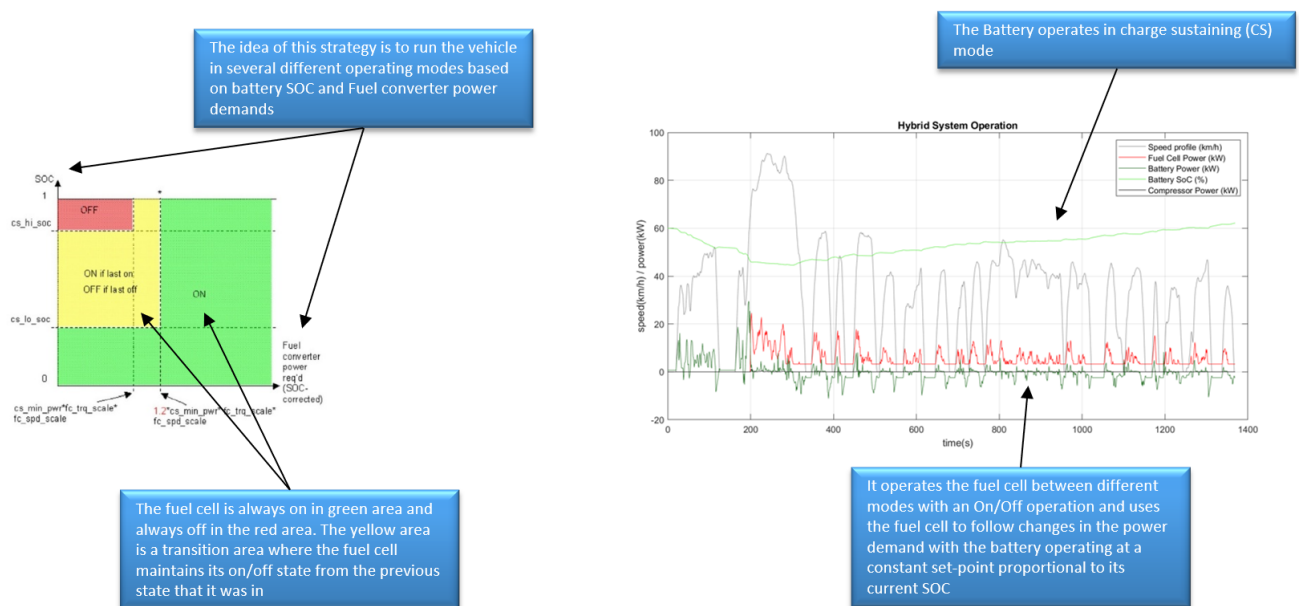


Figure 5.20 – Mode based control strategy example

Mean controller parameters used (tuned for every cycle to balance the state of charge):

- Initial battery SoC=0.60
- Highest desired battery SoC=0.8
- Lowest desired battery SoC=0.4
- Initial FC state=off
- Minimum operating power (W)=15% of maximum fuel converter power
- Maximum operating power (W) [exceeded only if SoC<Lowest desired battery SoC]= 95% of maximum fuel converter power
- Corrective factor to keep the battery SoC inside the limits [extra FC power output (W)]=7000
- Minimum time Fc remains off (s) [enforced unless SOC<=Lowest desired battery SoC]=90
- Maximum rate of increase of power (W/s)=2000
- Maximum rate of decrease of power (W/s)=-4000
- Charge sustaining strategy=on
- Fuel cell not always on

5.4.1. Results using the FTP driving cycle

The main outputs of the vehicle system are represented as follows:

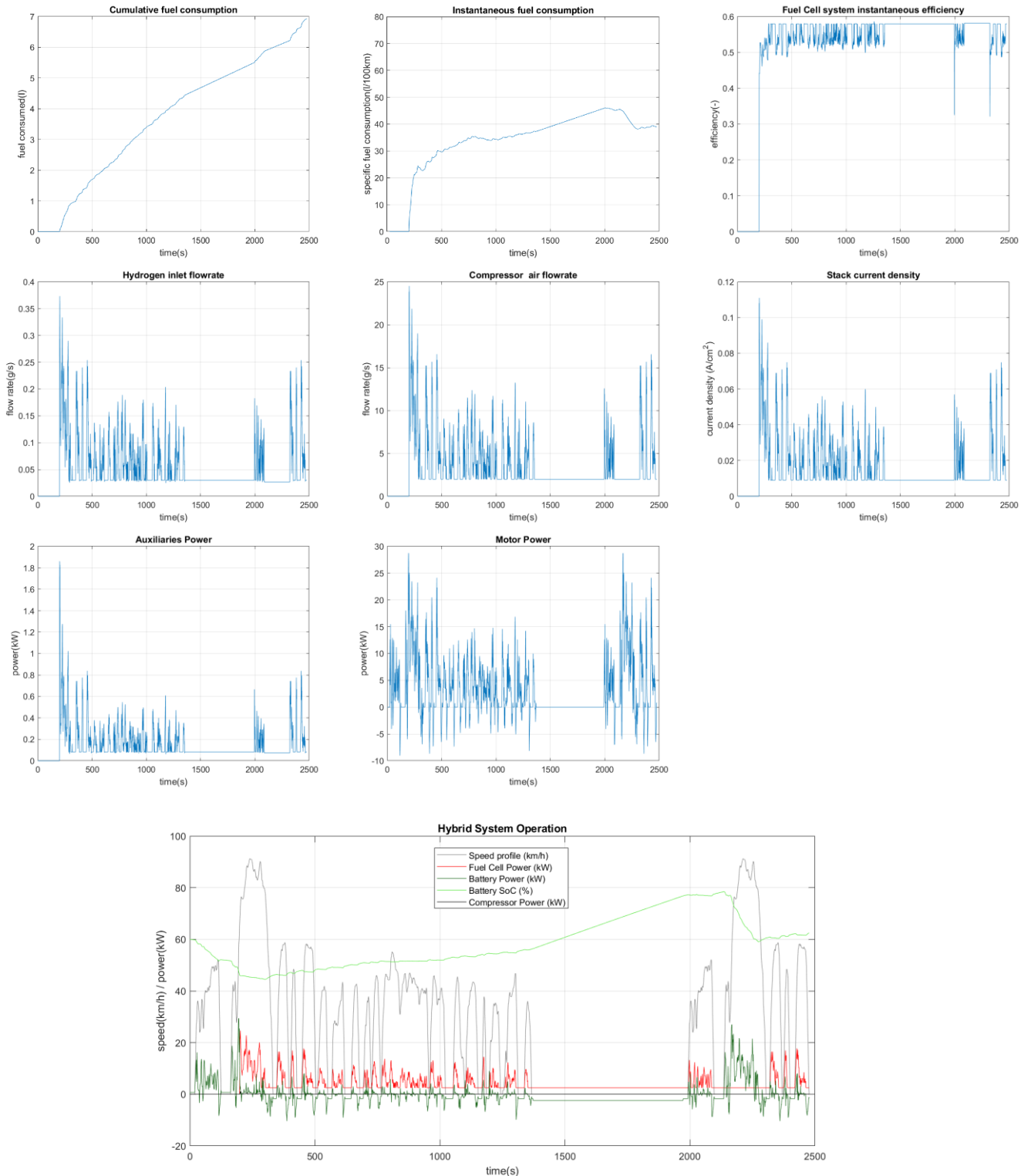


Figure 5.21 – Results on FTP driving cycle: a) Cumulative consumption b) Instantaneous specific consumption c) Fuel cell system efficiency d) Hydrogen flowrate e) Air flowrate f) Current density g) Auxiliary system power h) Motor power i) Hybrid system operation

5.4.2. Results using the NEDC driving cycle

The main outputs of the vehicle system are represented as follows:

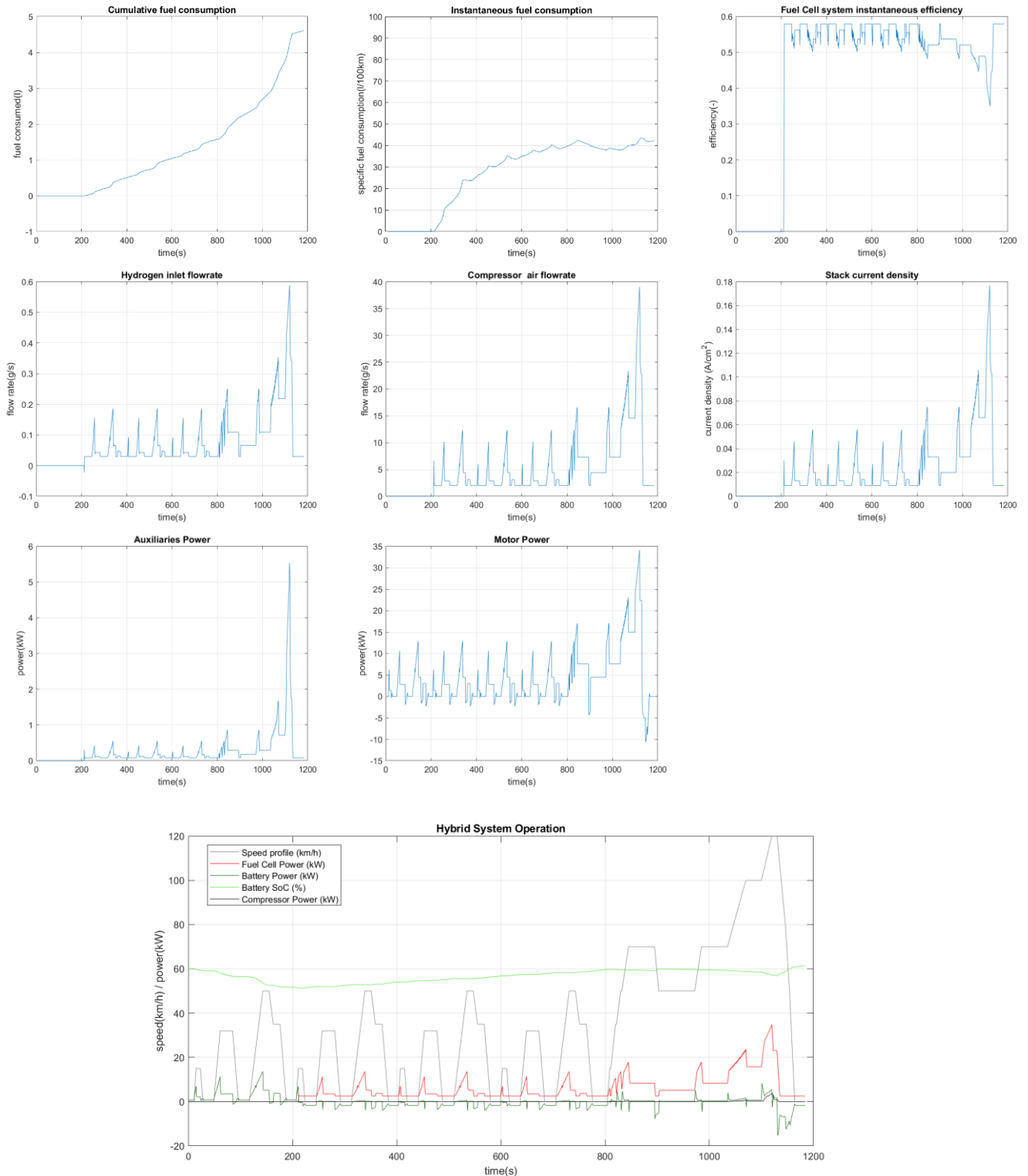


Figure 5.22 – Results on NEDC driving cycle: a) Cumulative consumption b) Instantaneous specific consumption c) Fuel cell system efficiency d) Hydrogen flowrate e) Air flowrate f) Current density g) Auxiliary system power h) Motor power i) Hybrid system operation

5.4.3. Results using the UDDS driving cycle

The main outputs of the vehicle system are represented as follows:

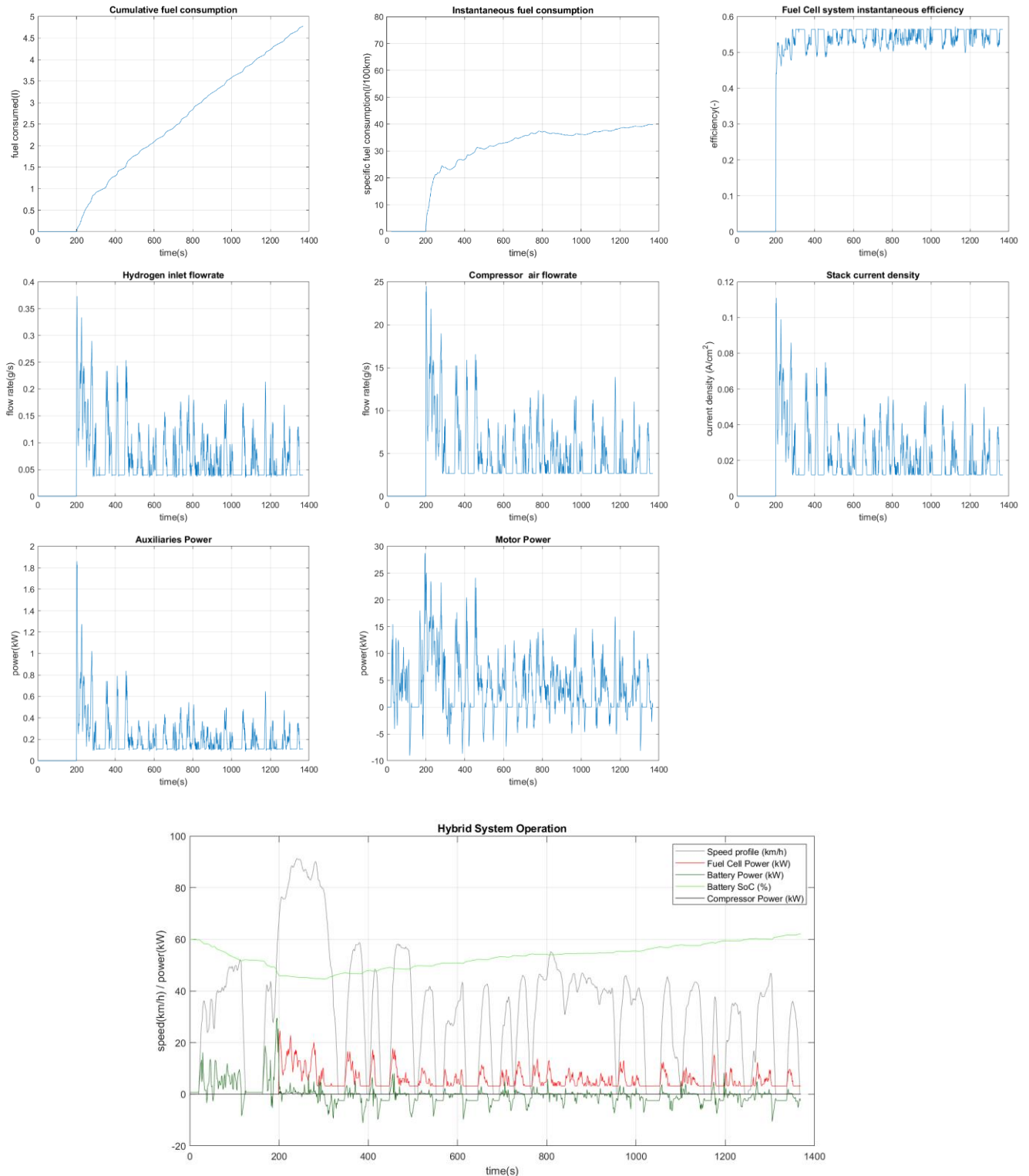


Figure 5.23 – Results on UDDS driving cycle: a) Cumulative consumption b) Instantaneous specific consumption c) Fuel cell system efficiency d) Hydrogen flowrate e) Air flowrate f) Current density g) Auxiliary system power h) Motor power i) Hybrid system operation

5.4.4. Results using the US06 driving cycle

The main outputs of the vehicle system are represented as follows:

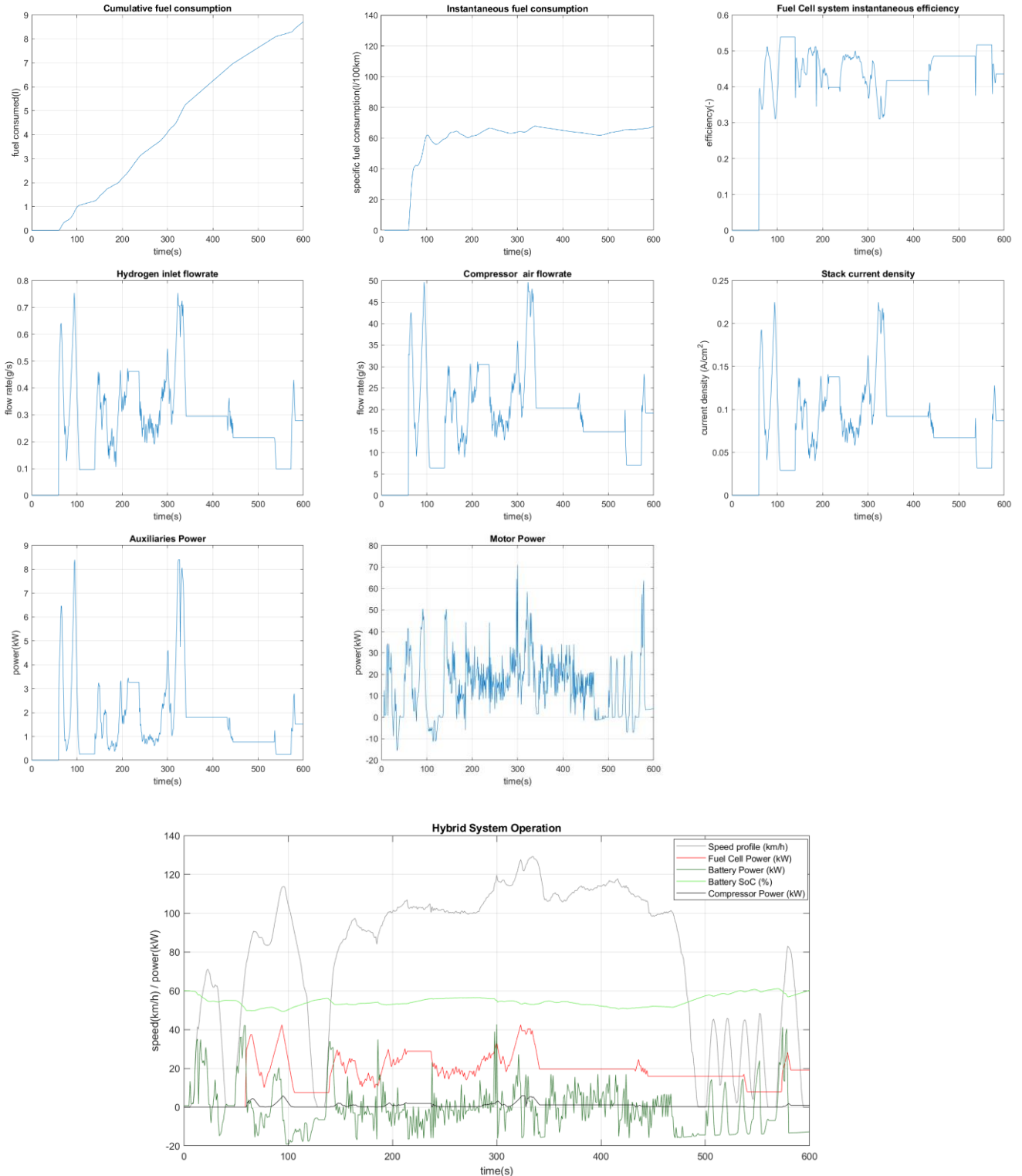


Figure 5.24 – Results on US06 driving cycle: a) Cumulative consumption b) Instantaneous specific consumption c) Fuel cell system efficiency d) Hydrogen flowrate e) Air flowrate f) Current density g) Auxiliary system power h) Motor power i) Hybrid system operation

5.4.5. Results using the WLTP driving cycle

The main outputs of the vehicle system are represented as follows:

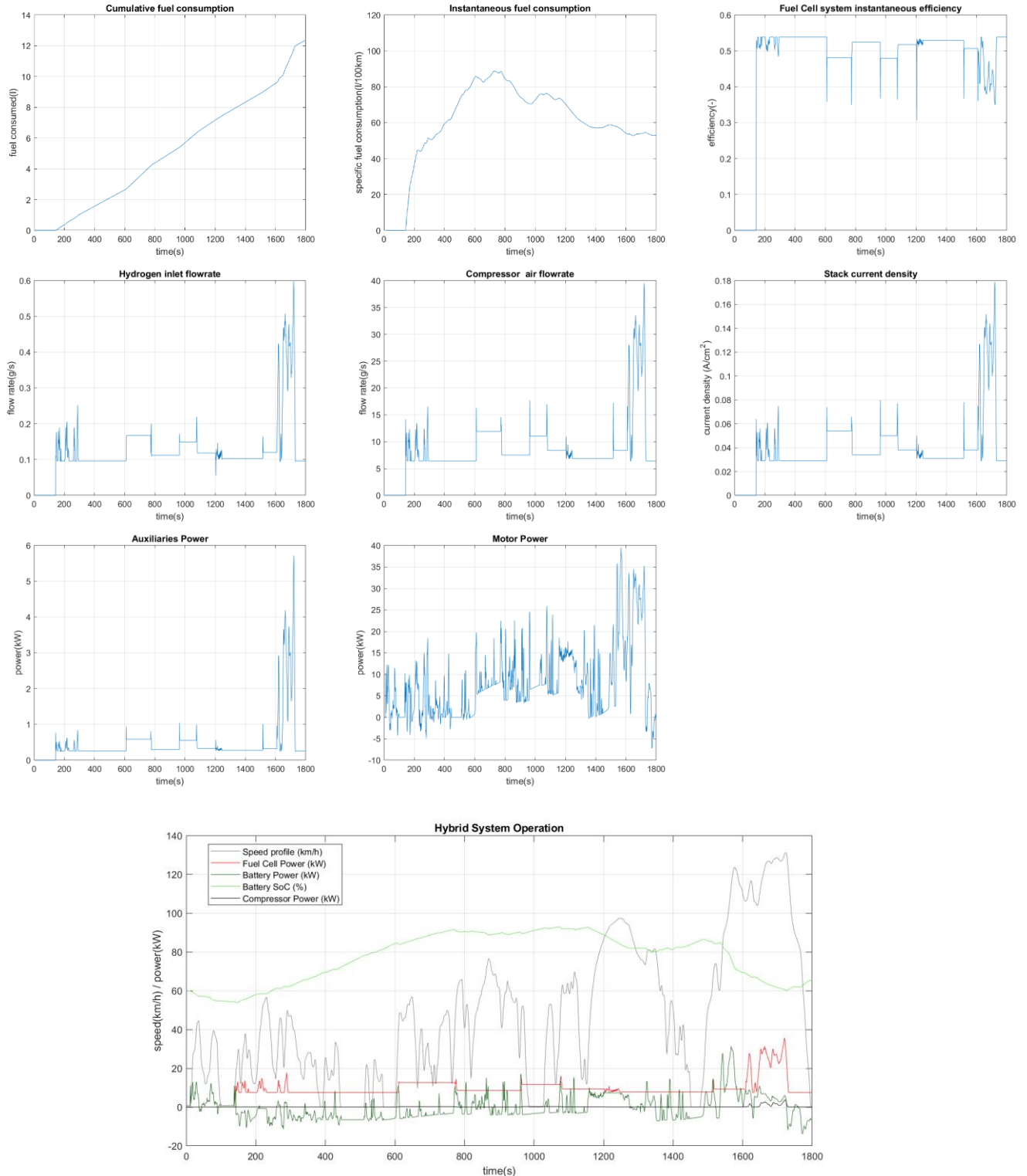


Figure 5.25 – Results on WLTP driving cycle: a) Cumulative consumption b) Instantaneous specific consumption c) Fuel cell system efficiency d) Hydrogen flowrate e) Air flowrate f) Current density g) Auxiliary system power h) Motor power i) Hybrid system operation

5.5. Constant Fuel Cell output control strategy

The goal of this strategy is keeping the fuel cell at near constant power output (which must satisfy the average demand) and using the battery to satisfy instantaneous power demand. In these simulations the fuel cell output power has been constrained between 15% and 30% of the maximum, because it corresponds to its best efficiency zone. The Battery operates in charge sustaining (CS) mode.

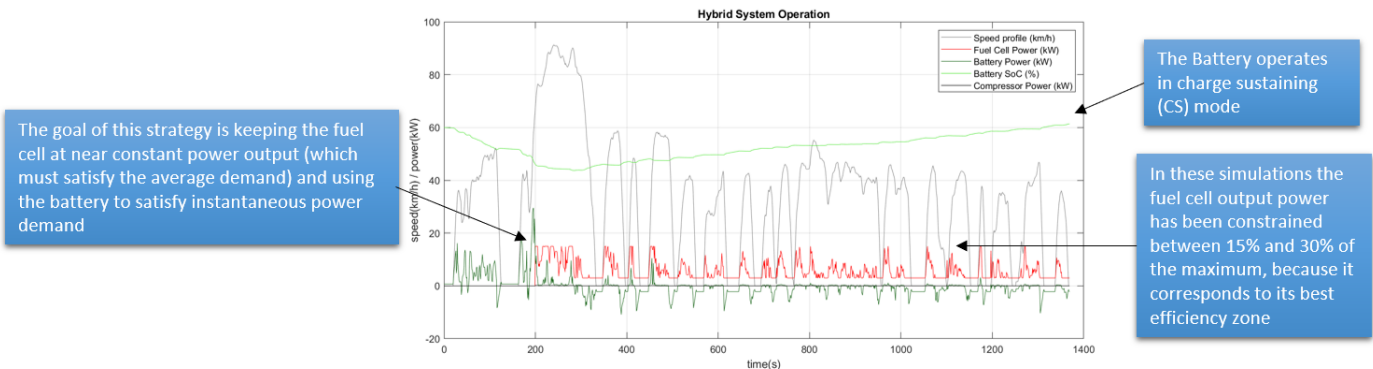


Figure 5.26 – Constant fuel cell output control strategy example

Mean controller parameters used (tuned for every cycle to balance the state of charge):

- Initial battery SoC=0.60
- Highest desired battery SoC=0.8
- Lowest desired battery SoC=0.4
- Initial FC state=off
- Minimum operating power(W)=15% of maximum fuel converter power
- Maximum operating power(W) [exceeded only if SoC<Lowest desired battery SoC]= 30% of maximum fuel converter power
- Corrective factor to keep the battery SoC inside the limits [extra FC power output (W)]=10000
- Minimum time Fc remains off (s) [enforced unless SOC<=Lowest desired battery SoC]=200
- Maximum rate of increase of power (W/s)=15000
- Maximum rate of decrease of power (W/s)=-25000
- Charge sustaining strategy=on
- Fuel cell not always on

5.5.1. Results using the FTP driving cycle

The main outputs of the vehicle system are represented as follows:

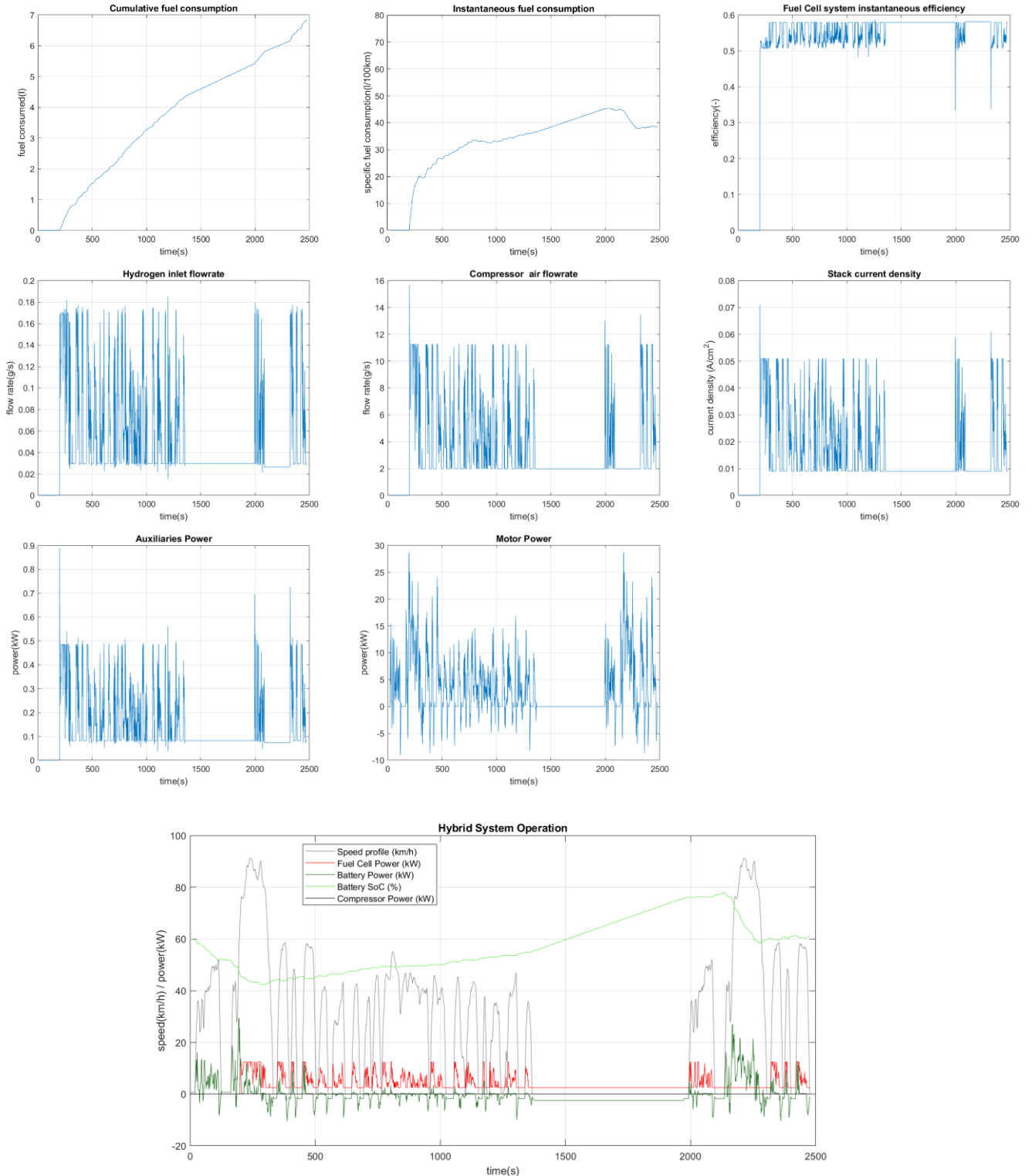


Figure 5.27 – Results on FTP driving cycle: a) Cumulative consumption b) Instantaneous specific consumption c) Fuel cell system efficiency d) Hydrogen flowrate e) Air flowrate f) Current density g) Auxiliary system power h) Motor power i) Hybrid system operation

5.5.2. Results using the NEDC driving cycle

The main outputs of the vehicle system are represented as follows:

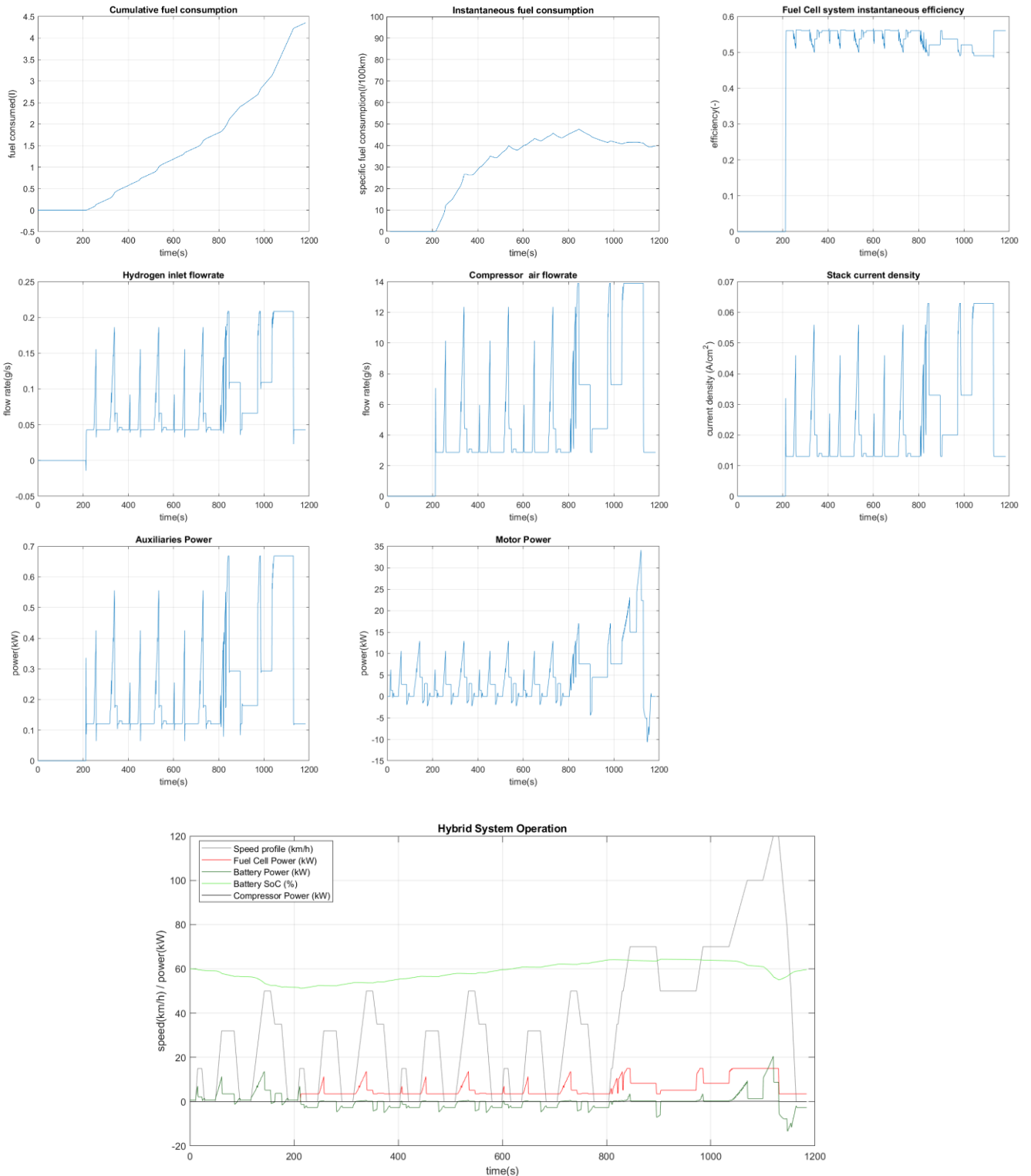


Figure 5.28 – Results on NEDC driving cycle: a) Cumulative consumption b) Instantaneous specific consumption c) Fuel cell system efficiency d) Hydrogen flowrate e) Air flowrate f) Current density g) Auxiliary system power h) Motor power i) Hybrid system operation

5.5.3. Results using the UDDS driving cycle

The main outputs of the vehicle system are represented as follows:

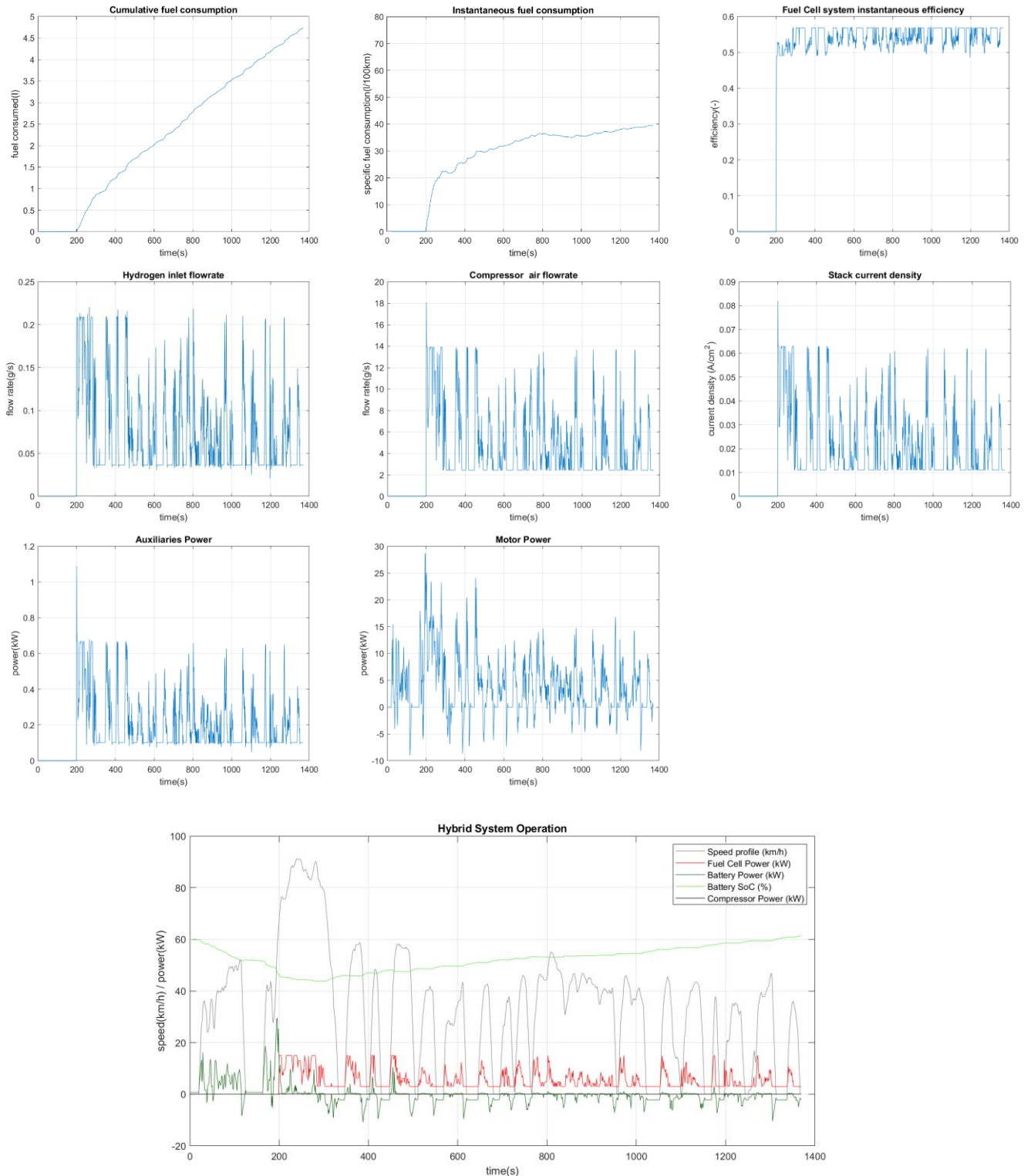


Figure 5.29 – Results on UDDS driving cycle: a) Cumulative consumption b) Instantaneous specific consumption c) Fuel cell system efficiency d) Hydrogen flowrate e) Air flowrate f) Current density g) Auxiliary system power h) Motor power i) Hybrid system operation

5.5.4. Results using the US06 driving cycle

The main outputs of the vehicle system are represented as follows:



Figure 5.30 – Results on US06 driving cycle: a) Cumulative consumption b) Instantaneous specific consumption c) Fuel cell system efficiency d) Hydrogen flowrate e) Air flowrate f) Current density g) Auxiliary system power h) Motor power i) Hybrid system operation

5.5.5. Results using the WLTP driving cycle

The main outputs of the vehicle system are represented as follows:

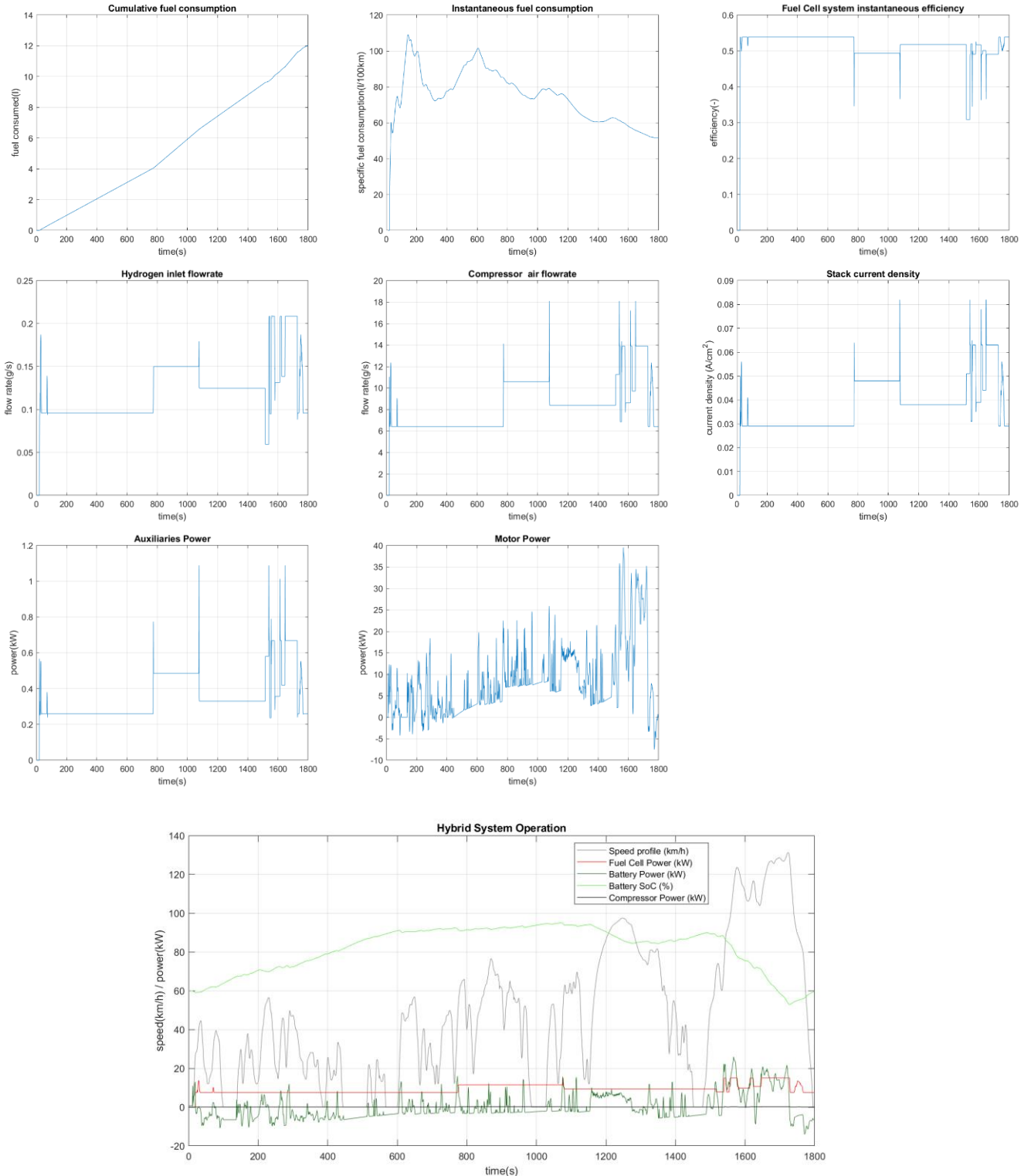


Figure 5.31 – Results on WLTP driving cycle: a) Cumulative consumption b) Instantaneous specific consumption c) Fuel cell system efficiency d) Hydrogen flowrate e) Air flowrate f) Current density g) Auxiliary system power h) Motor power i) Hybrid system operation

5.6. Strong load following control strategy

The propulsion of the vehicle is mainly entrusted to the fuel cell while the battery is used to produce additional power when required and to make up for the losses of the auxiliaries. It can be seen as a more 'reactive' version of the mode based control strategy. The Battery operates in charge sustaining (CS) mode.

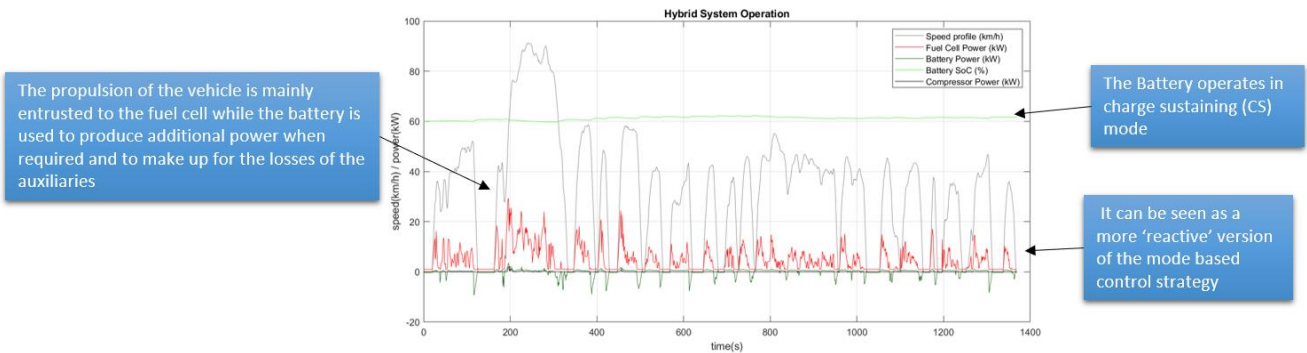


Figure 5.32 – Strong load following control strategy example

Mean controller parameters used (tuned for every cycle to balance the state of charge):

- Initial battery SoC=0.60
- Highest desired battery SoC=0.8
- Lowest desired battery SoC=0.4
- Initial FC state=off
- Minimum operating power (W)=1000
- Maximum operating power (W) [exceeded only if SoC<Lowest desired battery SoC]= Maximum allowable by the fuel converter
- Corrective factor to keep the battery SoC inside the limits [extra FC power output (W)]=5000
- Minimum time Fc remains off (s) [enforced unless SOC<=Lowest desired battery SoC]=0
- Maximum rate of increase of power (W/s)=40000
- Maximum rate of decrease of power (W/s)=-40000
- Charge sustaining strategy=on
- Fuel cell always on (unless key is off)

5.6.1. Results using the FTP driving cycle

The main outputs of the vehicle system are represented as follows:

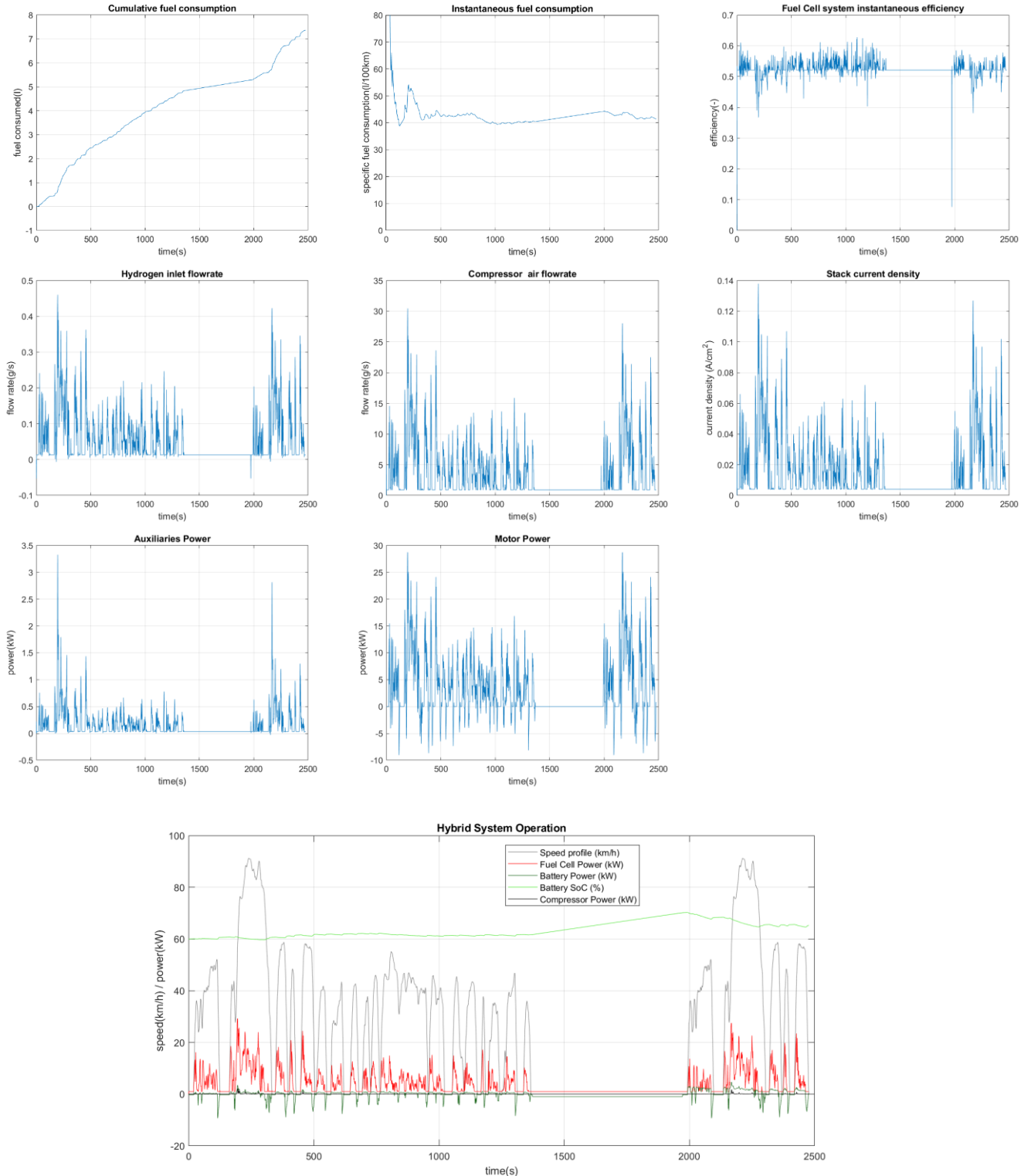


Figure 5.33 – Results on FTP driving cycle: a) Cumulative consumption b) Instantaneous specific consumption c) Fuel cell system efficiency d) Hydrogen flowrate e) Air flowrate f) Current density g) Auxiliary system power h) Motor power i) Hybrid system operation

5.6.2. Results using the NEDC driving cycle

The main outputs of the vehicle system are represented as follows:

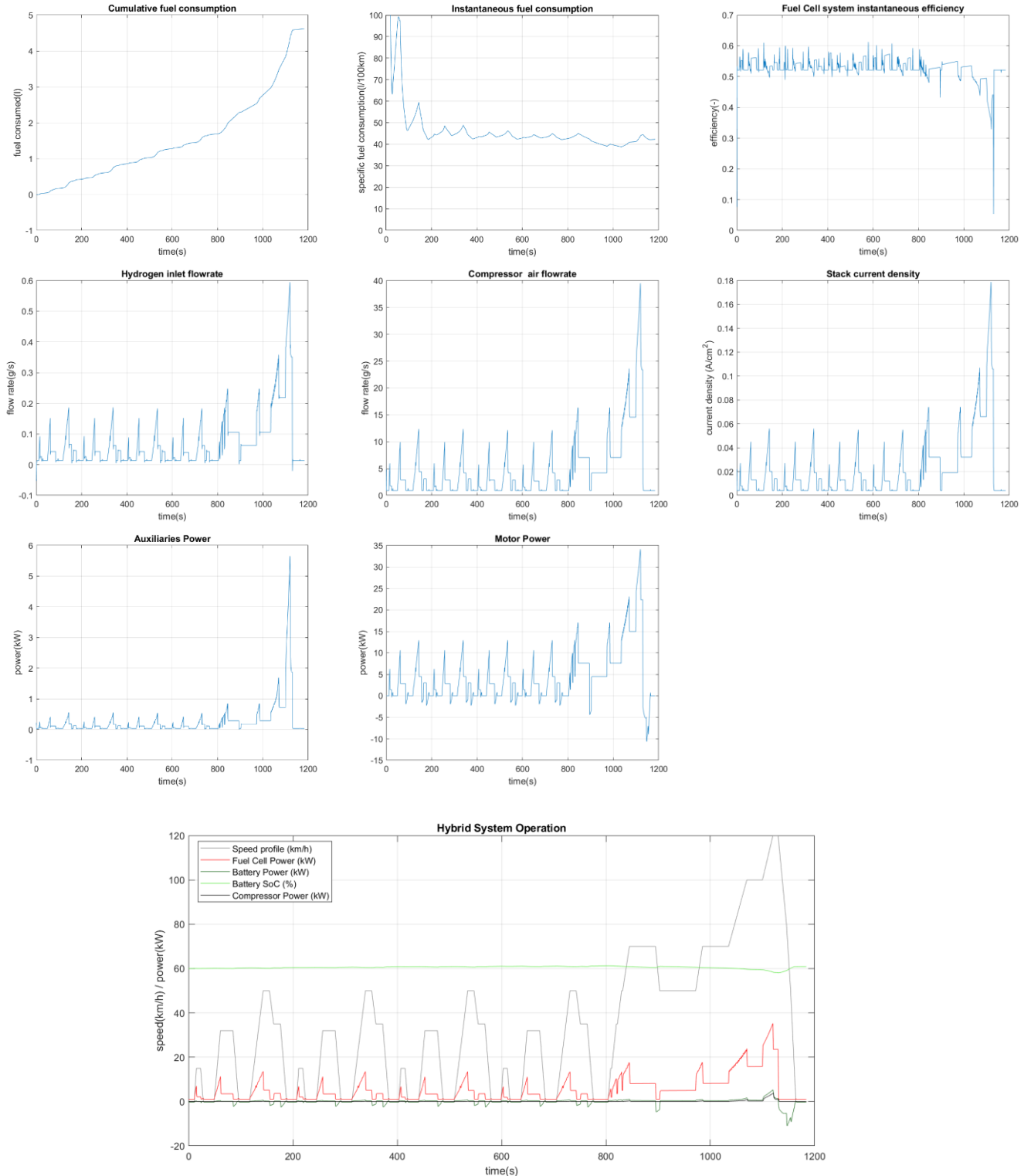


Figure 5.34 – Results on NEDC driving cycle: a) Cumulative consumption b) Instantaneous specific consumption c) Fuel cell system efficiency d) Hydrogen flowrate e) Air flowrate f) Current density g) Auxiliary system power h) Motor power i) Hybrid system operation

5.6.3. Results using the UDDS driving cycle

The main outputs of the vehicle system are represented as follows:

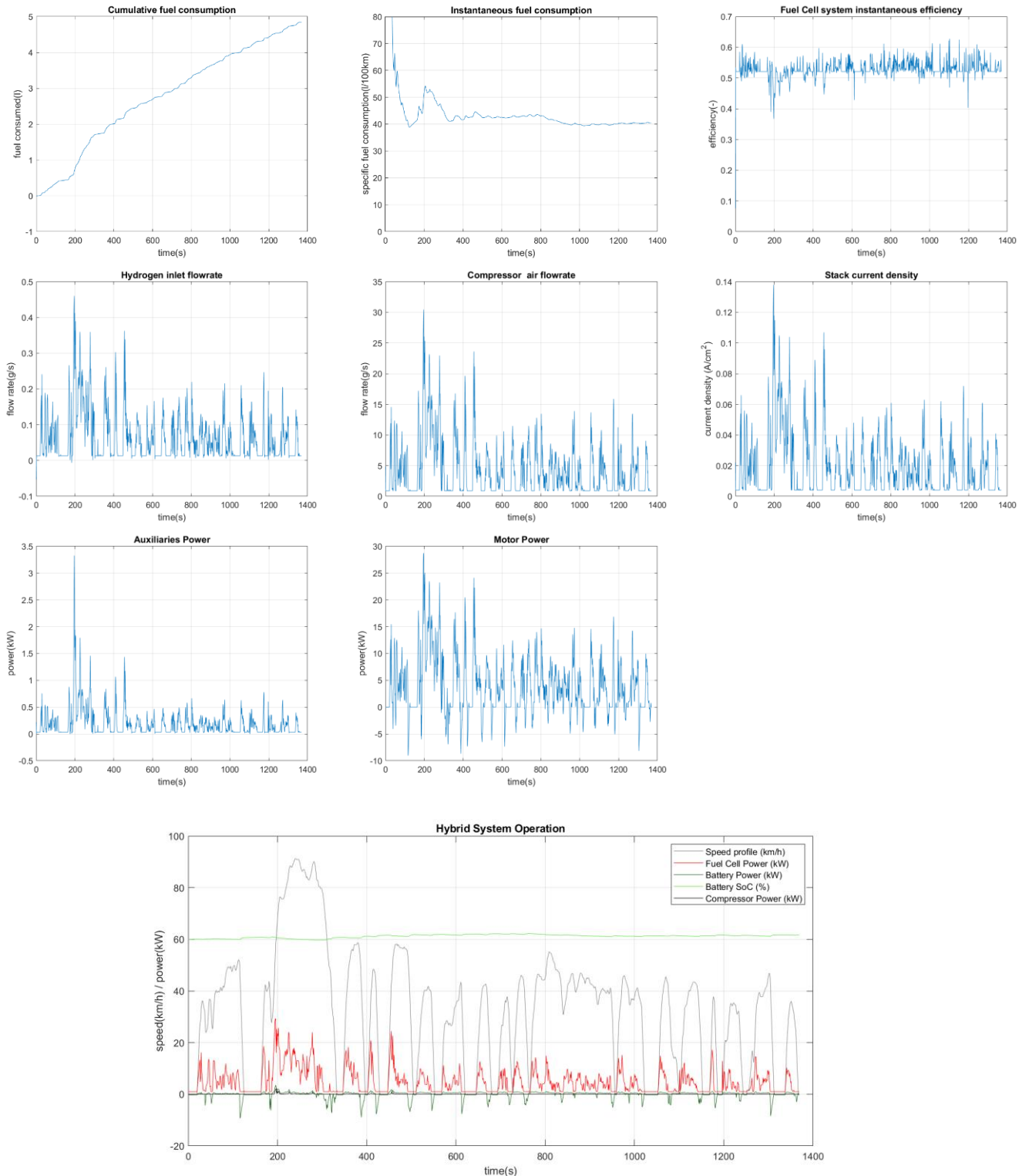


Figure 5.35 – Results on UDDS driving cycle: a) Cumulative consumption b) Instantaneous specific consumption c) Fuel cell system efficiency d) Hydrogen flowrate e) Air flowrate f) Current density g) Auxiliary system power h) Motor power i) Hybrid system operation

5.6.4. Results using the US06 driving cycle

The main outputs of the vehicle system are represented as follows:

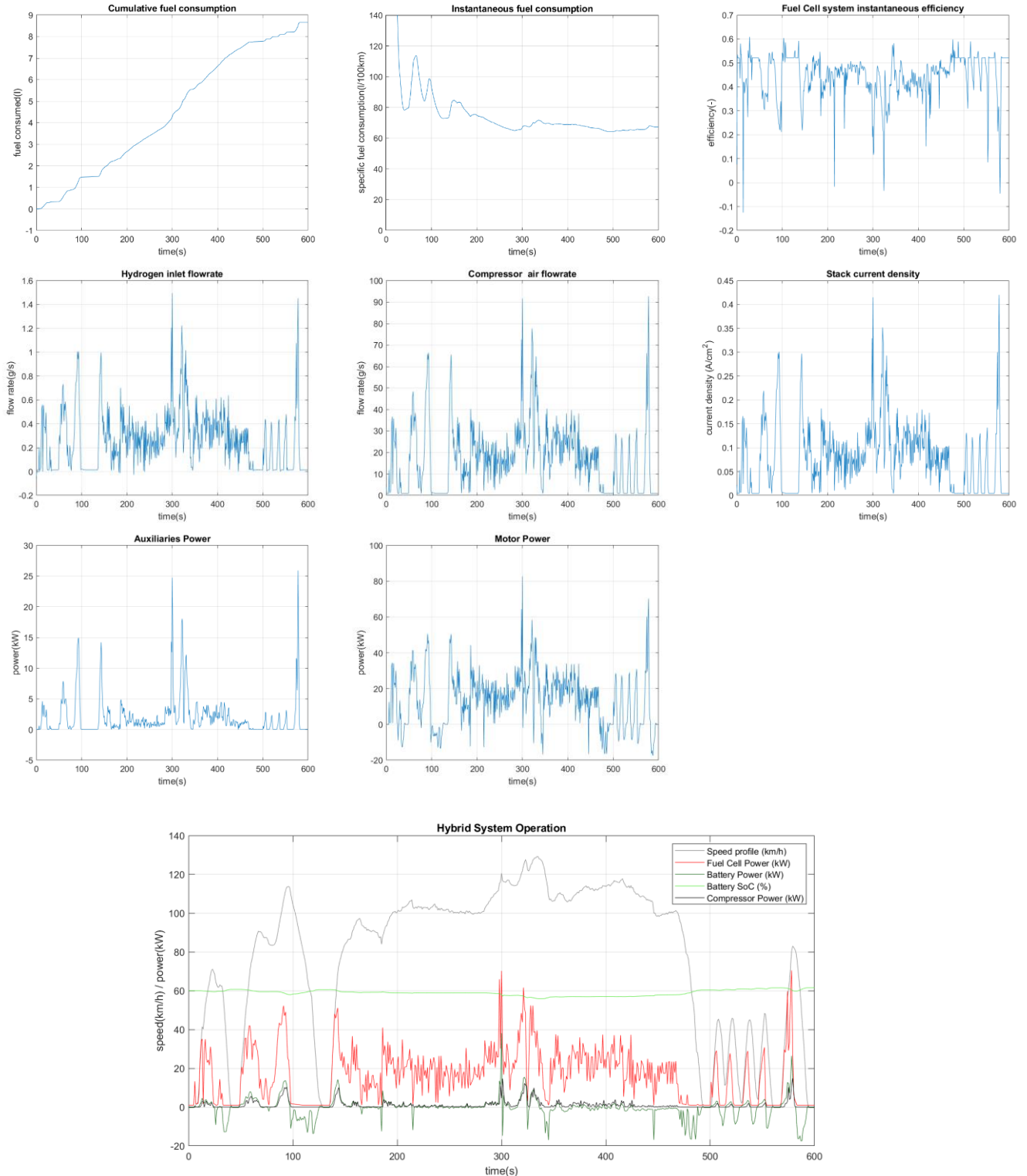


Figure 5.36 – Results on US06 driving cycle: a) Cumulative consumption b) Instantaneous specific consumption c) Fuel cell system efficiency d) Hydrogen flowrate e) Air flowrate f) Current density g) Auxiliary system power h) Motor power i) Hybrid system operation

5.6.5. Results using the WLTP driving cycle

The main outputs of the vehicle system are represented as follows:

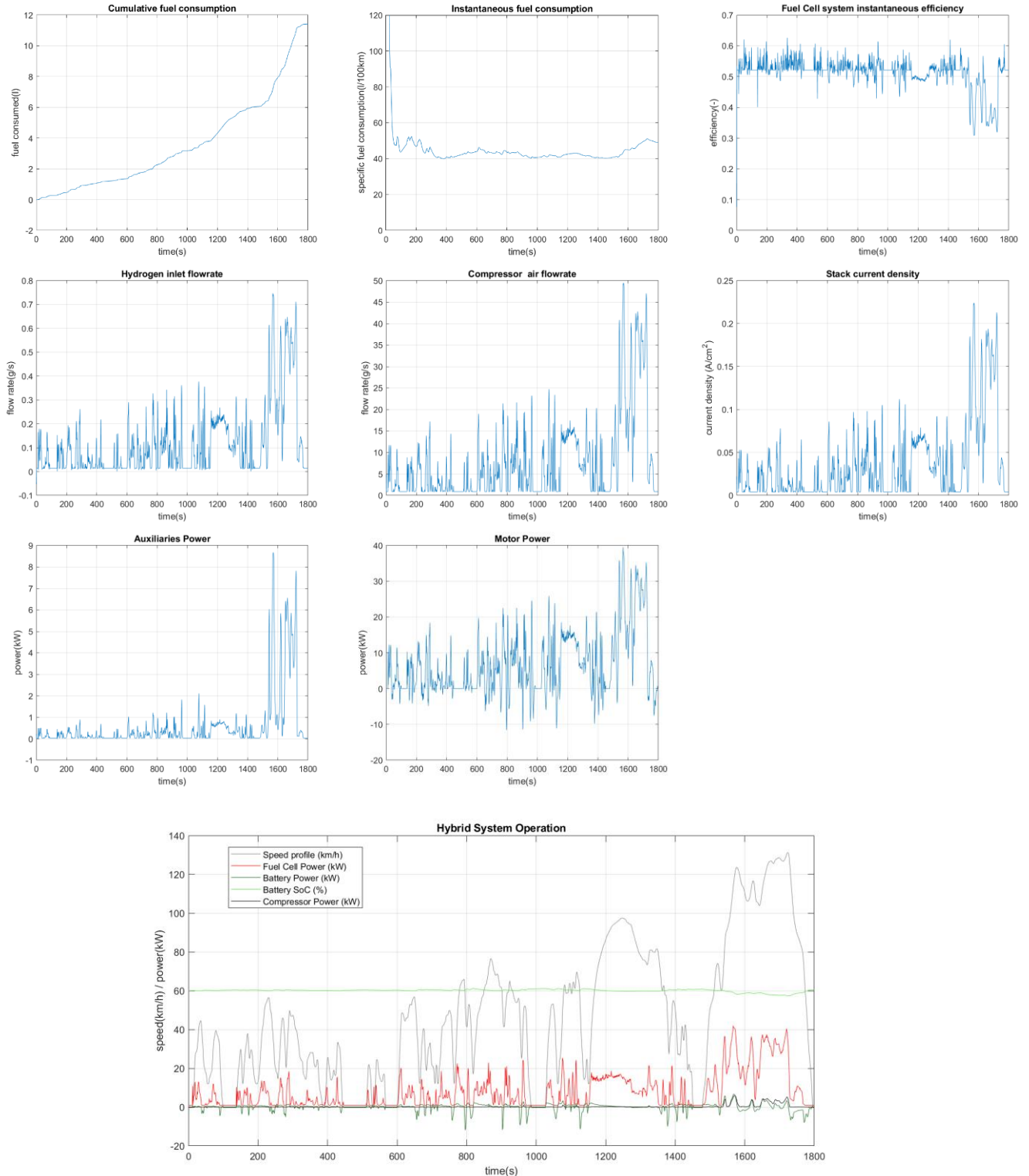


Figure 5.37 – Results on WLTP driving cycle: a) Cumulative consumption b) Instantaneous specific consumption c) Fuel cell system efficiency d) Hydrogen flowrate e) Air flowrate f) Current density g) Auxiliary system power h) Motor power i) Hybrid system operation

5.7. Adaptive control strategy

It tries to find at each time interval the best power split between Fuel Cell and battery through the minimization of a global energy function. In the Simulink, the block diagram has been changed. The Battery operates in charge depleting (CD) mode.

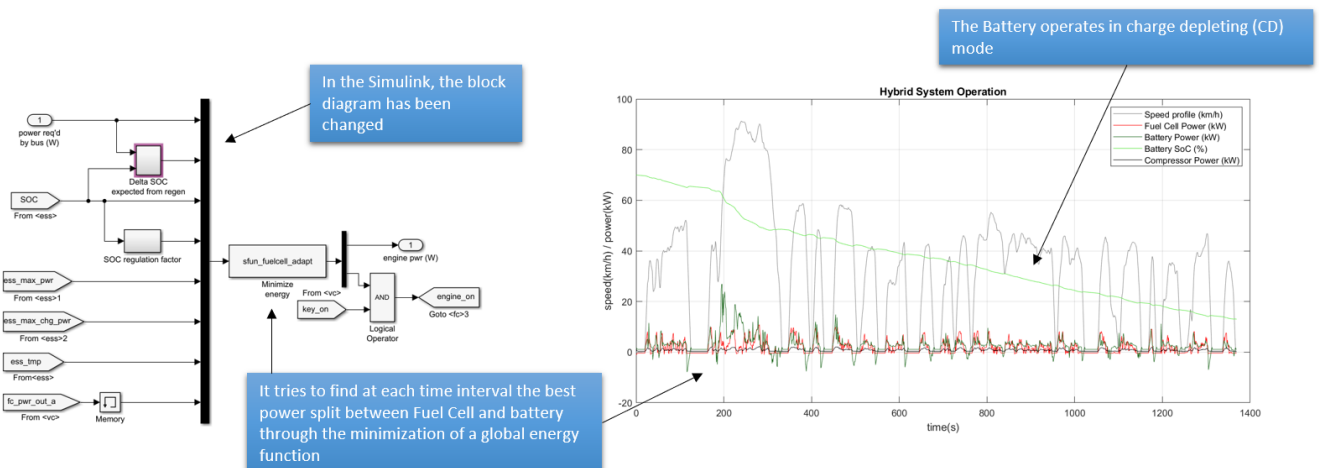


Figure 5.38 – Adaptive control strategy example

Mean controller parameters used (tuned for every cycle to balance the state of charge):

- Initial battery SoC=0.70
- Highest desired battery SoC=0.8
- Lowest desired battery SoC=0.4
- Initial FC state=off
- Minimum operating power (W) = 0
- Maximum operating power (W) [exceeded only if SoC<Lowest desired battery SoC]= 40000
- Corrective factor to keep the battery SoC inside the limits [extra FC power output (W)]=10000
- Minimum time Fc remains off (s) [enforced unless SOC<=Lowest desired battery SoC]=200
- Maximum rate of increase of power (W/s)=3000
- Maximum rate of decrease of power (W/s)=-3000
- Charge depleting strategy=on
- Fuel cell always on
- Regenerative average time (s)=30

5.7.1. Results using the FTP driving cycle

The main outputs of the vehicle system are represented as follows:

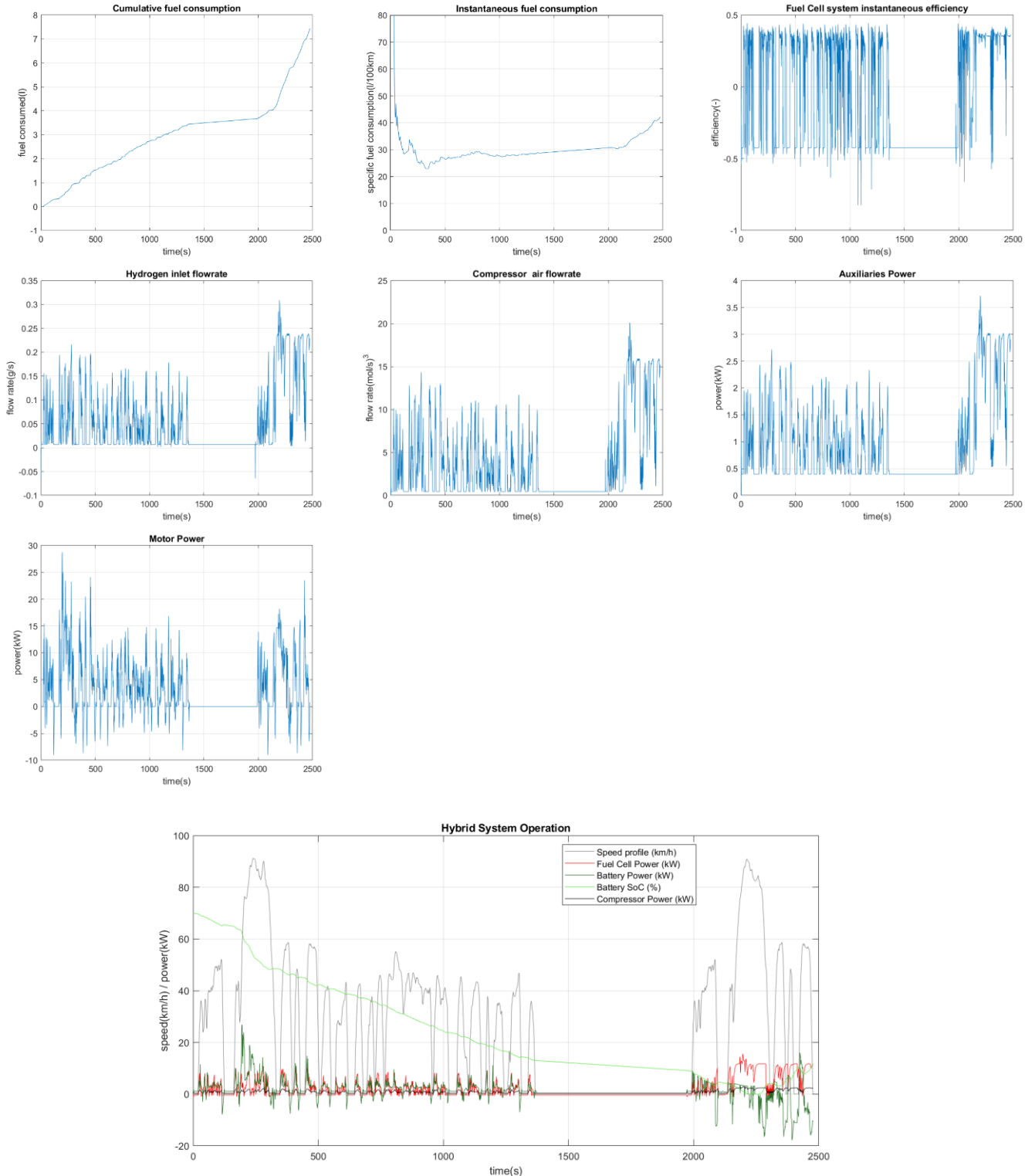


Figure 5.39 – Results on FTP driving cycle: a) Cumulative consumption b) Instantaneous specific consumption c) Fuel cell system efficiency d) Hydrogen flowrate e) Air flowrate f) Auxiliary system power g) Motor power h) Hybrid system operation

5.7.2. Results using the NEDC driving cycle

The main outputs of the vehicle system are represented as follows:

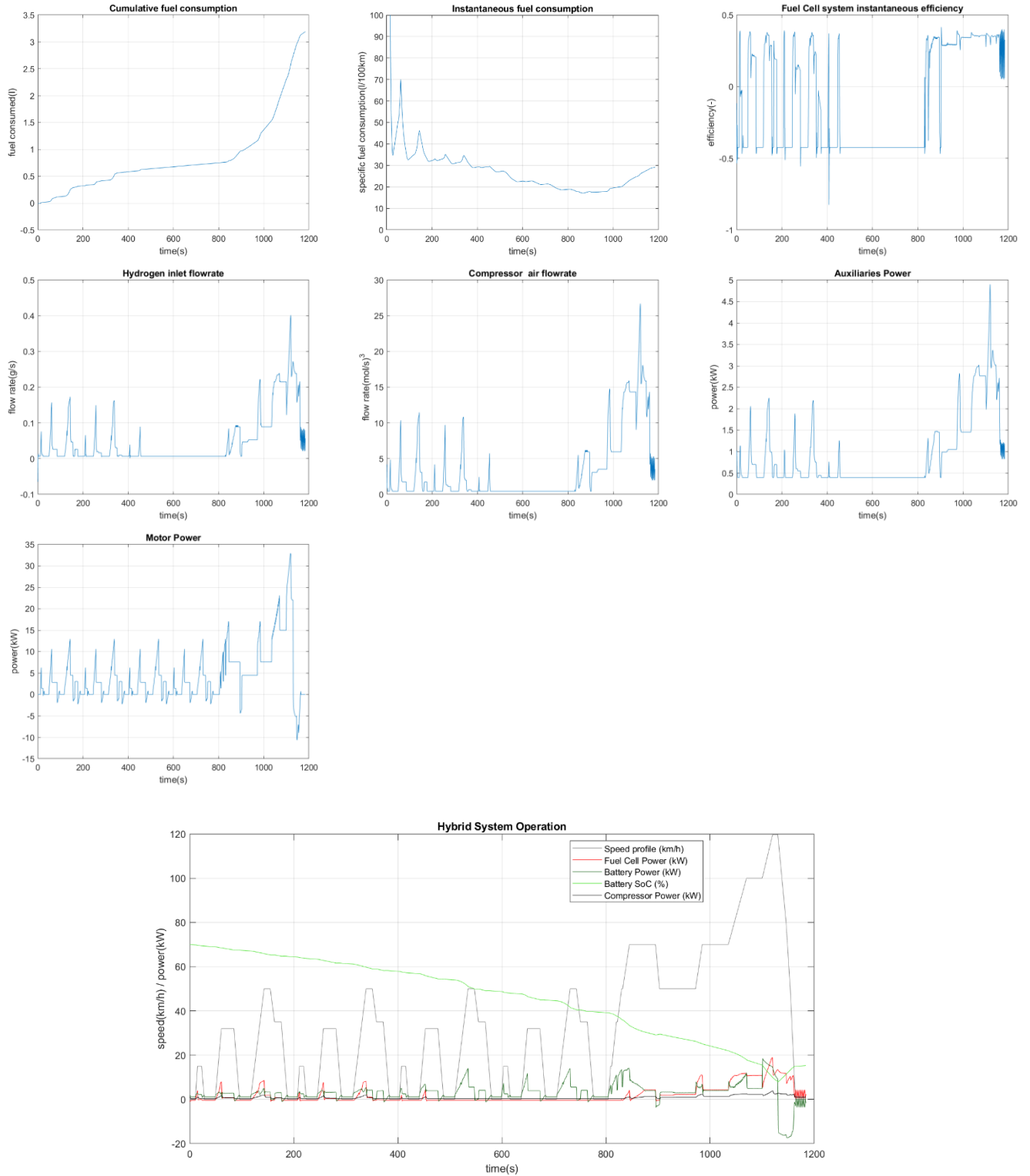


Figure 5.40 – Results on NEDC driving cycle: a) Cumulative consumption b) Instantaneous specific consumption c) Fuel cell system efficiency d) Hydrogen flowrate e) Air flowrate f) Auxiliary system power g) Motor power h) Hybrid system operation

5.7.3. Results using the UDDS driving cycle

The main outputs of the vehicle system are represented as follows:

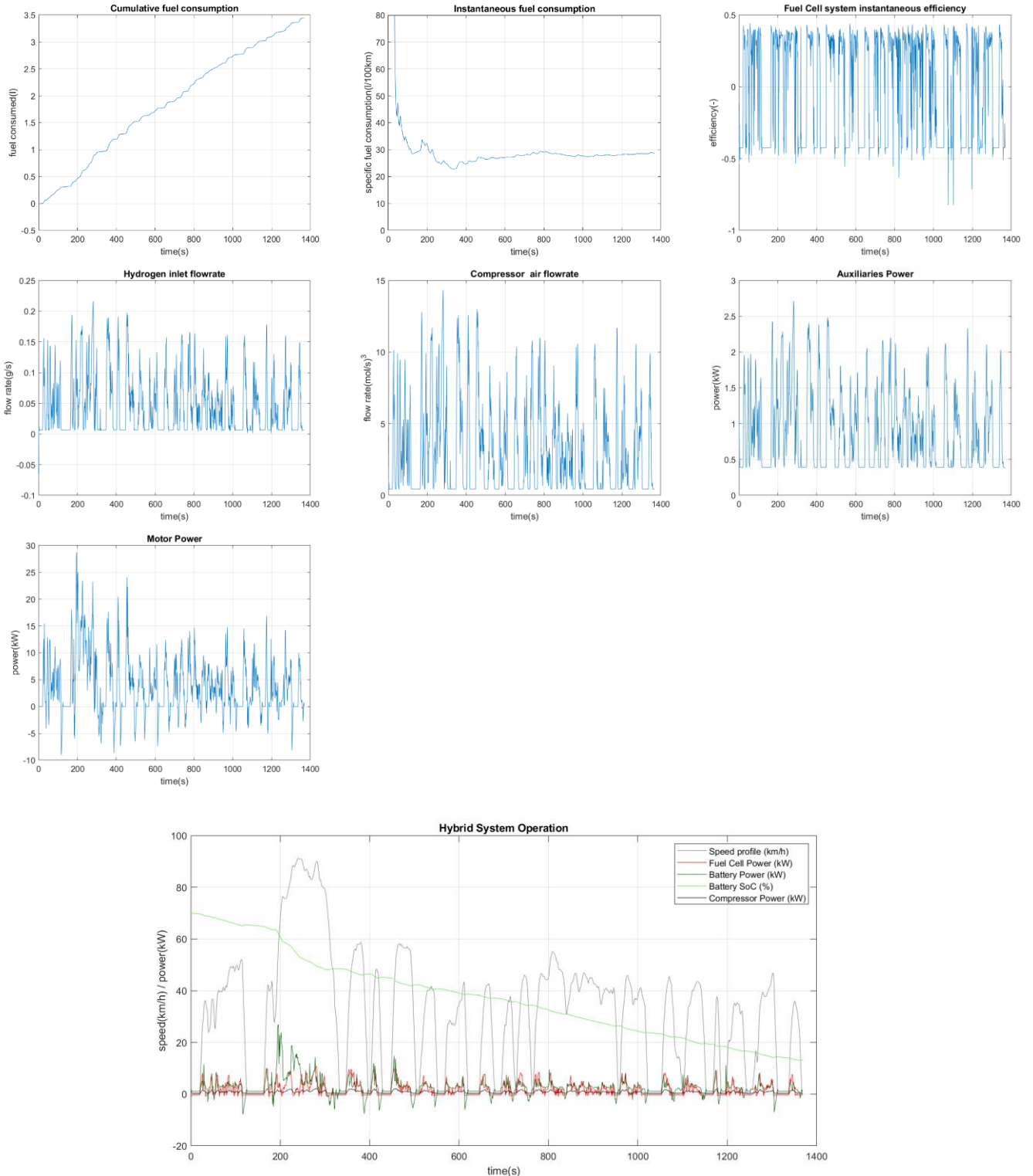


Figure 5.41 – Results on UDDS driving cycle: a) Cumulative consumption b) Instantaneous specific consumption c) Fuel cell system efficiency d) Hydrogen flowrate e) Air flowrate f) Auxiliary system power g) Motor power h) Hybrid system operation

5.8. Control strategies considerations and comparison

A summary table of the results and a comparison graph is represented for the low load cycles.

	FTP			NEDC			UDDS		
	Average cycle fuel consumption (l/100km)	Average efficiency of the fuel cell system during the cycle (-)	Fuel consumed in one cycle (l)	Average cycle fuel consumption (l/100km)	Average efficiency of the fuel cell system during the cycle (-)	Fuel consumed in one cycle (l)	Average cycle fuel consumption (l/100km)	Average efficiency of the fuel cell system during the cycle (-)	Fuel consumed in one cycle (l)
Thermostat control strategy	40.21	0.460	11.30	48.38	0.210	12.38	38.12	0.316	15.99
Range extender control strategy	32.39	0.549	6.75	58.56	0.517	4.33	33.47	0.538	4.69
Mode based control strategy	33.89	0.515	6.93	27.44	0.447	4.61	28.83	0.465	4.78
Constant fuel cell output control strategy	32.64	0.515	6.83	30.29	0.444	4.36	28.04	0.466	4.73
Strong load following control strategy	43.71	0.525	7.36	46.84	0.525	4.62	44.82	0.528	4.84
Adaptive control strategy	30.43	-0.059	7.45	27.20	-0.102	3.19	29.29	-0.006	3.45

Table 5.1 – Low load cycles results

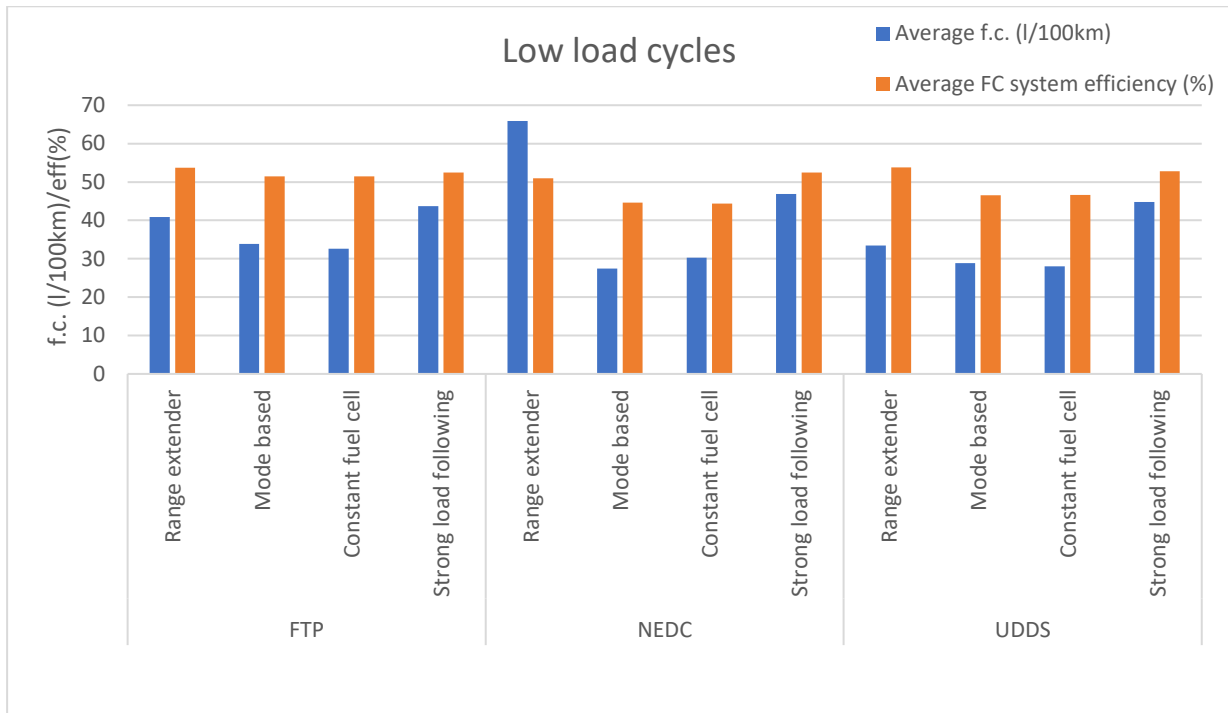


Table 5.2 – Low load cycles comparison

The thermostat control strategy has not been displayed because its results were not convenient in any cycle.

The adaptive control strategy has not been displayed even if it gave low fuel consumption values because it would be necessary to know in advance the profile to avoid discharging the battery too early. It could be a good solution for Plug-in hybrids working in the city.

The best results in these cycles were given by the Constant fuel cell output in the FTP and UDDS and by the Mode based in the NEDC.

Good values were achieved also with the Strong load following control strategy (higher consumption but higher efficiency which imply a higher usage of the fuel cell).



Also for the high load cycles, a summary table of the results and a comparison graph are represented (the adaptive control strategy could not follow the speed profile in the high load cycles and so they were not displayed):

	US06			WLTP		
	Average cycle fuel consumption (l/100km)	Average efficiency of the fuel cell system during the cycle (-)	Fuel consumed in one cycle (l)	Average cycle fuel consumption (l/100km)	Average efficiency of the fuel cell system during the cycle (-)	Fuel consumed in one cycle (l)
Thermostat control strategy	67.60	0.379	11.37	168.14	0.376	33.67
Range extender control strategy	67.48	0.456	8.41	58.50	0.420	13.14
Mode based control strategy	56.57	0.406	8.72	60.10	0.472	12.37
Constant fuel cell output control strategy	62.90	0.460	7.92	74.43	0.512	12.04
Strong load following control strategy	106.96	0.449	8.67	60.48	0.511	11.42
Adaptive control strategy	-	-	-	-	-	-

Table 5.3 – High load cycles results

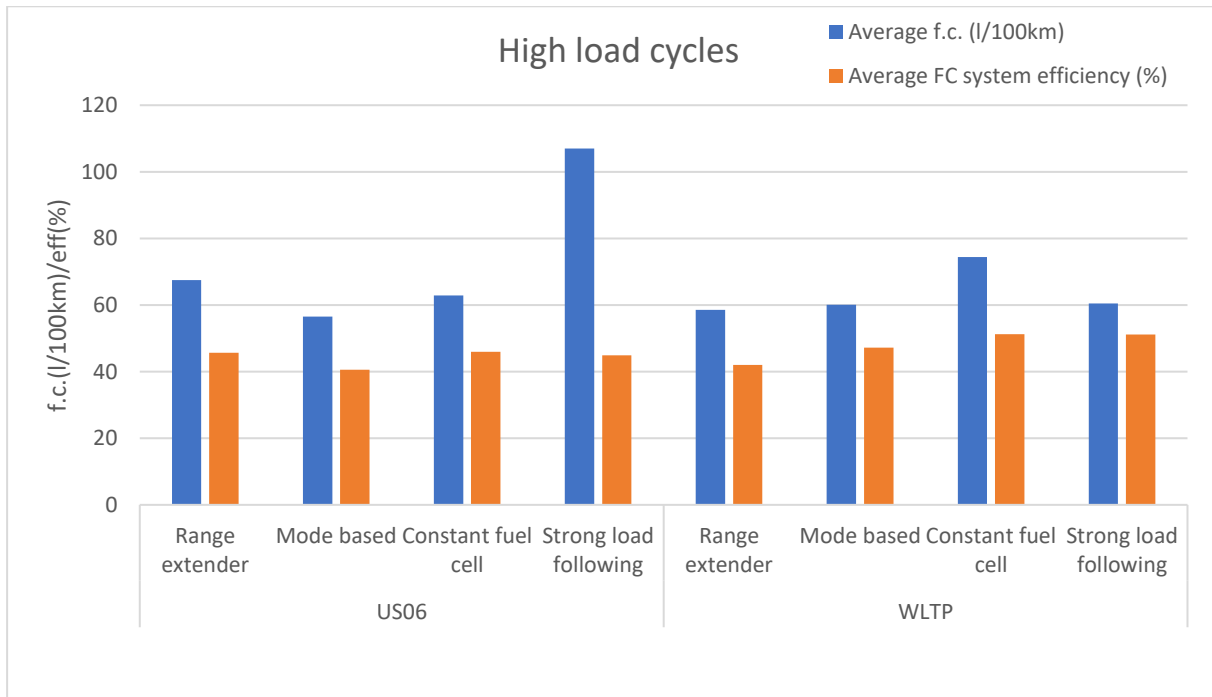


Table 5.4 – High load cycles comparison

The thermostat control strategy has not been displayed because its results were not convenient in any cycle.

The adaptive control strategy has not been displayed even if it gave low fuel consumption values because it would be necessary to know in advance the profile to avoid discharging the battery too early. It could be a good solution for Plug-in hybrids working in the city.

In the US06, the Constant fuel cell output control strategy has higher efficiency and higher fuel consumption than the Mode based control strategy. This could be explained by the less usage of the battery.

In the WLTP, the Mode based and the Strong load following have very similar outputs while the Constant fuel cell consumes a little bit more.

The Toyota Mirai control strategy has a behavior close to the Strong load following one tested here. This could be due to the fact that the results of this control strategy are satisfying both for the low load and high load cycles. It is also the more versatile not knowing in advance the cycle.

6. Simulating Toyota Mirai

Since it has been found that the simulation method of the control strategies was stable, for validation purposes the data used for the vehicle simulation has been put as close as possible to the one of the 2017 Toyota Mirai fuel cell vehicle. This allowed comparing the simulation results to the ones obtained by reverse engineering in the test bench of the Argonne National Lab (ANL) [20]. In the following sections, the main assumptions done in the simulation are described. In the modelling of the components Toyota data has been picked if declared, if those data were not present they were picked by the Argonne testing results and if they were not present even there, data of vehicles with similar technologies have been picked. After having described the vehicle modelling, the results of the simulations are shown.

6.1. Chassis and load parameters modelling

Parameters:

- Vehicle curb weight (with standard equipment and without any passenger): 1850 kg (source: Toyota datasheets)
- Frontal area: it has roughly been considered $0.8 \times \text{width} \times \text{height} = 2.23 \text{ m}^2$
- Weight fraction in front when standing still: it has been put equal to 0.55 since the new Mirai 2021 declared a distribution of 0.5/0.5 and has 3 tanks with another one behind the rear wheels. This value is also consistent for a front wheel drive car.
- Centre of gravity (CoG) height: it has roughly been put at $\frac{1}{4}$ of the total height (considering the component distribution) $\rightarrow 0.385 \text{ m}$
- Cargo Mass: Two passengers of 75 kg + 40 kg of luggage have been considered. Total: 190kg
- Wheel dimensions: 215/55R17 (source: Toyota datasheets)
- Drag coefficient: 0.29 (source: Toyota datasheets)

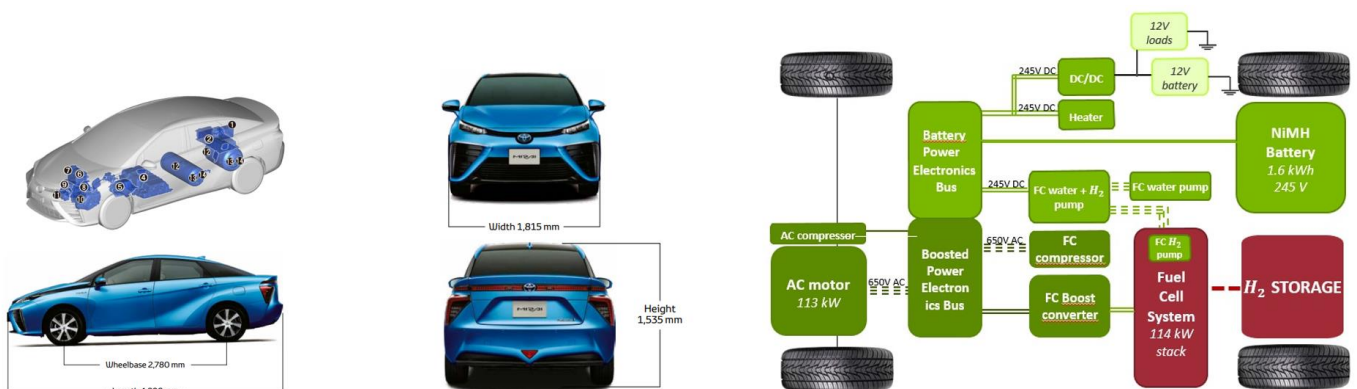


Figure 6.1 – Toyota Mirai dimensions and components distribution

6.2. Battery modelling

Toyota Mirai is equipped with a 6.5 Ah Nickel Metal Hydride battery (244.8V).

The most similar battery data found was of the 1998 Prius [21] (source: NREL testing on Insight which has the same battery of Prius with 20 modules instead of 40). The 1998 Prius shape of the parameters taken into account has been kept, but they have been adapted to the different nominal values given by Toyota datasheets for Toyota Mirai.

Number of modules= 40
Minimum voltage of the module: 6 V
Maximum voltage of the module: 9 V
Module mass:1.09 kg

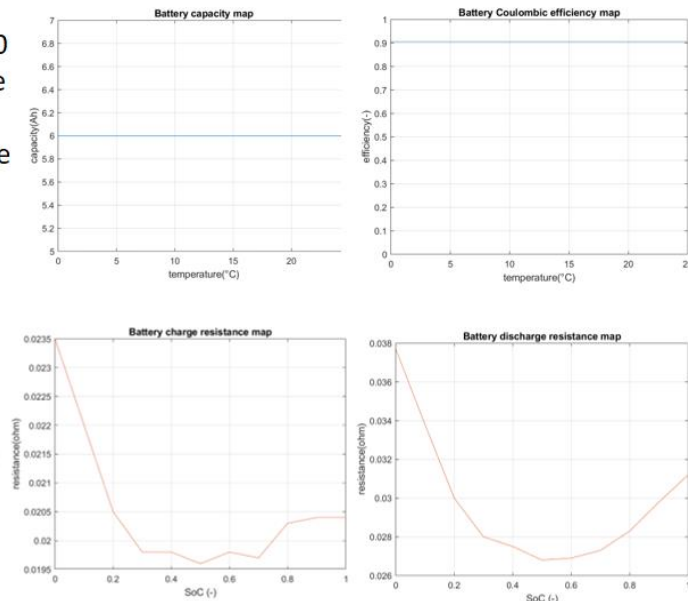


Figure 6.2 – Battery used in the 1998 Toyota Prius: 6 Ah 288V NiMe

Number of modules= 34
Minimum voltage of the module: 4 V
Maximum voltage of the module: 9.5 V
Module mass:1.37 kg

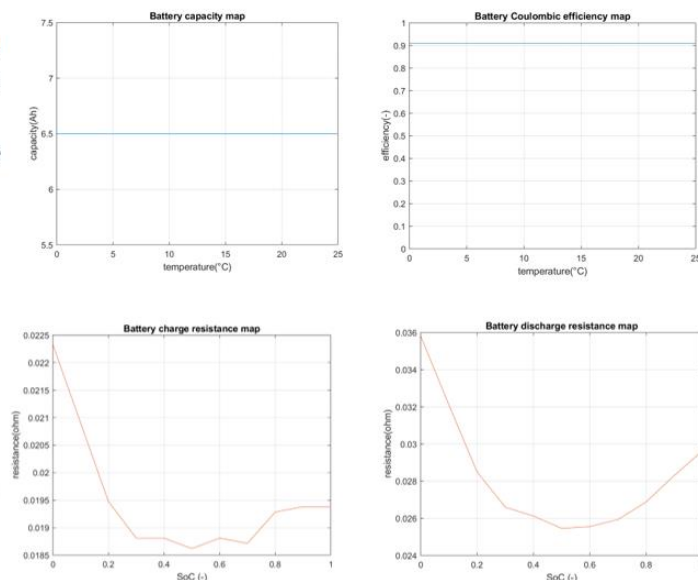


Figure 6.3 – Toyota Mirai 2017 6.5 Ah 244.8V NiMe battery estimation

6.3. Electric motor modelling

The electric motor of Toyota Mirai is a 114-kW AC Permanent magnet Electric generator (335 Nm max). The most similar motor data found was of the 2010 Toyota Prius [22]. Prius is not a Fuel Cell Vehicle but it is a hybrid vehicle with a motor similar to the Mirai one (both are permanent magnet motors and the technology could be similar because they are of the same brand).

To construct the Mirai motor map the efficiencies of the 2010 Prius have been imitated, while the torque-speed characteristic has been constructed in order to satisfy the max power constraint at the base speed with the maximum torque given by Toyota datasheets (335 Nm).

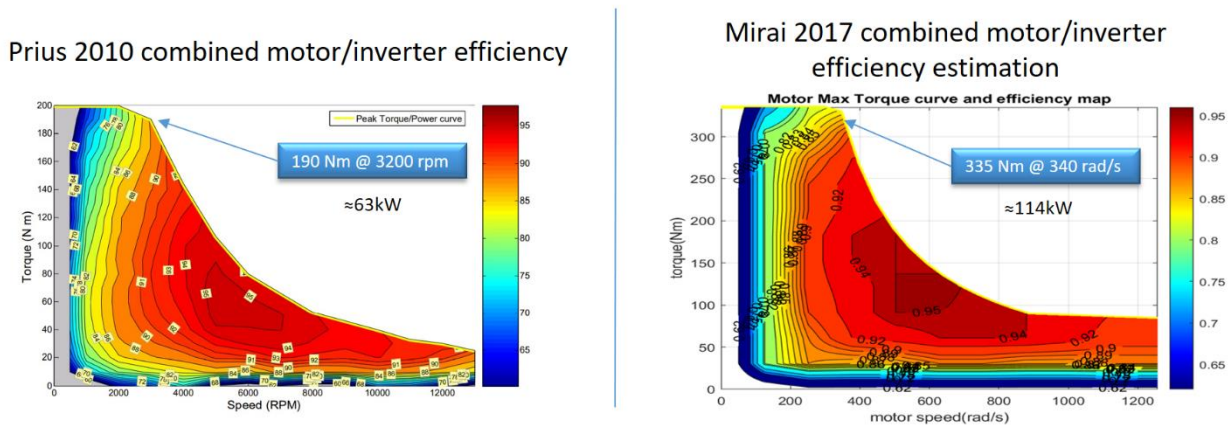


Figure 6.4 – Prius 2010 and Toyota Mirai motor modelling comparison

6.4. Fuel Cell system modelling

The following data were found for the Toyota Mirai fuel cell system:

- Maximum output electric power of stack: 114 kW
- Number of cells in a stack: 370
- Exchange current density: $1.9 \frac{A}{cm^2}$
- Single cell voltage: 0.67 V
- Total tanks volume/weight: 122.4 l - 88 kg

The only data available were Toyota datasheets and the Argonne reverse engineering tests. The KTH model has been used as a starting point and has been modified to respect the requirements imposed by the Toyota Mirai system.

At first the stack efficiency curve has been found by the Argonne lab testing data and then it has been reconstructed sampling point by point.

The KTH model calculates iteratively the number of cells needed and the current density needed to satisfy the power requirement. The Mirai instead has a fixed number of cells in the stack and has a predetermined current density range. For this reason the iterative procedure has been removed and instead the polarization curve (with the power lines intersected) present in the Argonne data has been used. The KTH model sets an initial current density value and a minimum voltage of the cell. It calculates then the voltage of the cell using the equivalent circuit

and the present value of current density. After the voltage is calculated the current density is incremented by one step. This iterative procedure continues until the cell voltage limit is not respected anymore. The cell number required is then found as the total power required to the stack divided by the power that the single cell can give.

Instead of the KTH method, a polarization curve method used to find current density and cell voltage has been used. The polarization curve map with the power lines has been reconstructed sampling point by point in the following way:

1. Pick a power value
2. Find the intersection with the curve
3. Read the current density and the cell voltage values

This map is interpolated during the operations starting from the effective power required (which is given by the previous block).

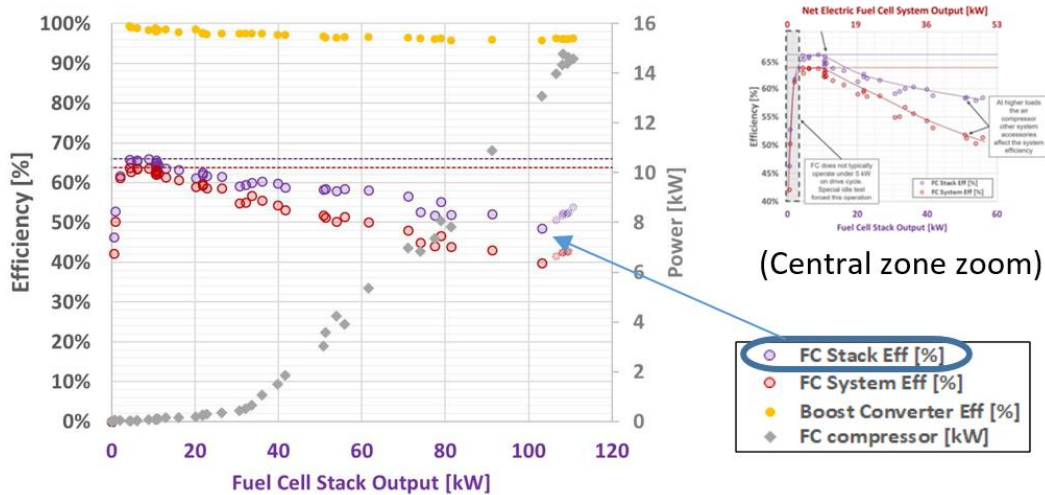


Figure 6.5 – Stack efficiency measured by the Argonne LAB

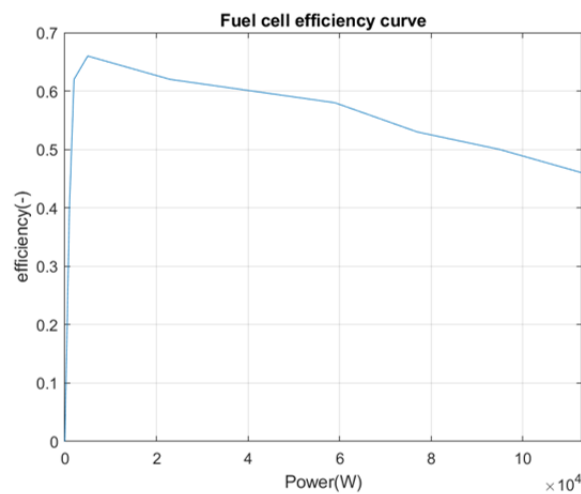


Figure 6.6 – Stack efficiency curve used in the simulation (found sampling the curve in figure 6.5)

```

i=0.1 [A/cm2]
Ecell=0.8 [V]
} Initial values imposed

while (Ecell>0.75)
Ecell=Voc-(R2*(Tcell+273))/(0.5*F)*log(i/(j0*Po))-i*Rm;
i=i+0.001;
end;

if N==0
N=Pe1/(i*A*Ecell);
else
N=N;
end
} The cell number required
is found as the total
power required to the
stack divided by the
power that the single cell
can give

Iterative
operation
continues
until the cell
voltage limit
is not
respected
anymore

```

Figure 6.7 – KTH iterative procedure

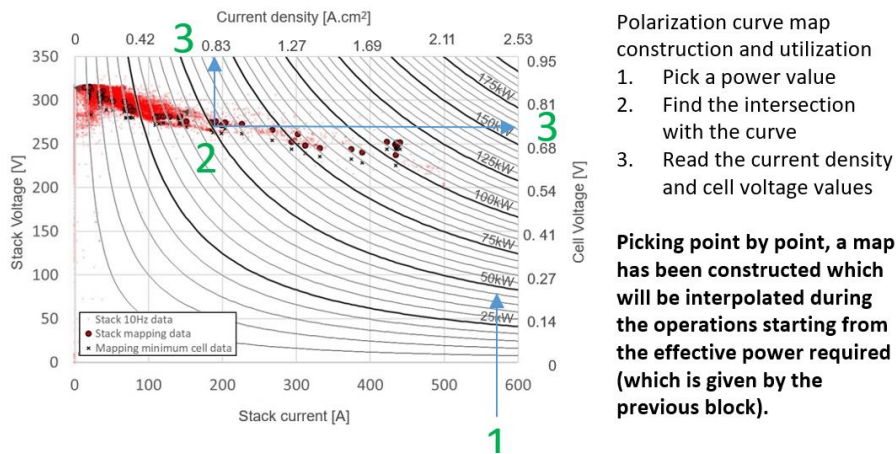


Figure 6.8 – Polarization curve method

The difference in cell number and current density with the two methods is substantial. The method used with the polarization curve gives results closer to the real operation of Toyota Mirai.

The results with the KTH iterative method are very different from those of Toyota Mirai. The cell number found by iteration in the US06 cycle is 1594 (very different from Mirai which has 370 cells).

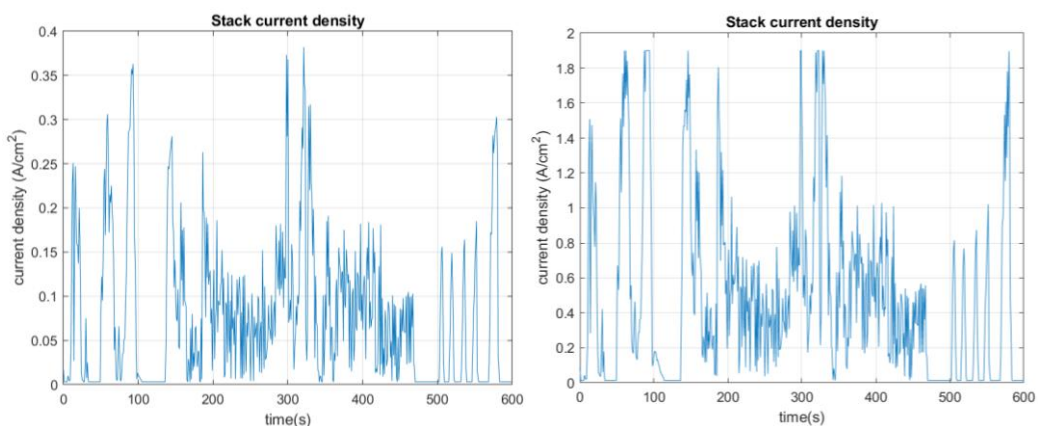


Figure 6.9 – Current density with KTH method (left) / with Polarization curve method (right)

For what concerns the Fuel cell stack auxiliaries, the air compressor map has been found by reverse from some graphs of the Argonne testing, while the other auxiliaries modelling have been kept as the KTH model (Bernoulli approach) because of the lack of data.

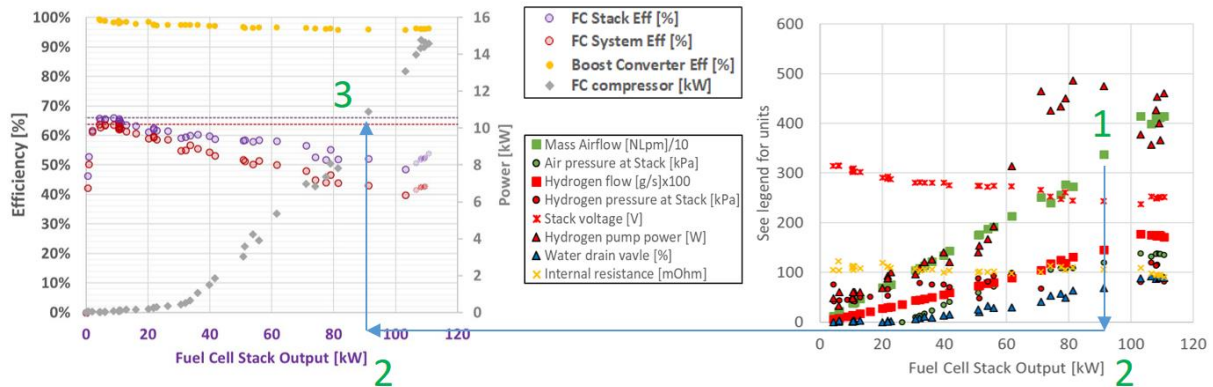


Figure 6.10 – Air compressor map estimation procedure

To find the compressor power for each mass airflow value this procedure has been followed:

1. Pick a mass airflow point from the graph at the right
2. Find the corresponding Stack output power
3. Pick the corresponding compressor power from the graph at the left

To find the air pressure at the stack for each mass airflow value it is sufficient to watch the graph at the right.

To find the corresponding temperature, consider an isentropic transformation with $\gamma=1.4$.

$$T_2 = T_1 \left(\frac{P_2}{P_1} \right)^{\frac{\gamma-1}{\gamma}} \quad (6.1)$$

6.5. Parameters not taken into account: humidifier-less stack

Differently from the other fuel cell systems, Toyota Mirai's one does not have the external humidifiers at the anode and cathode inlets [23]. The water generated downstream of the cathode is returned upstream of it through internal circulation inside the anode. This is helped by the fact that in the system, air and hydrogen flow are in opposite directions in order to make water recirculation easier. Conventional stacks use straight grooves which have the problem of water accumulation which is a problem for oxygen diffusion and gives a non-uniform power generation. The Toyota Mirai system has a complex 3D mesh air flow field which promotes the oxygen diffusion to the catalyst layer using turbulence. The shape has also been optimized to draw the excess water generated at the electrode to the back surface. In the simulations it has not been considered that the Mirai stack is humidifier-less.

This has been done in order to simplify the analysis and keep the validity of the results also for more general systems.

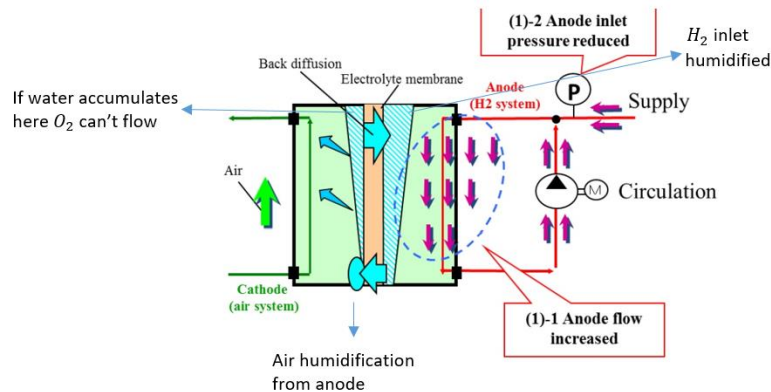


Figure 6.11 – Opposite flow directions and water recirculation in humidifier-less system

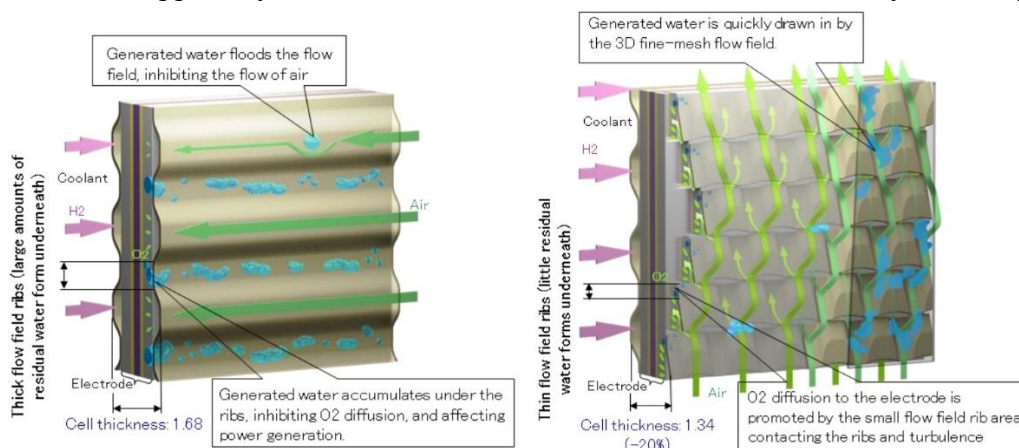


Figure 6.12 – Conventional flow field structure (left) / 3D Toyota flow field structure (right)

6.6. Simulation results

Five different driving cycles have been tested: FTP, NEDC, UDDS, US06, WLTP

Only the strong load following strategy has been tested since it has been previously found to be the more similar to how Toyota Mirai operates. The parameters used in the control strategy block have been fitted to be as close as possible to the real operation of the car:

- Initial battery SoC=0.60
- Highest desired battery SoC=0.68
- Lowest desired battery SoC=0.52
- Initial FC state=off
- Minimum operating power (W)=1000
- Maximum operating power (W) [exceeded only if SoC<Lowest desired battery SoC]=113000
- Corrective factor to keep the battery SoC inside the limits [extra FC power output (W)]=20000
- Minimum time Fc remains off (s) [enforced unless SOC<=Lowest desired battery SoC]=0
- Maximum rate of increase of power (W/s)=150000
- Maximum rate of decrease of power (W/s)=-150000
- Charge sustaining strategy=on
- Fuel cell always on (unless key is off)

6.6.1. Results using the FTP driving cycle

The main outputs of the vehicle system are represented as follows:

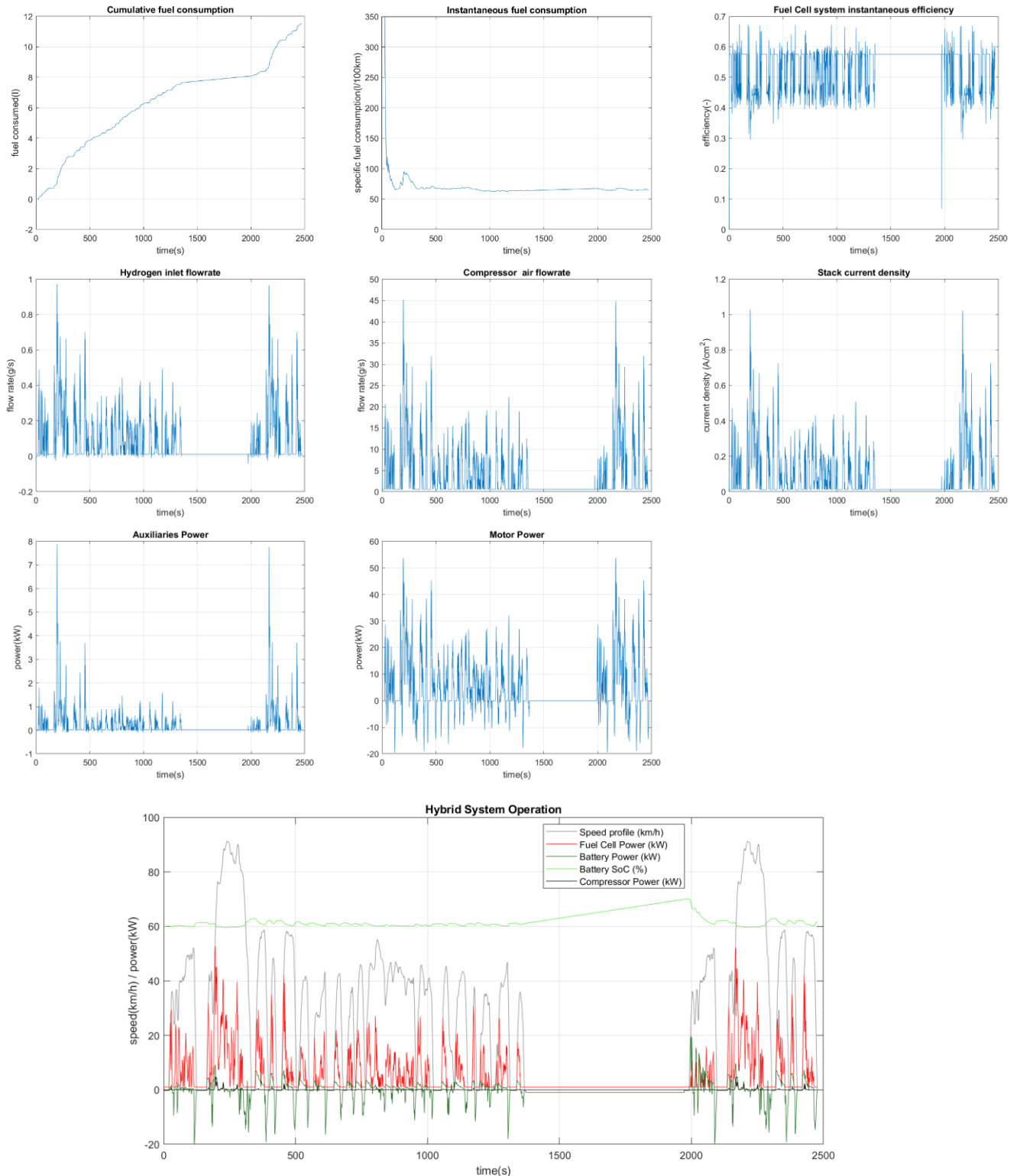


Figure 6.12 – Results on FTP driving cycle: a) Cumulative consumption b) Instantaneous specific consumption c) Fuel cell system efficiency d) Hydrogen flowrate e) Air flowrate f) Current density g) Auxiliary system power h) Motor power i) Hybrid system operation

6.6.2. Results using the NEDC driving cycle

The main outputs of the vehicle system are represented as follows:

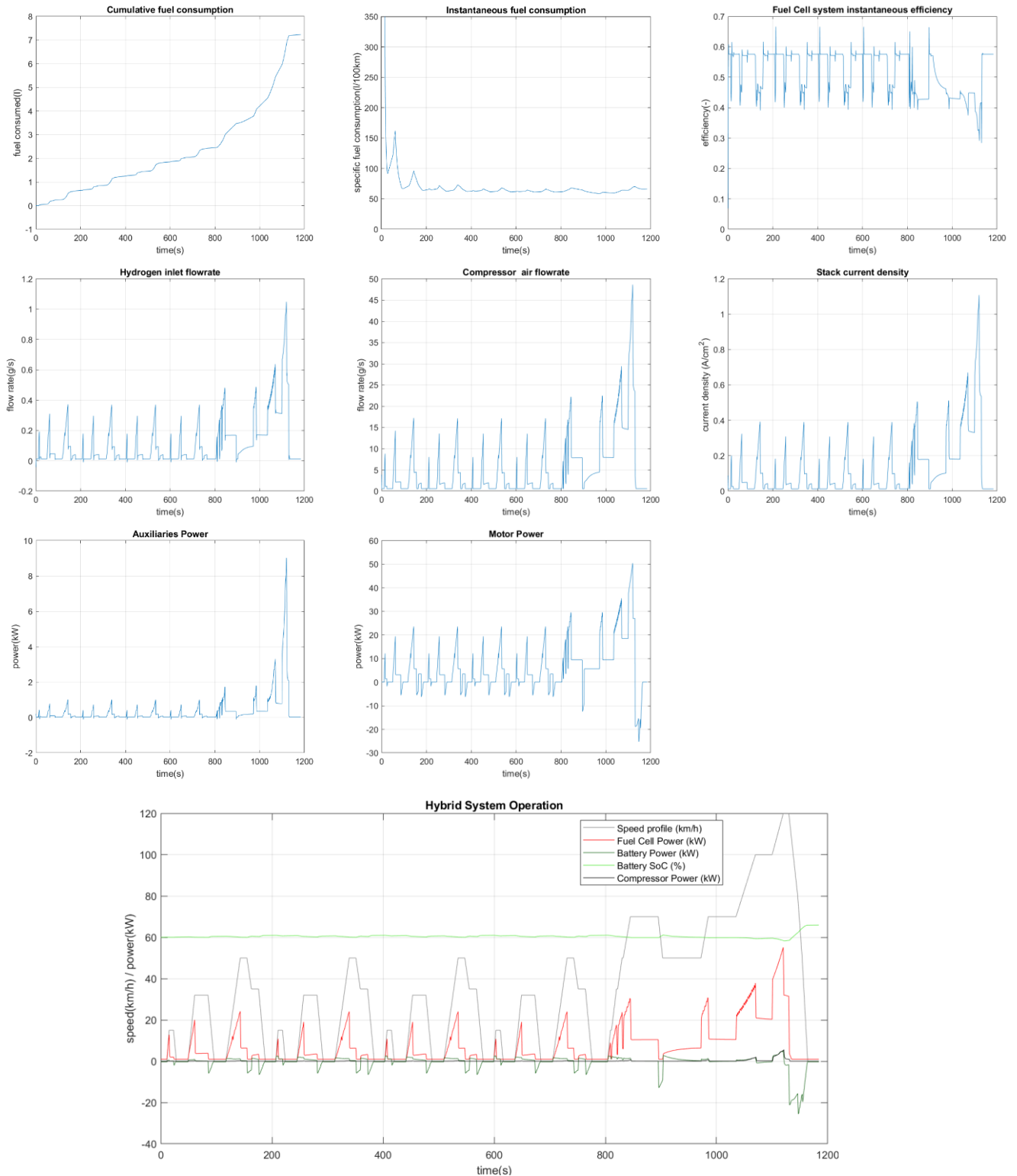


Figure 6.13 – Results on NEDC driving cycle: a) Cumulative consumption b) Instantaneous specific consumption c) Fuel cell system efficiency d) Hydrogen flowrate e) Air flowrate f) Current density g) Auxiliary system power h) Motor power i) Hybrid system operation

6.6.3. Results using the UDDS driving cycle

The main outputs of the vehicle system are represented as follows:

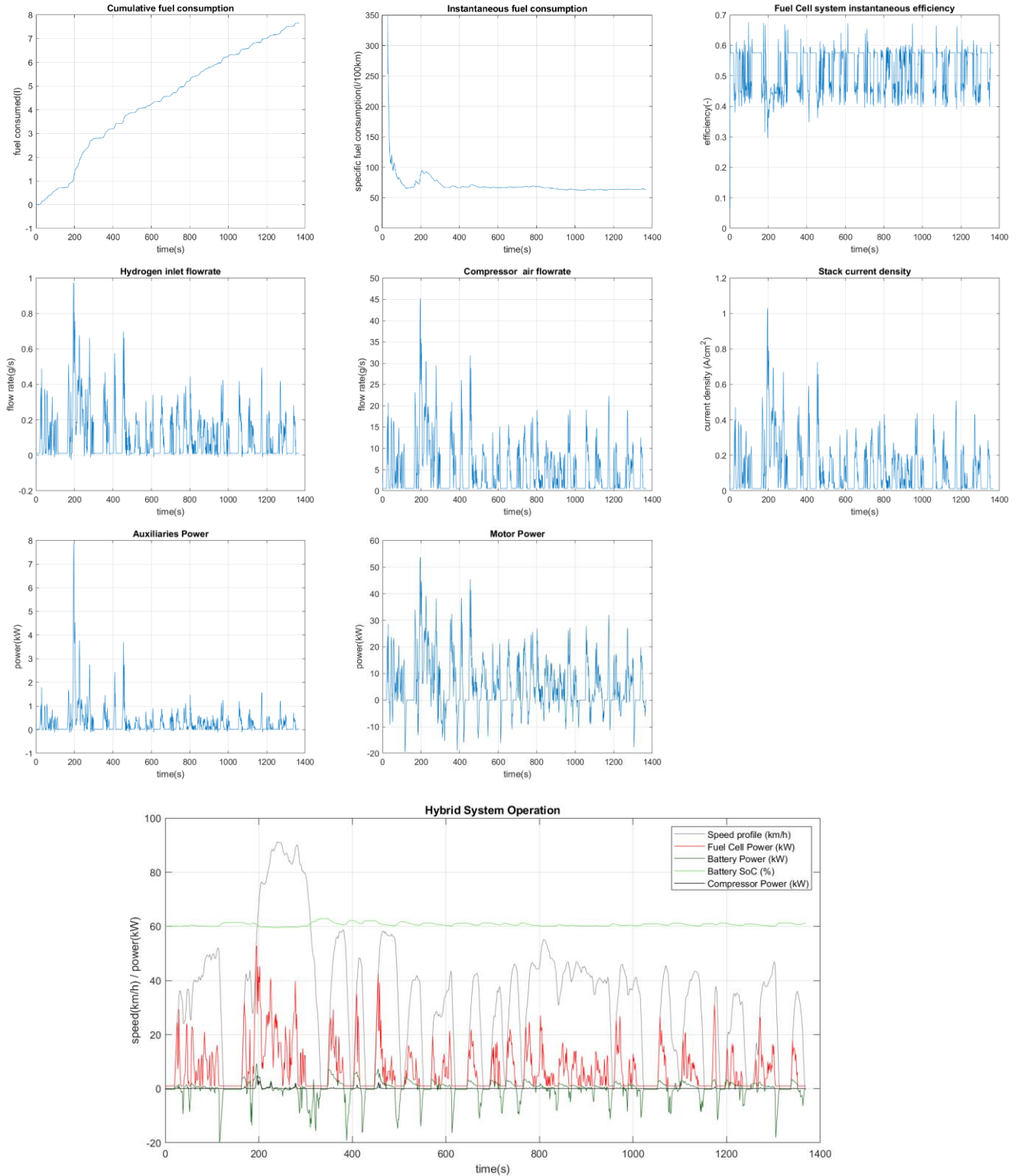


Figure 6.14 – Results on UDDS driving cycle: a) Cumulative consumption b) Instantaneous specific consumption c) Fuel cell system efficiency d) Hydrogen flowrate e) Air flowrate f) Current density g) Auxiliary system power h) Motor power i) Hybrid system operation

6.6.4. Results using the US06 driving cycle

The main outputs of the vehicle system are represented as follows:

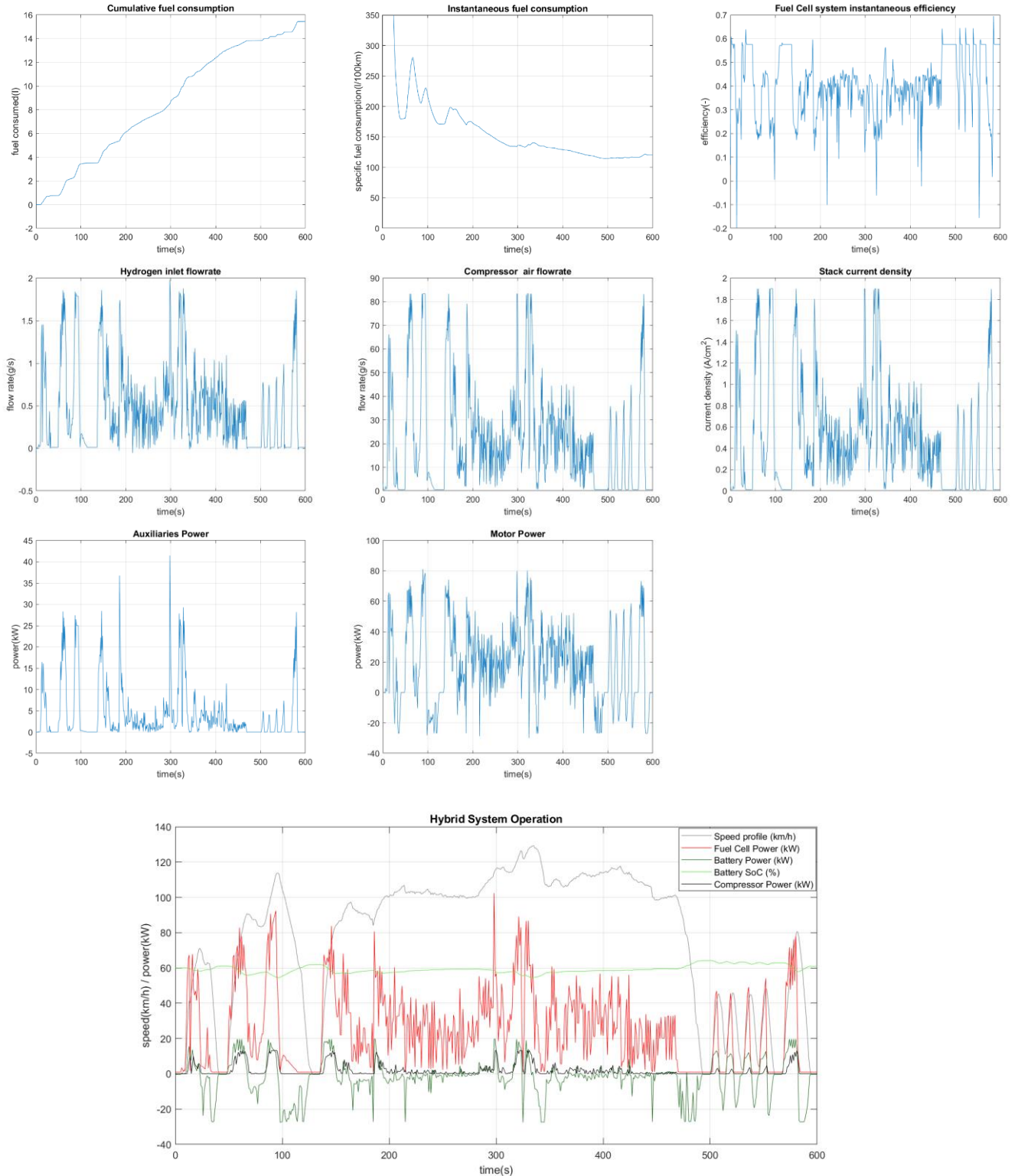


Figure 6.15 – Results on US06 driving cycle: a) Cumulative consumption b) Instantaneous specific consumption c) Fuel cell system efficiency d) Hydrogen flowrate e) Air flowrate f) Current density g) Auxiliary system power h) Motor power i) Hybrid system operation

6.6.5. Results using the WLTP driving cycle

The main outputs of the vehicle system are represented as follows:

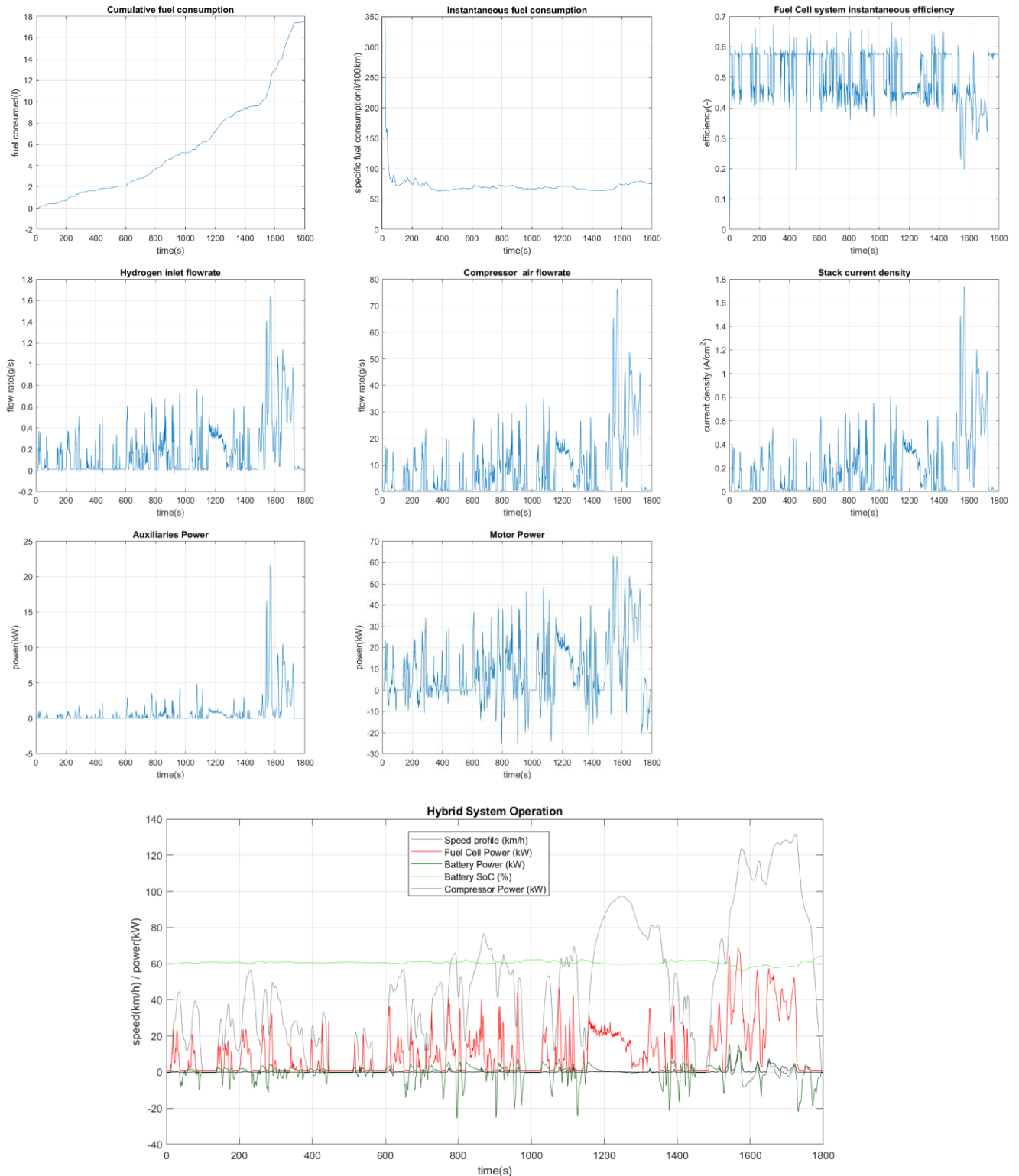


Figure 6.16 – Results on WLTP driving cycle: a) Cumulative consumption b) Instantaneous specific consumption c) Fuel cell system efficiency d) Hydrogen flowrate e) Air flowrate f) Current density g) Auxiliary system power h) Motor power i) Hybrid system operation

6.7. Cycle results comparison

The results of the simulations of Toyota Mirai are summarized in the following table:

	FTP	NEDC	UDDS	US06	WLTP
Average cycle fuel consumption (l/100km)	69.22	69.09	72.24	168.10	81.32
Average efficiency of the fuel cell system during the cycle (-)	0.534	0.521	0.522	0.406	0.506
Fuel consumed in one cycle (l)	11.53	7.23	7.66	15.45	17.47

Table 6.1 – Result summary

Also a comparison table of the results in the different cycles is shown:

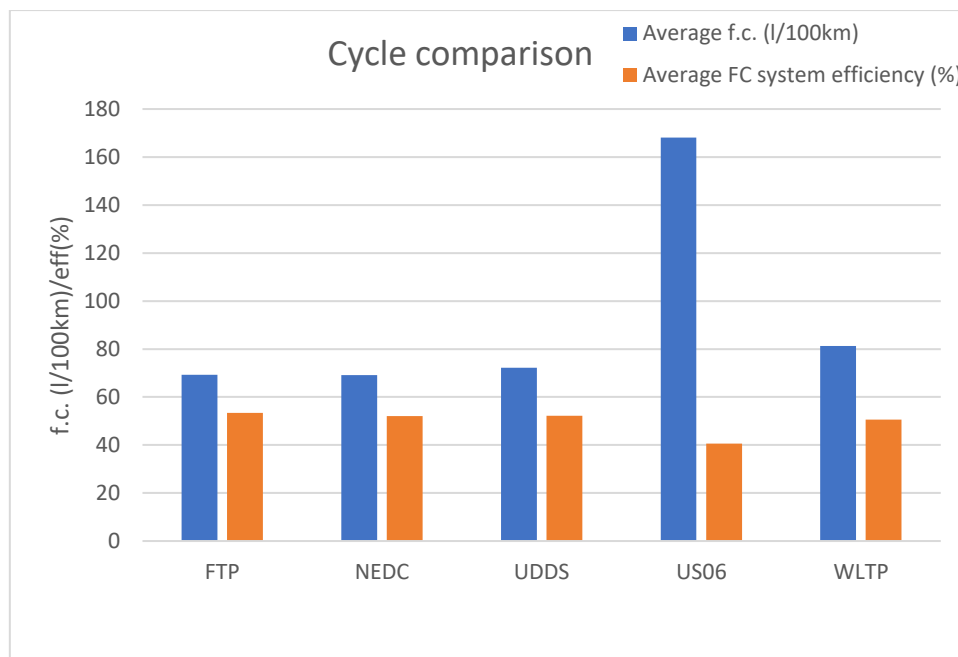


Table 6.2 – Cycle comparison

The FTP, NEDC, UDDS give very similar results since they are all low load cycles. The US06 is the cycle which gives lower efficiency of the FC system and higher specific fuel consumption. This is because the cycle spends the majority of its time at high load. The WLTP is the most balanced cycle because it has both low load and high load parts. The new profile is more dynamic than the low load cycles and this can help to avoid cycle beating. This profile gives higher efficiency of the fuel cell system and lower fuel consumption respect to the US06 because its high load part in relation to the total load is less.

7. Comparison with Argonne National Lab results

For validation purposes, the results obtained simulating the Toyota Mirai in the MATLAB/Simulink environment have been compared with those obtained by reverse engineering by the Argonne National Lab in 2017. Since one low load cycle (NEDC) and one high load cycle (US06) are present in the reverse engineering paper, those are the cycles which are taken into account.

7.1. NEDC

The hybrid system operation found in the dynamometer is compared with the one found in the simulation.

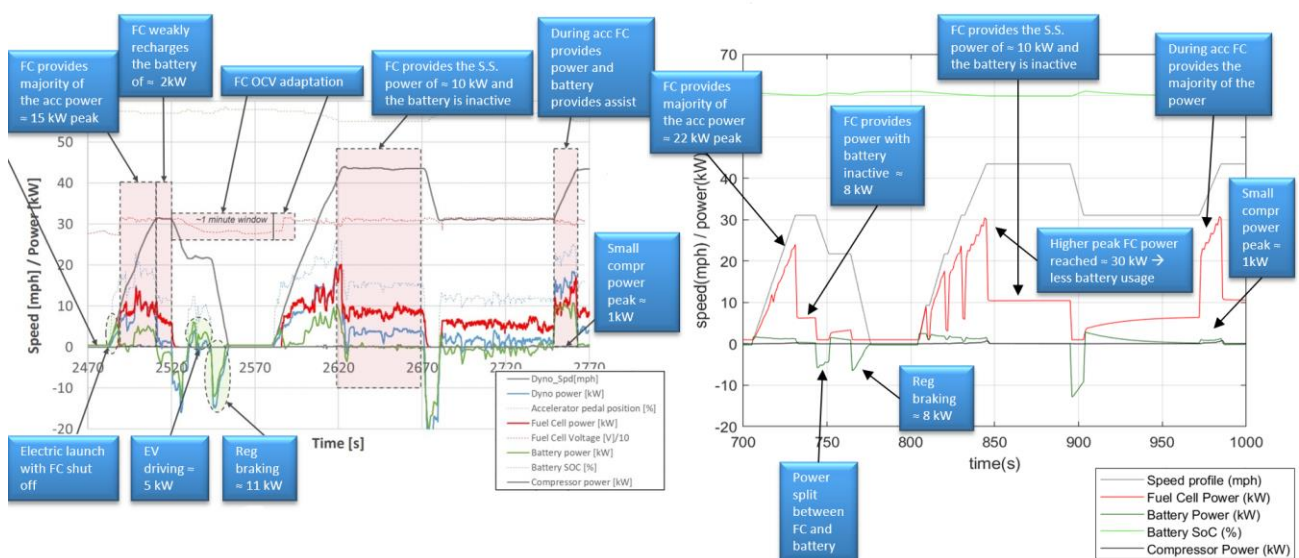


Figure 7.1 – NEDC hybrid system operation of the Argonne lab (left) / of the Simulation (right)

Considerations on the results found:

- The general shape of the Fuel Cell curve and of the Battery curve is well reproduced
- The obtained punctual results are very similar
- The main differences found are:
 - a) The Fuel cell is used slightly more respect to the Argonne Lab results
 - b) Battery assist is smaller than the results found by the Argonne Lab
 - c) When the velocity of the speed profile is 0, the Fuel Cell is operated in idle instead of being cut-off (as Argonne)

7.2. US06

The hybrid system operation found in the dynamometer is compared with the one found in the simulation.

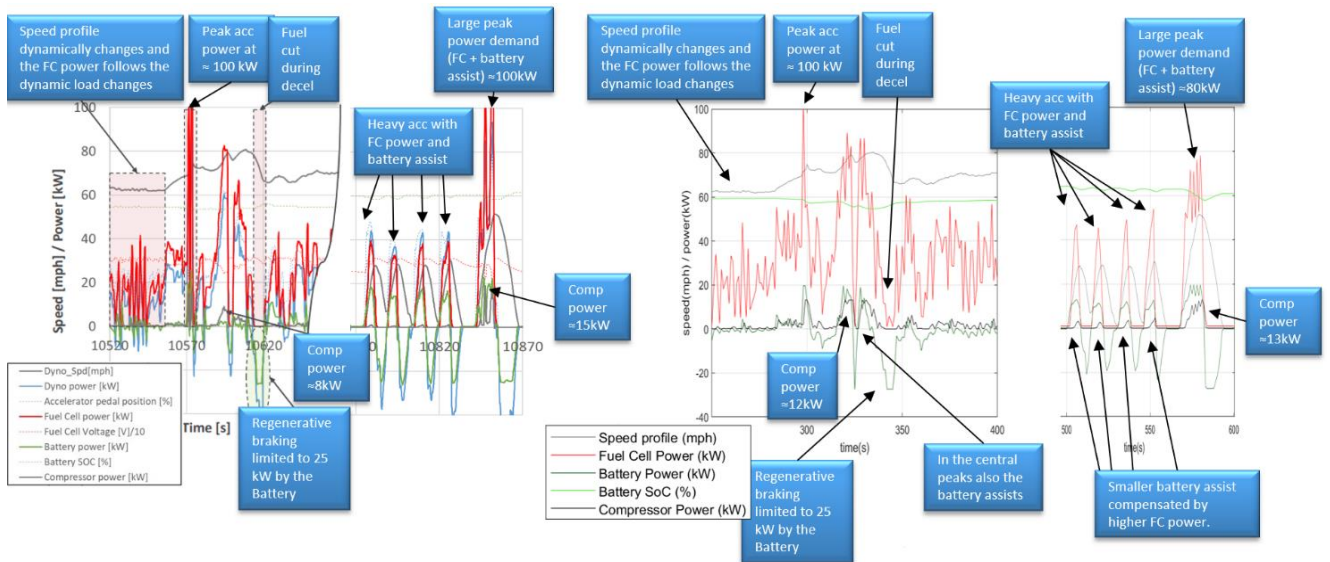


Figure 7.2 – US06 Hybrid system operation of the Argonne lab (left) / of the Simulation (right)

Considerations on the results found:

- The general shape of the Fuel Cell curve and of the Battery curve is well reproduced
- The obtained punctual results are very similar
- The main differences found are:
 - a) In the middle peaks the air compressor power is higher than Argonne Lab results
 - b) In the middle peaks also the battery assists the Fuel cell, differently from what shown by Argonne
 - c) In the sequence of equal peaks at the end, the battery assist is slightly smaller but this is compensated by a higher Fuel Cell usage
 - d) In the last peak, the power requested is considerably smaller than the Argonne data



8. Conclusions

In this thesis work, a MATLAB/Simulink model, which simulates the whole vehicle system of a hybrid fuel cell vehicle in various driving cycles, has been created. This model has been found to be fast and to give stable and reliable results. The model has been applied at first to test different possible control strategies to find the optimal power split between the fuel cell stack and the battery. In this first part, the data of an average small car have been considered. In these simulations six possible control strategies have been tested (thermostat, range extender, mode based, constant fuel cell output, strong load following and adaptive) through three low load driving cycles (FTP, NEDC, UDDS) and two high load ones (US06, WLTP). In the low load cycles, the best specific fuel consumption values were obtained by the constant fuel cell output in the FTP and UDDS and by the mode based in the NEDC. The strong load following control strategy gave slightly higher fuel consumption values but also higher average efficiency of the fuel cell system (which implies a higher usage of the fuel cell). In the high load cycles, the best fuel consumption is achieved by the mode control strategy but the best fuel cell efficiency is obtained by the constant fuel cell output control strategy. The strong load following control strategy does not give the best results either in high load cycles or in low load cycles but are still satisfactory for both. The advantage of this control strategy is that it is the more versatile not knowing in advance the cycle since the state of charge of the battery has small changes during the cycle. Toyota Mirai has a control strategy similar to the last described.

The model has then been used to simulate the hybrid operation of the 2017 Toyota Mirai vehicle over the five different control strategies. The FTP, NEDC and UDDS all give low fuel consumption values (especially the NEDC) since they are low load cycles. The US06 is the cycle with the higher specific fuel consumption and lower fuel cell system efficiency. This can be explained by the fact that the cycle spends the majority of its time at high load. The WLTP cycle is the most balanced since it has both low load and high load parts and is more dynamic than the other cycles to avoid cycle beating. For validation purposes, the results of the Toyota Mirai simulations over the NEDC and US06 are compared with those obtained by reverse engineering by the Argonne National Lab (ANL). The general shape of both the fuel cell and battery operation curve are well represented for both cycles. In the NEDC the fuel cell is used slightly more with less battery assist than what found by Argonne lab. In the US06 cycle, the middle peaks have a slightly higher compressor power and more battery assist than the Argonne results and the last peak has a smaller power request. These differences could be present due to the lack of precise and accurate data relative to some of the vehicle components such as the motor and the fuel cell stack configuration. In particular, in order to simplify the analysis and keep the validity of the results for more general systems it has not been considered that the stack is humidifier-less in this vehicle.



References

- [1] Erjavec, J. (2012). Hybrid, electric, and fuel-cell vehicles. Cengage Learning.
- [2] Agaesse, Tristan. (2016). PhD manuscript –draft- Simulations of one and two-phase flows in porous microstructures, from tomographic images of gas diffusion layers of proton exchange membrane fuel cells.
- [3] Barbir, F. (2012). PEM fuel cells: theory and practice. Academic press.
- [4] Hoogers, G. (Ed.). (2002). Fuel cell technology handbook. CRC press.
- [5] Haraldsson, K. (2005). On direct hydrogen fuel cell vehicles: modelling and demonstration (Doctoral dissertation, KTH).
- [6] Eshani, M., Gao, Y., Gay, S. E., & Emadi, A. (2005). Modern electric, hybrid electric and fuel cell vehicles. Fundamentals, Theory, and Design. Boca Raton, FL: CRC.
- [7] Guzzella, L., & Sciarretta, A. (2007). Vehicle propulsion systems (Vol. 1). Springer-Verlag Berlin Heidelberg.
- [8] Dell, R. M., Moseley, P. T., & Rand, D. A. (2014). Towards sustainable road transport. Academic Press.
- [9] Fenton, J., & Hodgkinson, R. (2001). Lightweight electric/hybrid vehicle design.
- [10] Ravello, V., (2019/2020). Electric and Hybrid propulsion system course lecture notes.
- [11] Thomas, C. E. (2009). Fuel cell and battery electric vehicles compared. international journal of hydrogen energy, 34(15), 6005-6020.
- [12] Markel, T., Brooker, A., Hendricks, T., Johnson, V., Kelly, K., Kramer, B., ... & Wipke, K. (2002). ADVISOR: a systems analysis tool for advanced vehicle modeling. Journal of power sources, 110(2), 255-266.
- [13] Prathibha, P. K., Samuel, E. R., & Unnikrishnan, A. (2020). Parameter study of electric vehicle (EV), hybrid EV and fuel cell EV using advanced vehicle simulator (ADVISOR) for different driving cycles. In Green Buildings and Sustainable Engineering (pp. 491-504). Springer, Singapore.
- [14] Turkmen, A. C., Solmaz, S., & Celik, C. (2017). Analysis of fuel cell vehicles with advisor software. Renewable and Sustainable Energy Reviews, 70, 1066-1071.
- [15] Zoppello, M. (2010). Power management nei veicoli ibridi ed elettrici.
- [16] Karpinski-Leydier, M. (2012). Optimal Control of Li-Ion Hydrogen Fuel Cell Hybrid Vehicles (Master's thesis, University of Waterloo).
- [17] Cipollone, R., Di Battista, D., Marchionni, M., & Villante, C. (2014). Model based design and optimization of a fuel cell electric vehicle. Energy Procedia, 45, 71-80.
- [18] ISO 23274-1. (2019). Hybrid-electric road vehicles - Exhaust emissions and fuel consumption measurements - Part 1:Non-externally chargeable vehicles.
- [19] Morita, K., Shimamura, K., Yamaguchi, S., Furumachi, K., Osaki, N., Nakamura, S., ... & Kawai, T. (2009). Development of a fuel economy and exhaust emissions test method with HILS for heavy-duty HEVs. SAE International Journal of Engines, 1(1), 873-887.
- [20] Lohse-Busch, H., Stutenberg, K., Duoba, M., & Iliev, S. (2018). Technology assessment of a fuel cell vehicle: 2017 Toyota Mirai (No. ANL/ESD-18/12). Argonne National Lab.(ANL), Argonne, IL (United States).
- [21] Kelly, K. J., & Rajagopalan, A. (2001). Benchmarking of OEM hybrid electric vehicles at NREL. National Renewable Energy Laboratory.
- [22] Efficiency, E., & Energy, R. (2011). Evaluation of the 2010 toyota prius hybrid synergy drive system.
- [23] Yumiya, H., Kizaki, M., & Asai, H. (2015). Toyota fuel cell system (TFCS). World Electric Vehicle Journal, 7(1), 85-92.